

UC San Diego

UC San Diego Electronic Theses and Dissertations

Title

Coxsackievirus Persistence in the Neonatal Central Nervous System : Investigating the Interplay between the Host Response and Viral Persistence in Neural Stem and Progenitor Cells

Permalink

<https://escholarship.org/uc/item/1tk4j9dn>

Author

Tsueng, Ginger

Publication Date

2013

Peer reviewed|Thesis/dissertation

UNIVERSITY OF CALIFORNIA, SAN DIEGO

SAN DIEGO STATE UNIVERSITY

Coxsackievirus Persistence in the Neonatal Central Nervous System:
Investigating the Interplay between the Host Response and Viral Persistence in
Neural Stem and Progenitor Cells

A dissertation submitted in partial satisfaction of the
requirements for the degree Doctor of Philosophy

in

Biology

by

Ginger Tsueng

Committee in charge:

University of California, San Diego

Professor Nicholas Spitzer
Professor Elina Zuniga

San Diego State University

Professor Ralph Feuer, Chair
Professor Kelly Doran
Professor Greg Harris

2013

The Dissertation of Ginger Tsueng is approved, and it is acceptable in quality and form for publication on microfilm and electronically:

Chair

University of California, San Diego

San Diego State University

2013

DEDICATION

This dissertation is dedicated my parents, J, W, A, & V T; my fellow ex-Nereids (especially MJS, SyTe, Dee, King Huong, Hunter K, and KS Lam), my dear Cookie, Tky, and ABI.

EPIGRAPH

“There is nothing like looking, if you want to find something. You certainly usually find something, if you look, but it is not always quite the something you were after.”

J.R.R. Tolkien

TABLE OF CONTENTS

SIGNATURE PAGE.....	iii
DEDICATION.....	iv
EPIGRAPH.....	v
TABLE OF CONTENTS.....	vi
LIST OF ABBREVIATIONS.....	ix
LIST OF FIGURES AND TABLES.....	xi
ACKNOWLEDGEMENTS.....	xiii
VITA.....	xv
ABSTRACT OF THE DISSERTATION.....	xix
INTRODUCTION TO THE DISSERTATION.....	1
CHAPTER 1: Examining the susceptibility of different neural cell types to CVB3 infection.....	4
Introduction.....	5
Materials and Methods.....	6
Results.....	6
Discussion.....	16
Acknowledgements.....	20
CHAPTER II: Coxsackievirus B3 Hypervirulence Followed by Virus Attenuation Upon Establishment of Persistent Infection in Neural Progenitor and Stem Cells.....	21
Introduction.....	22
Materials & Methods.....	24
Isolation and production of a recombinant coxsackievirus.....	24
Isolation, culture, and infection of neurospheres.....	24

Cell counts	25
Detection and isolation of viral variants	25
Virus multi-step growth curves.....	26
Examination of viral virulence by plaque assay	26
Differentiation and immunostaining.....	27
Fluorescence microscopy and ImageJ analysis	27
Western blots	27
Sequencing and analysis.....	28
Results	29
Coxsackievirus B3 persists in cultured neural progenitor and stem cells.....	29
Virus production over time in persistently-infected NPSCs.....	30
Changes in CVB3 plaque size observed over time in supernatants sampled from infected NPSC cultures	32
Multistep growth curve for viral isolates obtained from persistently-infected NPSCs.....	34
Sequence analysis of viral isolates from persistently-infected NPSCs.....	35
Persistently-infected NPSCs continue to express of nestin and other markers of neural cell lineage differentiation.....	37
Persistently-infected NPSCs have an increased propensity to spontaneously differentiate under normal culturing conditions.....	38
mCAR expression levels in NPSCs vary depending on differentiation status, but are not entirely suppressed in persistently-infected NPSCs.....	39
Discussion	40
Figures	48
Acknowledgements	54
CHAPTER III: The role of Type I Interferons in Establishing a Carrier - State Infection and Selecting for Attenuated Viral Variants Following Coxsackievirus	55

Infection in Neural Stem Cell Cultures.....	55
Introduction.....	56
Materials & Methods.....	58
Isolation and production of a recombinant coxsackievirus.....	58
Isolation, culture, and infection of neurospheres.....	58
Superinfection infection of uninfected or persistently-infected C57BL/6 NPSCs.....	59
Interferon β treatment.....	60
Detection of Endogenous Interferon β	60
Plaque Assays and Plaque Size Determination.....	61
Priming of the Innate Immune Response in NPSCs.....	61
Results.....	62
CVB3-infected NPSCs are less susceptible to new CVB3 infections.....	62
NPSCs are capable of producing Type I Interferons.....	65
The type I interferon response is protective against CVB3 in NPSCs.....	65
The decreased susceptibility to superinfection in Persistently-infected NPSCs is specific to CVB3.....	68
The lack of a functional Type I interferon response affects the ability of the virus to evolve and persist.....	70
Discussion.....	71
Figures.....	75
Acknowledgements.....	85
CONCLUSION OF THE DISSERTATION.....	86
REFERENCES.....	92

LIST OF ABBREVIATIONS

CAR	Coxsackievirus adenovirus receptor
CNS	Central nervous system
CPE	Cytopathic Effects
CVB3	Coxsackievirus B3
eGFP	Enhanced green fluorescent protein
GFAP	glial fibrillary acidic protein
hrs	Hours
IFN	Interferon
R K/O	Receptor knock out
LCMV	Lymphocytic choriomeningitis virus
Mbp	Myelin basic protein
mL	Milliliter
MOI	Multiplicity of infection
NPSCs	Neural progenitor and stem cells
OD	Optical density
pfu	Plaque forming units
PI	Post-infection
Poly I:C	Polyinosinic:polycytidylic acid
qRT-PCR	Quantitative real time polymerase chain reaction
Surv	CVB3-infection survivors (carrier-state NPSCs)
U/mL	Functional Units per milliliter
UV	Ultraviolet

μL	microliter
μg	microgram
VSV	Vesicular Stomatitis Virus

LIST OF FIGURES AND TABLES

Figure 1.1. Neurospheres grown in culture are highly susceptible to eGFP-CVB3 infection.....	7
Figure 1.2. CVB3 preferentially infected nestin-positive and NG2+ cells within neurospheres.	9
Figure 1.3. Virus replication and cytopathic effects in neurospheres inoculated from actin promoter-GFP transgenic mice and infected with DsRed-CVB3. ..	10
Figure 1.4. Quantification of virus-induced cell death over time in neurospheres following infection with two recombinant coxsackieviruses.....	11
Figure 1.5. Differentiation of NPSCs following treatment with fetal bovine serum.	12
Figure 1.6. Higher levels of viral protein expression and CPE were observed in NPSCs than in differentiated NPSCs.	13
Figure 1.7. Higher levels of viral titers were observed in NPSCs than in differentiated NPSCs.....	14
Figure 1.8. Reduction in CVB3 replication and viral protein expression in highly differentiated NPSCs expressing neural differentiation markers and lacking nestin expression.	15
Figure 1.9. CVB3 infection and alteration of hte NPSC differentiation pathway.	17
Figure 2.1. CVB3 persists as a carrier-state infection in cultured NPSCs.	43
Figure 2.2. Quantification of viral titers, viable cells, and interferon- β production over time in persistently-infected NPSCs.....	44
Figure 2.3. Viral isolates obtained at different time points during the establishment of persistent infection in NPSCs exhibited an initial increase, followed by a gradual reduction in plaque size.	45
Figure 2.4. Viral isolates obtained temporally from persistently-infected NPSCs showed an initial increase, followed by a step-wise reduction in growth curve kinetics.	46
Figure 2.5. Unique mutations observed in viral isolates derived from persistently-infected NPSCs.	48

Figure 2.5 continued. Unique mutations observed in viral isolates derived from persistently-infected NPSCs.	49
Figure 2.6. Persistently-infected NPSCs differentiate into the three downstream neural cell lineages similar to uninfected NPSCs.....	50
Figure 2.7. Persistently-infected NPSCs have an altered propensity to spontaneously differentiate.....	51
Figure 2.8. mCAR levels fluctuate in persistently-infected NPSCs, and are not necessarily suppressed.....	52
Supplementary Figure 2.1. mCAR levels fluctuate in persistently-infected NPSCs, and are not necessarily suppressed.....	53
Table 2.1. Primer sequences utilized for viral genome amplification and sequence analysis for hypervirulent and attenuated viral isolates.	47
Figure 3.1. Persistently-infected cells are resistant to superinfection.	75
Figure 3.2. Superinfection occurs in naïve NPSCs upon concurrent inoculation.	76
Figure 3.3. Interferon is produced during the course of infection.....	77
Figure 3.4. Interferon β treatment inhibits viral protein expression.	78
Figure 3.5. The induction of the type I interferon response is transiently protective in the absence of exogenous interferons.	79
Figure 3.6. Priming the innate immune response may protect cells from virus-induced CPE.	80
Figure 3.7. Persistently-infected NPSCs are still vulnerable to superinfection by VSV.	81
Figure 3.8. The type I interferons are important for CVB3 evolution.....	82
Supplementary Figure 3.1. Persistently-infected NPSCs do not exhibit superinfection by CVB3.....	83
Supplementary Figure 3.2. Infected and persistently-infected NPSCs can still be superinfected by LCMV.	84

ACKNOWLEDGEMENTS

I would like to thank my exceptional mentor, Dr. Ralph Feuer, for his patience, wit, perceptiveness, and flexibility—all of which fostered an environment of cooperation, dedication, delight, and growth in his laboratory. Thank you for pushing me forward when I needed the push, providing hints when I got a little lost, and otherwise allowing me to explore the rest of the way.

I would like to acknowledge my fellow Feuer Lab students whose previous research shed insights for my own, and who will carry forward the research beyond the scope of my own.

I would like to acknowledge the ARCS Foundation, the Inamori Foundation, and Gen Probe, whose generous support has enabled me to concurrently complete this work as well as a Masters in Business Administration. You have my greatest respect and my deepest gratitude for your continued investment in science and the struggling researchers behind it.

I would like to thank all of my committee members, Dr. Doran, Dr. Harris, Dr. Spitzer, and Dr. Zuniga for the time and assistance they have provided in improving the research described in this dissertation.

Chapter 1, in full, is a reprint of the material as it appears in *Journal of Virology* 2011. Tsueng, G; Tabor-Godwin, JM; Gopal, A; Ruller, CM; Deline, S; An, N; Frausto, RF; Milner, R; Crocker, SJ; Whitton, JL; Feuer, R. The dissertation author was the primary investigator and author of this paper.

Chapter 2, in part is currently being prepared for submission for publication of the material. Tsueng, G; Rhoades, RE; Deline, S; Feuer, R. The dissertation author was the primary investigator and author of this material.

Chapter 3, in part is currently being prepared for submission for publication of the material. Tsueng, G; Rahawi, S; Deline, S; Tabor-Godwin, JM; Ruedas, J; Perrault, J; Cornell, CT; Whitton, JL; Feuer, R. The dissertation author was the primary investigator and author of this material.

VITA

EDUCATION

Doctor of Philosophy in Biology - September 2013
University of California at San Diego and San Diego State University
Joint Doctoral Program in Biology – Cell and Molecular Biology

Master in Business Administration – May 2013
San Diego State University

Bachelor of Science in Biochemistry/Cell Biology and Psychology – June 2002
With Minors in Political Science and English Writing
University of California at San Diego

HONORS, AWARDS, AND PATENT INVENTORSHIP

January 2013	Finalist, CSUPERB I2P Competition
December 2012	Finalist, Lavin VentureStart Competition
December 2012	CSUPERB Travel Award
December 2012	SDSU Instructionally Related Travel Award, San Diego State University
February 2012	2 nd Place APICS West Coast Case Competition, APICS
August 2010 - 2011	Inamori Fellowship, Inamori Foundation
August 2010 - 2013	PhD/MBA Fellowship, Gen-Probe
August 2010 - 2013	ARCS Scholarship, ARCS Foundation
December 2009	SDSU Instructionally Related Travel Award, San Diego State University
August 2009	US Patent 7572606, Issued to Nereus Pharmaceuticals
August 2007 - 2008	SDSU In State Tuition Scholarship, San Diego State University
May 2008	US Patent 7375129, Issued to Nereus Pharmaceuticals
September 1998 - 2002	Del Mar Thoroughbred sponsored Regents Scholarship, University of California, San Diego

PUBLICATIONS

Tabor-Godwin JM, **Tsueng G**, Sayen R, et al. The Role of Autophagy during Cocksackievirus Infection in Neural Progenitor and Stem Cells. *Autophagy*. 2012 Jun 1;8(6)

Tsueng G, Tabor-Godwin JM, Deline S, Gopal A, Ruller CM, Frausto RF, An N, Crocker SJ, Milner R, Whitton JL, and Feuer R Cocksackievirus Preferentially Replicates and Induces Cytopathic Effects in Undifferentiated Neural Progenitor Cells. *J Virol*, 2011.

Rhoades RE, Tabor-Godwin JM, **Tsueng G**, Feuer R. Enterovirus infections of the central nervous system. *Virology*, 2011.

Tsueng G and Lam KS. A preliminary investigation on the growth requirement for monovalent cations, divalent cations and medium ionic strength of marine actinomycete *Salinispora*. *Appl Microbiol Biotechnol*. 2010 May; 86(5):1525–1534

Tsueng G and Lam KS. The effect of cobalt and vitamin B12 on the production of salinosporamides by *Salinispora tropica*. *J Antibiot (Tokyo)*. 2009 Apr;62(4):213-6.

Manam RR, Macherla VR, **Tsueng G** et al. Antiprotealide is a natural product. *J Nat Prod*. 2009 Feb 27;72(2):295-7

Tsueng G and Lam KS. Growth of *Salinispora tropica* strains CNB440, CNB476 and NPS21184 in non-saline, low sodium media. *Appl. Microbiol. Biotechnol*. 2008 Oct;80(5):873-80

McArthur KA, Mitchell SS, **Tsueng G** et al. Lynamycin A-E: Chlorinated bisindole pyrrole antibiotics from a novel marine actinomycete. *J Nat Prod*. 2008 Oct;71(10):1732-7

Sunga MJ, Teisan S, **Tsueng G** et al. Seawater requirement for the production of lipoxazolidinones by marine actinomycete strain NPS8920. *J Ind Microbiol Biotechnol*. 2008 Jul;35(7):761-

Tsueng G, Teisan S, Lam KS. Defined salt formulations for the growth of *Salinispora tropica* strain NPS21184 and the production of salinosporamide A (NPI-0052) and related analogs. *Appl Microbiol Biotechnol*. 2008 Apr;78(5):827-32.

Tsueng G, Lam KS. A low-sodium salt formulation for the fermentation of salinosporamides by *Salinispora tropica* strain NPS21184. *Appl Microbiol Biotechnol*. 2008 Apr;78(5):821-6.

Lam KS, **Tsueng G**, McArthur KA et al. Effects of halogens on the production of salinosporamides by the obligate marine actinomycete *Salinispora tropica*. *J Antibiot (Tokyo)*. 2007 Jan;60(1):13-9

Tsueng G, McArthur KA, Potts BC, Lam KS. Unique butyric acid incorporation patterns for salinosporamides A and B reveal distinct biosynthetic origins. *Appl Microbiol Biotechnol*. 2007 Jul;75(5):999-1005.

Tsueng G, Lam KS. Stabilization effect of resin on the production of potent proteasome inhibitor NPI-0052 during submerged fermentation of *Salinispora tropica*. *J Antibiot (Tokyo)*. 2007 Jul;60(7):469-72

SCIENTIFIC PRESENTATIONS

October 2012	Society for Neuroscience Annual meeting (Poster)
March 2012	SDSU Student Research Symposium (Talk)
February 2012	SDSU Graduate Student Seminar Series (Talk)
March 2011	SDSU Student Research Symposium (Poster)
March 2011	ARCS 2011 Scientist of the Year Event (Poster)
February 2011	SDSU Graduate Student Seminar Series (Talk)
November 2010	Society for Neuroscience Annual meeting (Poster)
April 2010	San Diego Cell Biology Meeting (Poster)
April 2010	SDSU Graduate Student Symposium (Poster)
February 2010	SDSU Student Research Symposium (Poster)
December 2009	American Society for Cell Biology annual meeting (poster)
October 2009	SDSU Graduate Student Seminar Series (Talk)
May 2009	SDSU Graduate Student Seminar Series (Talk)

- August 2008 Society for Industrial Microbiology annual meeting
(Poster)
- July 2004 Society for Industrial Microbiology annual meeting
(Poster)

PROFESSIONAL EXPERIENCE

- 2002 – 2003 Laboratory Assistant, Nereus Pharmaceuticals
- 2003 – 2005 Research Associate I, Nereus Pharmaceuticals
- 2005 – 2006 Research Associate II, Nereus Pharmaceuticals
- 2006 – 2008 Research Associate III, Nereus Pharmaceuticals
- 2008 – 2009 Research Scientist I, Nereus Pharmaceuticals
- 2010 – 2013 Webmaster, SDSU Feuer Lab
<http://www.bio.sdsu.edu/Pub/feuer/>
- 2012 – 2013 Web designer, Webmaster, SDSU Glembotski Lab
<http://www.bio.sdsu.edu/Pub/glembotski/>

ASSOCIATION MEMBERSHIPS

- September 2010 - Society for Neuroscience Student Member
Current
- August 2009 – American Society for the Advancement of Science
Current Student Member
- August 2009 American Society for Cell Biology Student Member

TEACHING EXPERIENCE

- Spring 2010 Graduate Laboratory Instructor for Introduction to
Microbiology, San Diego State University
- Spring 2009 Graduate Laboratory Instructor for Introduction to
Microbiology, San Diego State University

ABSTRACT OF THE DISSERTATION

Coxsackievirus Persistence in the Neonatal Central Nervous System:
Investigating the Interplay between the Host Response and Viral Persistence in
Neural Stem and Progenitor Cells

by

Ginger Tsueng

Doctor of Philosophy in Biology

University of California, San Diego 2013

San Diego State University 2013

Professor Ralph Feuer, Chair

Newborn infants are particularly vulnerable to neurotropic infections of coxsackievirus which can potentially cause serious central nervous system (CNS) diseases such as meningitis and encephalitis. Coxsackievirus is also capable of persisting in the host CNS for extensive periods of time; however, the mechanism by which the virus evades clearance by the host remains unclear. *In vivo* models of Coxsackievirus infection have previously revealed

that the virus isolated from persistent infection is not infectious, suggesting the evolution of the virus over the course of infection. In order to disaggregate the effects of the adaptive immune response and other complicating factors from the actual infection of the central nervous system, we therefore wish to develop and utilize an *in vitro* model of Coxsackievirus infection using Neural Progenitor and Stem Cells (NPSCs) and a recombinant Coxsackievirus B3 expressing enhanced GFP (eGFP). In developing and utilizing this model we hope to explore the interaction between the host innate immune response and the virus and the impact of these interactions on the evolution of the virus and the development of disorders in the infected host CNS.

INTRODUCTION TO THE DISSERTATION

Coxsackievirus is a small, positive-sense, RNA virus in the Enterovirus genus which is capable of causing inflammatory disease in the tissues it infects. Different serotypes of Coxsackievirus have been demonstrated to have varying degrees of tropism for different tissue types (Hyypia et al., 1993). Coxsackievirus B3 (CVB3) has tropism for the heart, pancreas, and the central nervous system (CNS) (Cheung et al., 2005). Because CVB3 is also capable of persisting in the host tissues, it has been associated with chronic diseases such as chronic myocarditis and dilated cardiomyopathy (Chapman and Kim, 2008). The persistence of the CVB3 in the heart is partially attributable to the immune response which creates selective pressures on the virus, causing 5' UTR deletions, attenuating the cytolytic virus to a less cytolytic form (Kim et al., 2008). Although reduced in cytolytic capabilities, the presence of the virus may be sufficient to trigger an on-going inflammatory response resulting in the observed chronic myocarditis.

CVB3 has also been observed to infect the central nervous system (CNS). As the CNS is considered an immunoprivileged site, the immune response plays a very important role in modulating the course of infection in the CNS. During acute infections in a neonatal mouse model, Coxsackievirus has been observed to induce the infiltration of immune cells into the CNS resulting in aseptic meningitis and encephalitis (Feuer et al., 2009). However, the effects of persistent infection and chronic immune activation on the course of CNS development have not yet been fully explored. Infants are

suspected to be particularly susceptible to infection and disease primarily because their NPSCs are in a higher proliferative state than those found in adults and also because their immune responses are not as adept at suppressing the virus.

The Feuer lab utilizes an *in vivo* neonatal mouse model to examine the effects of Coxsackievirus infections in the neonatal CNS. Using this model, the Feuer lab has demonstrated that CVB3 has tropism for actively proliferating cells and neural progenitors in the neonatal CNS (Feuer et al., 2005), and is capable of persisting for at least 90 days post-infection (Feuer et al., 2009). Interestingly enough, after 30 days post-infection, the virus is no longer detectable by plaque assay, and its presence must be determined using nested RT-PCR. This suggests that the persisting virus is attenuated, and the attenuation of the virus may play an important role in enabling the virus to persist. Further, the host innate immune response may play an important role in the attenuation of the virus and consequently, its persistence.

To decouple the course of CVB3 infection in the CNS from the adaptive immune response and other convoluting factors, we developed an *in vitro* infection model consisting of Neural Progenitor and Stem Cells (NPSCs) cultured from neonatal mice. This model allows us to investigate how the host innate immune response affects the persistence of the virus and to examine how the infection affects CNS development in the host. NPSCs are capable of proliferating for an indeterminate number of rounds, and can differentiate into the three lineages of the CNS: neurons, astrocytes, and oligodendrocytes.

In culture, they form spherical aggregates called neurospheres either by proliferation or migration (Mori et al., 2007). The NPSCs which make up the neurospheres can be quite heterogeneous with variations in their sizes, viability, mitotic potential, differentiation, and apoptotic potentials (Bez et al., 2003).

While *in vivo* experiments have determined that proliferating cell types like NPSCs are preferentially infected by CVB3, our *in vitro* neurosphere model of infection will enable us to examine the susceptibility of more differentiated neural cell types to CVB3 infection. By utilizing a recombinant coxsackievirus B3 expressing enhanced GFP (eGFP-CVB3), we can track the course of infection in real time and study how the virus interacts with the host cells of the CNS. Furthermore, NPSCs have also been found to be responsive to interferon- β treatments, making our *in vitro* model of infection relevant and interesting. At high doses (1000U/mL) of interferon- β , neural precursor proliferation appeared to be inhibited as determined by lower OD detection, and lack of apoptosis as determined by caspase 3/7 levels (Wellen et al., 2009). Additionally, Wellen et al. found that differentiation potential remained unchanged; however, the neurite outgrowth lengths were significantly shorter in differentiated cells derived from interferon- β treated neural precursor cells. **Therefore, our hypothesis is that the host immune response creates selective pressures which alter the virus in the CNS. This alteration allows for the persistence of the virus in the CNS, which in turn can affect the resident NPSC population, and lead to developmental disorders of the CNS.**

**CHAPTER 1: Examining the susceptibility of different neural cell types to CVB3
infection**

Coxsackievirus Preferentially Replicates and Induces Cytopathic Effects in Undifferentiated Neural Progenitor Cells[∇]

Ginger Tsueng,¹ Jenna M. Tabor-Godwin,¹ Aparajita Gopal,¹ Chelsea M. Ruller,¹ Steven Deline,¹ Naili An,¹ Ricardo F. Frausto,² Richard Milner,³ Stephen J. Crocker,^{2,†} J. Lindsay Whitton,² and Ralph Feuer^{1,*}

Cell and Molecular Biology Joint Doctoral Program, Department of Biology, San Diego State University, San Diego, California 92182-4614¹; Department of Immunology and Microbial Science, SP30-2110, The Scripps Research Institute, La Jolla, California 92037²; and Department of Molecular and Experimental Medicine, The Scripps Research Institute, La Jolla California 92037³

Received 28 October 2010/Accepted 25 March 2011

Enteroviruses, including coxsackieviruses, exhibit significant tropism for the central nervous system, and these viruses are commonly associated with viral meningitis and encephalitis. Previously, we described the ability of coxsackievirus B3 (CVB3) to infect proliferating neuronal progenitor cells located in the neonatal subventricular zone and persist in the adult murine central nervous system (CNS). Here, we demonstrate that cultured murine neurospheres, which comprise neural stem cells and their progeny at different stages of development, were highly susceptible to CVB3 infection. Neurospheres, or neural progenitor and stem cells (NPSCs), isolated from neonatal C57BL/6 mice, supported high levels of infectious virus production and high viral protein expression levels following infection with a recombinant CVB3 expressing enhanced green fluorescent protein (eGFP) protein. Similarly, NPSCs isolated from neonatal actin-promoter-GFP transgenic mice (actin-GFP NPSCs) were highly susceptible to infection with a recombinant CVB3 expressing DsRed (*Discosoma* sp. red fluorescent protein). Both nestin-positive and NG2⁺ progenitor cells within neurospheres were shown to preferentially express high levels of viral protein as soon as 24 h postinfection (p.i.). By day 3 p.i., viral protein expression and viral titers increased dramatically in NPSCs with resultant cytopathic effects (CPE) and eventual cell death. In contrast, reduced viral replication, lower levels of CPE, and diminished viral protein expression levels were observed in NPSCs differentiated for 5 or 16 days in the presence of fetal bovine serum (FBS). Despite the presence of CPE and high levels of cell death following early CVB3 infection, surviving neurospheres were readily observed and continued to express detectable levels of viral protein as long as 37 days after initial infection. Also, CVB3 infection of actin-GFP NPSCs increased the percentage of cells expressing neuronal class III β -tubulin following their differentiation in the presence of FBS. These results suggest that neural stem cells may be preferentially targeted by CVB3 and that neurogenic regions of the CNS may support persistent viral replication in the surviving host. In addition, normal progenitor cell differentiation may be altered in the host following infection.

Nonpolio enterovirus infections are thought to be directly responsible for a majority of clinical cases of viral meningitis and encephalitis in the United States every year. An estimated 10 to 15 million symptomatic enterovirus infections every year may account for up to 75,000 cases of meningitis hospitalizations in the United States alone (35). In particular, coxsackievirus B (CVB) and enterovirus 71 have been routinely identified in patients suffering from viral meningitis. Other serious central nervous system (CNS) diseases may result following enterovirus infection, including acute disseminating myelitis (12) and acute transverse myelitis (20). Despite the significance of these viruses in human disease, much remains to be determined regarding their neurotropism, immune activation

following infection, and potential long-lasting effects on the central nervous system in the surviving host.

We previously described a neonatal mouse model of coxsackievirus B3 (CVB3) infection whereby nestin-positive neural stem cells and myeloid cells were identified as the primary target cells during early infection (15, 16, 37). Eventually, many cells infected with CVB3 underwent apoptosis (15). However, host survival was commonly observed in parallel with detectable levels of viral RNA in the adult CNS for at least 90 days postinfection (p.i.). The ability of CVB3 to persist in other organs, in particular, the heart, has been well documented (6, 25) and may involve genetic alterations in the virus which may limit replication and cytopathic effects (CPE) in the host cell (23, 24, 36). We hypothesized that the continued presence of viral RNA and/or viral gene products may affect normal neural stem cell migration and/or differentiation in the developing CNS.

Relatively little is known about the susceptibility of neural stem cells to neurotropic viral infections. Surprisingly, neural stem cells residing in the CNS remain active into adulthood, replenishing neurons within the olfactory bulb and dentate gyrus (3, 19). As these neural stem cells give rise to mature

* Corresponding author. Mailing address: Cell and Molecular Biology Joint Doctoral Program, Department of Biology, San Diego State University, 5500 Campanile Drive, San Diego, CA 92182-4614. Phone: (619) 594-7377. Fax: (619) 594-0777. E-mail: rfeuer@sciences.sdsu.edu.

† Present address: Department of Neuroscience, Faculty of Medicine, University of Connecticut Health Center, Farmington, CT 06030-3401.

[∇] Published ahead of print on 6 April 2011.

neurons, their proliferative and activation status may render them attractive targets for neurotropic viruses. Also, the migratory nature of immature neuroblasts may assist in virus dissemination within the brain following infection of progenitor or stem cells (15). Recently, both human cytomegalovirus (7, 27), HIV-1 (31, 34), and Japanese encephalitis virus (9, 10) have been shown to target neural stem cells and may influence stem cell function (26, 29, 30) and immunogenicity (11).

We wished to investigate the ability of CVB3 to infect neural stem cells grown in culture in order to more clearly evaluate the consequences of CVB3 infection on stem cell survival and dysfunction in a less complex environment. Neural progenitor and stem cells (NPSCs) isolated from the brains of 1-day-old mice form neurosphere aggregates which can be passaged indefinitely in culture. NPSCs or their differentiated counterparts were infected with recombinant coxsackieviruses expressing either enhanced green fluorescent protein (eGFP-CVB3) or *Discosoma* sp. red fluorescent protein (DsRed-CVB3) and inspected for virus production and alterations in stem cell function. Also, the levels of virus replication and virus protein expression in NPSCs were compared to those of their differentiated counterparts. Our results suggest that virus production and protein expression levels were robust in undifferentiated neurospheres, yet differentiated cells appeared to be refractory to infection and virus protein expression.

Surprisingly, some NPSCs survived infection and supported a “carrier state” infection, provided that cultures were regularly replenished with fresh complete NPSC medium. We hypothesize that CVB3 may persist in a similar fashion *in vivo* within a quiescent subset of neural stem cells. Evaluating CVB3 infection of NPSCs in culture may help us understand factors influencing preferential viral replication in dividing progenitor cells, and these investigations may ultimately illuminate possible chronic alterations in neural progenitor cell differentiation during persistent infection within the surviving host.

MATERIALS AND METHODS

Isolation and production of a recombinant coxsackievirus. The generation of a recombinant coxsackievirus expressing eGFP has been described previously. Briefly, the CVB3 infectious clone (pH 3) (obtained from Kirk Knowlton at University of California at San Diego) was engineered to contain a unique *Sfi*I site, which facilitates the insertion of any foreign sequence into the CVB3 genome. The generation of recombinant coxsackievirus expressing the enhanced green fluorescent protein (eGFP-CVB3) and DsRed (DsRed-CVB3) has been described previously (14, 37). Virus titrations were carried out as described previously (14). Viral stocks were prepared on HeLa RW cells maintained in Dulbecco’s modified Eagle’s medium (DMEM; Invitrogen, Gaithersburg, MD) supplemented with 10% fetal bovine serum (FBS). Viral stocks were diluted in DMEM before inoculation.

Isolation, culture, and infection of neurospheres. Mouse experimentation conformed to the requirements of the San Diego State University Animal Research Committee and the National Institutes of Health. C57BL/6 mice and actin promoter-GFP transgenic mice were obtained from the Scripps Research Institute animal facilities or Harlan Sprague Dawley (Harlan Laboratories, San Diego, CA). Breeding pairs were checked every day. As described previously, NPSCs were derived from isolated cortices of newborn mice, mechanically and enzymatically dissociated, and then plated as single-cell suspensions in complete NPSC medium consisting of DMEM/F12 medium supplemented with 2% B27 (Invitrogen), 20 ng/ml epidermal growth factor (EGF; Invitrogen), 20 ng/ml basic fibroblast growth factor (bFGF; Preprotech), 5 μ g/ml heparin (Sigma), and 0.5% penicillin-streptomycin (8). Free-floating neurospheres were separated and transferred into new flasks every 2 days. Neurospheres were vigorously dissociated and resuspended in NPSC culture medium to a concentration of 10^5 cells/ml

in a T-25 flask (BD Falcon). Neurospheres were plated onto chamber slides and infected with eGFP-CVB3 at various multiplicities of infection (MOI) in NPSC medium. Alternatively, NPSCs were differentiated for 5 or 16 days in differentiation medium consisting of DMEM supplemented with 1% FBS, N1 supplement (Sigma), and 0.5% penicillin-streptomycin. Following infection, differentiated cells were continuously cultured in either differentiation medium or in NPSC medium. Supernatants were harvested over time to determine viral titers. The percentage of dead cells was determined by trypan blue staining, followed by cell counting using a hemacytometer. Neurosphere cultures were replenished with complete NPSC medium and passed every 3 days up to 37 days postinfection. Infected neurospheres were examined over time using fluorescence microscopy.

Immunofluorescence microscopy. Live NPSCs or differentiated NPSC cultures infected with eGFP-CVB3 or DsRed-CVB3 were imaged using a Zeiss Axio Observer D.1 inverted fluorescent microscope with an ApoTome Imaging System. Alternatively, infected NPSCs were fixed in 4% paraformaldehyde and washed three times in phosphate-buffered saline (PBS). Viral protein expression was determined by native eGFP (green) or DsRed (red) expression. Fixed cells were blocked with 10% normal goat serum (NGS) and immunostained using the following antibodies: nestin (catalog item PRB-315C; Covance, Inc.) at 1:1,000, neuronal class III β -tubulin (PRB-435P; Covance, Inc.) at 1:1,000, glial fibrillary acidic protein ([GFAP] G 9269; Sigma, Inc.) at 1:1,000, NG2 (AB5320; Chemicon, Inc.) at 1:500, Olig2 (ab33427; Abcam, Inc.) at 1:1,000, and myelin basic protein (MBP) at 1:1,000 (AB980; Chemicon, Inc.). Primary antibodies were diluted in 2% NGS in PBS (150 to 200 μ l per slide) in a humidified chamber and incubated overnight. Slides were washed with PBS for 5 min (three times). Secondary antibodies (at 1:1,000) conjugated to Alexa-Fluor-594, Alexa-Fluor-488, or Alexa-Fluor-350 were diluted with 2% NGS in PBS (150 to 200 μ l per slide) and incubated overnight. Following incubation with the secondary antibody, slides were washed with PBS for 5 min (three times). Three to five representative images of the cultures were taken for each sampling time point at multiple magnifications.

ImageJ analysis. For each fluorescent image, three fluorescent channels for each image were exported separately without color overlay. Threshold adjustments were applied to generate a black and white image using NIH ImageJ (public domain software). These black and white images were analyzed using ImageJ to quantify fluorescent signal. In each case, marker expression was normalized prior to applying a Student *t* test to determine statistical significance. In C57BL/6 NPSCs infected with eGFP-CVB3, marker expression was normalized to 4’,6’-diamidino-2-phenylindole (DAPI). In actin-GFP NPSCs infected with DsRed-CVB3, marker expression was normalized to GFP.

RESULTS

CVB3 infection of primary neural progenitor and stem cells (NPSCs) in culture. We isolated and cultured primary NPSCs from both C57BL/6 and actin promoter-GFP transgenic mice in order to determine their ability to support CVB3 infection. NPSCs grown in culture formed neurospheres, which comprise both stem and progenitor cells. As expected, isolated neurospheres expressed high levels of nestin, a marker for neural stem and progenitor cells, as determined by immunofluorescence (data not shown). Neurospheres were infected at a multiplicity of infection (MOI) of 0.1 with a recombinant coxsackievirus B3 expressing eGFP (eGFP-CVB3), and viral protein expression (eGFP) was evaluated by immunofluorescence microscopy merged with Hoffman modulation contrast (Hoffman MC) over the course of 7 days (Fig. 1).

As early as 1 day postinfection (p.i.), virus protein expression was observed in a minority of cells within the neurosphere (Fig. 1A). An increase in virus protein expression was readily seen in neurospheres by day 2 p.i. (Fig. 1B). By day 4 p.i., nearly all cells within many neurospheres expressed large amounts of viral protein (Fig. 1C). In contrast, differentiated cells located near the periphery of the neurosphere which had attached to the surface of the chamber slide (most likely following the depletion of growth factors in the complete NPSC medium)

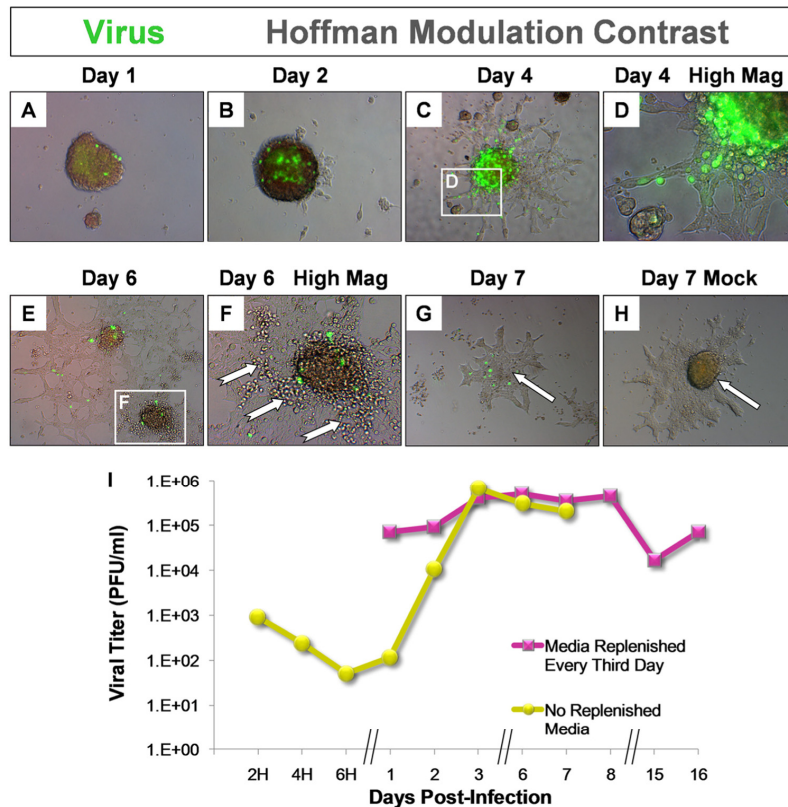


FIG. 1. Neurospheres grown in culture were highly susceptible to eGFP-CVB3 infection. NPSCs were isolated from the cortices of 1-day-old C57BL/6 mice, cultured to form neurosphere aggregates, and infected with eGFP-CVB3 (MOI of 0.1). Infected neurospheres were observed over time by fluorescence microscopy, and viral titers were determined by plaque assay. (A) Virus protein expression (green) was readily observed by day 1 p.i. (B and C) An increase in viral protein expression was seen until day 4 p.i. (D) Higher magnification of panel C showed the preferential infection of neurosphere aggregates with little to no viral protein expression in adherent cells with stretched morphology. (E) By day 6 p.i., virus protein levels were reduced, and signs of cytopathic effect (CPE) were readily observed at a higher magnification (F, notched white arrows). (G) By day 7 p.i., viral protein levels were low, many neurospheres had disappeared, and the remaining cells consisted of adherent cells (white arrow). (H) In contrast, neurospheres were readily apparent in mock-infected cultures (white arrow). (I) Viral titers increased over time and reached a maximum at day 3 p.i. (yellow). Also, infected NPSCs replenished with complete medium every 3 days supported a carrier state infection with high levels of infectious virus (pink).

failed to express appreciable levels of viral protein. Higher magnification of day 4 infected cultures illustrated the lack of viral protein expression in differentiated cells adjacent to heavily infected neurospheres (Fig. 1D). By day 6 p.i., the level of viral protein expression dropped dramatically (Fig. 1E), and cytopathic effects (CPE) were readily apparent near residual neurospheres (Fig. 1F, notched white arrows). At 7 days p.i., many infected neurospheres disappeared, presumably due to CPE (Fig. 1G, white arrow), and viral protein expression was limited to rounded cells or cellular debris while differentiated cells continued to lack viral protein expression. In contrast, unharmed neurospheres remained visible in mock-infected control cultures grown in parallel for 7 days (Fig. 1H, white arrow).

We evaluated the amount of infectious virus produced over time in these infected neurosphere cultures by plaque assay

(Fig. 1I, yellow line). Within 2 days p.i., viral titers increased dramatically in neurosphere cultures. By 3 days p.i., peak production of infectious virus was observed, which corresponded closely with viral protein expression levels, as determined by immunofluorescence microscopy. By day 6 p.i. and beyond, viral titers dropped, corresponding to the presence of CPE within the neurosphere cultures. Taken together, these results suggest that virus protein expression and viral replication were robust in stem and progenitor cells found within neurospheres; in contrast, differentiated cells adjacent to infected neurospheres appeared to be refractory to infection.

Also, NPSCs were infected with eGFP-CVB3 at a higher MOI (MOI of 100.0), replenished with complete NPSC medium every third day, and followed for infectious virus production by plaque assay for 16 days p.i. (Fig. 1I, pink line). High viral titers were observed in these NPSC cultures for up to 16

days p.i. Surprisingly, some NPSCs survived initial infection in the presence of replenished complete NPSC medium, and these infected NPSCs supported a carrier state infection characterized by a steady-state infection in which many or all of the cells became infected (18). These findings suggest the presence of a subpopulation of stem cells which may be resistant to virus-mediated CPE; a resistant primary stem cell may restore the neurosphere culture and generate additional target cells for the maintenance of virus production over time.

Preferential infection of nestin-positive and NG2⁺ cells in neurosphere cultures. Although NPSCs consist of nestin-positive stem cells, cells lacking nestin expression were also found within neurospheres. These nestin-negative cells may represent more committed progenitor cells or immature neuronal or glial cells. To determine which population of cells within a neurosphere were most susceptible to infection, NPSCs were infected with eGFP-CVB3 (MOI of 0.1), harvested 2 days later, and immunostained for nestin, as well as three additional downstream lineage markers including neuronal (neuronal class III β -tubulin) and glial cell (GFAP and NG2) markers. Neuronal class III β -tubulin is highly expressed within neuroblasts and immature neurons. GFAP is a marker commonly utilized to discriminate immature glial cells and astrocytes (28). NG2 has been used to identify oligodendrocyte precursor cells (4). A Zeiss Axio Observer with ApoTome Imaging System was utilized to detect the colocalization of infected cells and cells expressing downstream lineage molecules. The ApoTome Imaging System utilizes structured illumination technology allowing for the collection of optical sections and three-dimensional reconstruction.

Both nestin-positive and nestin-negative NPSCs expressed high levels of viral protein (Fig. 2A, white arrow and blue arrow, respectively). Also, we detected the expression of three downstream lineage markers within infected neurospheres at 2 days p.i. (Fig. 2A, β -tubulin, GFAP, and NG2 immunostaining). Viral protein expression was observed in cells expressing all three downstream markers although infection was preferentially within NG2⁺ cells. In Fig. 2A, higher magnification of a boxed field for each marker shows infected cells either expressing (white arrows) or failing to express (blue arrows) the marker. The number of infected cells expressing each marker was quantified over 2 days (Fig. 2B). Four cell populations were analyzed, and the proportion of infected cells was found to be highest in nestin-positive cells at day 1 and day 2 p.i. (66.7% and 75%, respectively). Also, an increasing percentage of NG2⁺ cells expressed detectable levels of viral protein at day 1 and day 2 p.i. (40% and 70.5%, respectively). The least percentage of infected cells was observed in β -tubulin-positive cells (9.1% and 14.9% at day 1 and day 2 p.i., respectively) and GFAP-positive (GFAP⁺) cells (10.4% and 14.8% at day 1 and day 2 p.i., respectively) although the percentage of double-positive cells increased for both populations over the course of 2 days. These results suggest that CVB3 may be preferentially infecting progenitor cells which follow the oligodendrocyte pathway or, alternatively, that the differentiation pathway of infected stem cells may be preferentially shifted toward the oligodendrocyte lineage.

Virus replication and cell death in actin promoter-GFP neurospheres infected with DsRed-CVB3. We tested the ability of an additional recombinant coxsackievirus expressing DsRed

(DsRed-CVB3) to infect an independent isolation of neurospheres from actin promoter-GFP transgenic mice (Fig. 3). Also, the infection of actin promoter-GFP neurospheres (actin-GFP NPSCs) was carried out at two multiplicities of infection (0.1 and 10.0) and followed over 7 days in culture. The eventual fate of infected neural stem cells surviving acute infection and followed via the adoptive transfer into the CNS will be of great interest in future studies involving actin-GFP NPSCs. Actin-GFP NPSCs were highly susceptible to infection with DsRed-CVB3 and supported high levels of viral protein expression (DsRed) at an MOI of 0.1 (Fig. 3A to E) and an MOI of 10.0 (Fig. 3F to J). At an MOI of 0.1, viral infection of actin-GFP NPSCs led to CPE at day 3 p.i. (Fig. 3C and L, white arrows). We observed accelerated CPE at the higher MOI in cultures infected with DsRed-CVB3 at day 2 p.i. (Fig. 3G and K, white arrows). The high level of viral protein expression (red) in actin-GFP NPSCs was represented by single-channel images (Fig. 3G, inset, and M). In contrast, no CPE was observed in mock-infected actin-GFP NPSCs at any time point (Fig. 3N). By 7 days p.i., only cellular debris remained for the majority of actin-GFP NPSCs infected at either a high or low MOI (Fig. 3E and J). High viral titers were observed over 7 days in actin-GFP NPSCs infected at either a high or low MOI (Fig. 3O). As expected, viral titers rose more quickly in actin-GFP NPSCs infected at a higher MOI (Fig. 3O).

We inspected the degree of cell death in NPSCs following CVB3 infection over the course of 3 days p.i. (Fig. 4). NPSCs isolated from C57BL/6 mice were infected with eGFP-CVB3 at two multiplicities of infection (MOI of 0.1 or 10.0), and viral protein expression was followed by fluorescence microscopy (Fig. 4B and C). Alternatively, actin-GFP NPSCs were infected with DsRed-CVB3 at two multiplicities of infection (MOI of 0.1 and 10.0) and compared directly to neurospheres infected with eGFP-CVB3 (Fig. 4E and Fig. F). Both recombinant coxsackieviruses induced rapid CPE in NPSCs at the greater MOI (MOI of 10.0) by day 3 p.i. (Fig. 4C and F, white arrows). Conversely, the greater level of CPE observed at the higher MOI may be due to more cells infected initially and yet more readily detected by our trypan blue staining protocol. By trypan blue staining, the percentage of dead cells was determined over time for C57BL/6 NPSCs infected with eGFP-CVB3 (Fig. 4G) and for actin-GFP NPSCs infected with DsRed-CVB3 (Fig. 4H). An increase in the percentage of dead cells was observed over 3 days with both recombinant viruses. Also, NPSCs infected at a greater MOI (MOI of 10.0) showed accelerated and higher levels of cell death by trypan blue staining at day 3 p.i., a time point when CPE was observed in cultures by fluorescence microscopy. These results demonstrate that neurospheres from two independent isolation procedures were similarly susceptible to infection and CPE using two recombinant coxsackieviruses.

Reduced virus replication in NPSCs differentiated with FBS. We inspected in greater detail the susceptibility of differentiated cells derived from NPSCs to CVB3. NPSCs were cultured in the presence of FBS in order to increase surface attachment and induce differentiation (Fig. 5). Prior to the addition of FBS, NPSCs expressed high levels of nestin; however, in the presence of FBS, neurosphere aggregates began to attach to the surface, reduced their expression of nestin, and expressed high levels of neuronal class III β -tubulin (Fig. 5A).

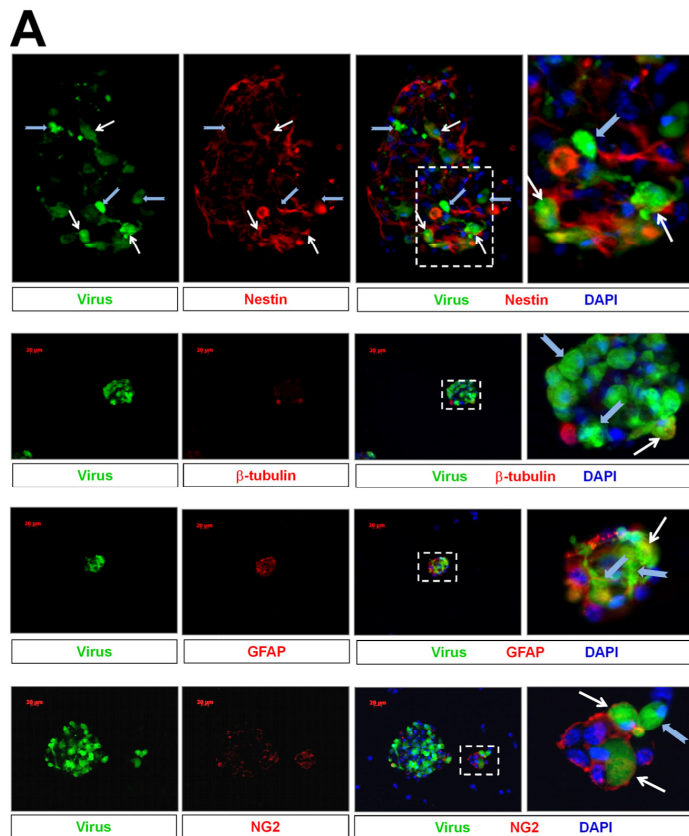


FIG. 2. CVB3 preferentially infected nestin-positive and NG2⁺ cells in neurospheres. NPSCs were infected with eGFP-CVB3, harvested at day 2 p.i., and stained for four cell markers (nestin, neuronal class III β -tubulin, GFAP, and NG2). Structured illumination immunofluorescence microscopy was carried out with a Zeiss Axio Observer with ApoTome Imaging System. (A) Both nestin-positive (white arrows) and nestin-negative cells (blue arrows) were susceptible to infection within neurosphere aggregates. Higher magnification of the boxed field showed both nestin-positive and nestin-negative infected cells (white arrows and blue arrows, respectively). Also, infected cells expressed cell lineage markers, including β -tubulin, GFAP, and NG2 cell markers. Higher magnification of the boxed field for each cell lineage marker showed both marker-positive (white arrows) and marker-negative (blue arrows) infected cells. (B) The percentage of infected cells expressing each marker at day 1 and day 2 p.i. was quantified and represented in a table form. Relatively high percentages of nestin-positive and NG2⁺ cells were infected with eGFP-CVB3 at day 1 and day 2 p.i. Lower percentages of infection were seen in cells expressing β -tubulin and GFAP at day 1 and day 2 p.i. Pos, positive; Neg, negative.

NPSCs were grown in the presence of FBS for 5 or 16 days and subsequently cultured with complete NPSC medium lacking FBS (Fig. 5B). NPSCs cultured in the presence of FBS for 16 days appeared to be in a more differentiated state and attached

more robustly to the culture surface than NPSCs cultured with FBS for only 5 days. Surprisingly, NPSCs differentiated for 5 days in the presence of FBS and replenished with NPSC medium lacking FBS showed a progressive return to spherical

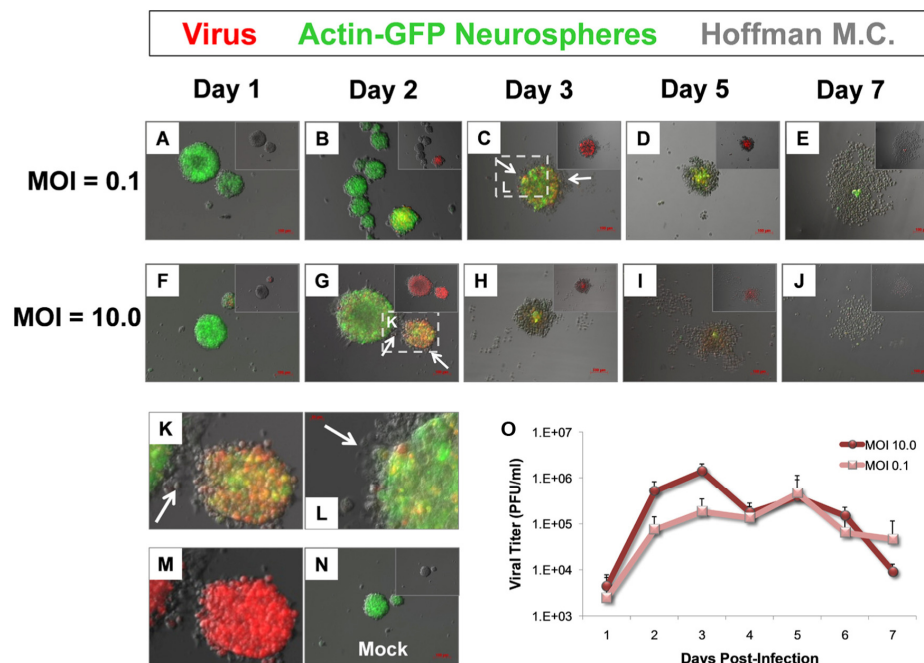


FIG. 3. Virus replication and cytopathic effects in neurospheres isolated from actin promoter-GFP transgenic mice and infected with DsRed-CVB3. Actin promoter-GFP (actin-GFP) NPSCs were isolated from the cortices of 1-day-old actin promoter-GFP transgenic mice, cultured to form neurosphere aggregates, and infected with DsRed-CVB3 (MOI of 0.1 and 10.0). Infected actin-GFP NPSCs were observed over 7 days by fluorescence microscopy, and viral titers were determined by plaque assay. (A to E) actin-GFP NPSCs infected at the lower MOI (MOI of 0.1) expressed high levels of virus protein in the majority of neurospheres (red in inset images without green signal) as soon as day 3 p.i. (white arrows). Cytopathic effects were seen at day 5 p.i. (F to J) Accelerated virus protein expression (red in inset images without green signal) at day 2 p.i. (white arrows) and CPE (at day 3 p.i.) were seen in actin-GFP NPSCs infected with the higher MOI (MOI of 10.0). (K and M) Higher magnification of panel G and a single-channel image (DsRed) revealed the relatively high level of virus protein expression and the presence of dying cells (white arrow) at day 2 p.i. in actin-GFP NPSCs infected at the higher MOI. (L) Similarly, higher magnification of panel C showed DsRed expression and the presence of dying cells (white arrow) at day 3 p.i. in actin-GFP NPSCs infected at the lower MOI. (N) No red signal or CPE was observed in mock-infected actin-GFP NPSCs. (O) Viral titers were determined for actin-GFP NPSCs infected at a low or high MOI.

neurosphere morphology at day 3 and day 7 posttreatment. Similarly, NPSCs differentiated for 16 days in the presence of FBS and replenished with NPSC medium lacking FBS also showed substantial morphological changes after 7 days in NPSC medium, suggesting “dedifferentiation” to neurosphere aggregates.

We inspected the expression levels of nestin, GFAP, neuronal class III β -tubulin (β -tubulin), and MBP in NPSCs differentiated for 5 or 16 days in the presence of FBS and replenished with complete NPSC medium lacking FBS or cultured in the presence of FBS (differentiation medium) (Fig. 5C). As expected, NPSCs treated for 5 or 16 days with FBS and cultured in differentiation medium expressed high levels of GFAP, β -tubulin, and MBP. Although nestin continued to be expressed in 5-day-differentiated cultures in differentiation medium, the cellular distribution of signal was altered (diffuse rather than filamentous). In contrast, 16-day-differentiated cultures in differentiation medium failed to express detectable levels of nestin, suggesting that these cells were well differentiated (Fig. 5C, white arrows). Paralleling the morphological results, 16-day-differentiated cultures in NPSC medium were induced to express moderate to high levels of nestin, suggest-

ing dedifferentiation, similar to what has been described previously (2, 21).

Five-day-differentiated or 16-day-differentiated NPSC cells were infected with eGFP-CVB3 and cultured either in NPSC medium or differentiation medium. Virus protein expression levels were evaluated by fluorescence microscopy up to 10 days following infection (Fig. 6). As determined previously, undifferentiated neurospheres cultured in NPSC medium and infected with eGFP-CVB3 supported robust levels of virus protein expression and CPE although surviving neurospheres were observed at day 7 and day 10 p.i. (Fig. 6, indicated by white arrows in the first column). The least amount of virus protein expression was observed in 16-day-differentiated NPSCs continuously cultured with FBS (Fig. 6, last column) although detectable levels of virus protein expression were eventually observed at day 10 p.i. within attached cells with stretched morphology. Also 5-day-differentiated NPSCs cultured continuously with FBS (Fig. 6, fourth column) expressed relatively low levels of virus protein. Little to no CPE was observed in either of these differentiated cultures continuously cultured with FBS.

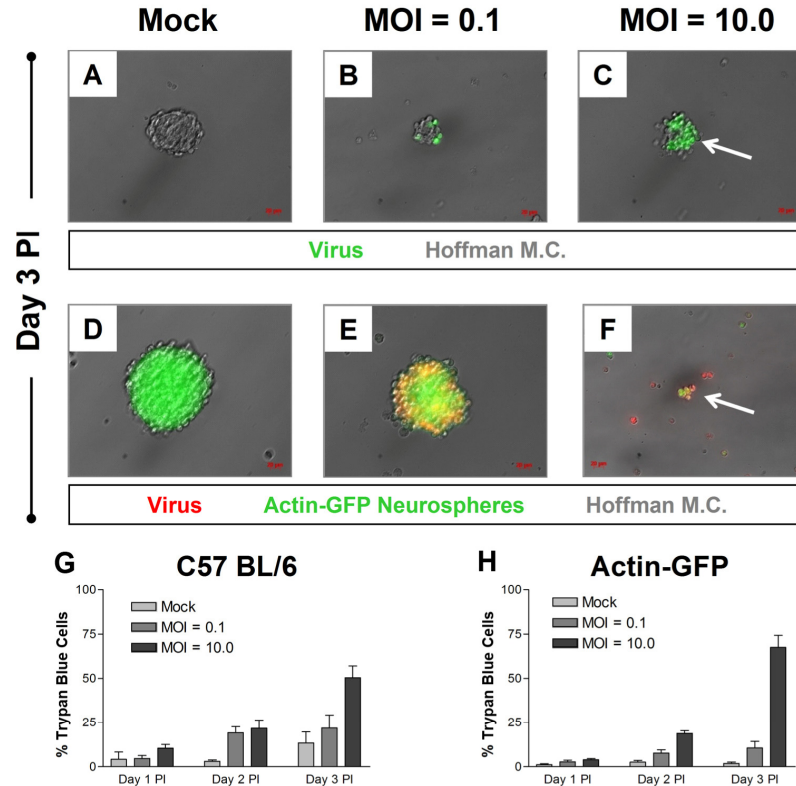


FIG. 4. Quantification of virus-induced cell death over time in neurospheres following infection with two recombinant coxsackieviruses. C57BL/6 NPSCs or actin-GFP NPSCs were mock-infected or infected with recombinant CVB3s (eGFP-CVB3 and DsRed-CVB3) at two MOI, observed by fluorescence microscopy, and stained for trypan blue at day 3 p.i. (A to C) Greater levels of virus protein (green) and accelerated CPE were observed in NPSCs infected with eGFP-CVB3 at the higher MOI (white arrow). (D to F) Similarly, greater levels of virus protein (red) and accelerated CPE were observed in actin-GFP NPSCs infected with DsRed-CVB3 at a higher MOI (white arrow). (G and H) The percentage of dead (trypan blue-positive) cells was determined in infected C57BL/6 and actin-GFP NPSCs using a hemacytometer. A greater percentage of dead cells was observed at each time point in both NPSC cultures infected at the higher MOI.

In 16-day-differentiated NPSC cultures replenished with NPSC medium, virus protein expression was observed at day 3 and continued to day 10 p.i. in the presence of low levels of CPE. In contrast to differentiated NPSCs continuously cultured with FBS, 5-day-differentiated NPSC cultures replenished with NPSC medium supported detectable virus protein expression levels very early (day 1 p.i.). At day 3 p.i., these cultures expressed high levels of virus protein in the presence of CPE (day 3 p.i.). The attached cells with a differentiated, stretched morphology in 5-day-differentiated cultures replenished with NPSC medium eventually gave rise to neurosphere aggregates with a spherical morphology, most likely reflecting dedifferentiation in these cells following the removal of FBS. The majority of 5-day-differentiated cultures replenished with NPSC medium underwent CPE by day 7 p.i.; however, surviving neurospheres were observed in these cultures (Fig. 6, indicated by a white arrow in the second column).

The morphology of many infected cells in 5-day-differentiated cultures replenished with NPSC medium suggested infec-

tion of immature neurons with long axonal extensions expressing high levels of virus protein (Fig. 7A, white arrows). Higher magnification showed the axonal processes of an infected cell extending and connecting to uninfected neighboring cells in these cultures (Fig. 7B and C, white arrows). In some cases, two infected neuronal cells with axonal processes made contact with uninfected cells separating both infected cells, suggesting preferential infection in cells with axonal morphology (Fig. 7D). Also, the presence of cellular blebbing was occasionally seen in adherent cells infected with CVB3, suggesting ongoing apoptosis in these cultures (Fig. 7E and F, blue arrows). Despite the high degree of CPE in the 5-day-differentiated cultures replenished with NPSC medium, surviving neurospheres could be observed at day 10 and day 37 p.i., suggesting dedifferentiation of the cultures and the presence of stem cells resistant to virus-mediated CPE and capable of renewing the neurosphere cultures (Fig. 7G and H, blue arrows). A closer inspection of neurospheres from day 37 p.i. indicated the continued expression of detectable levels of virus protein at this

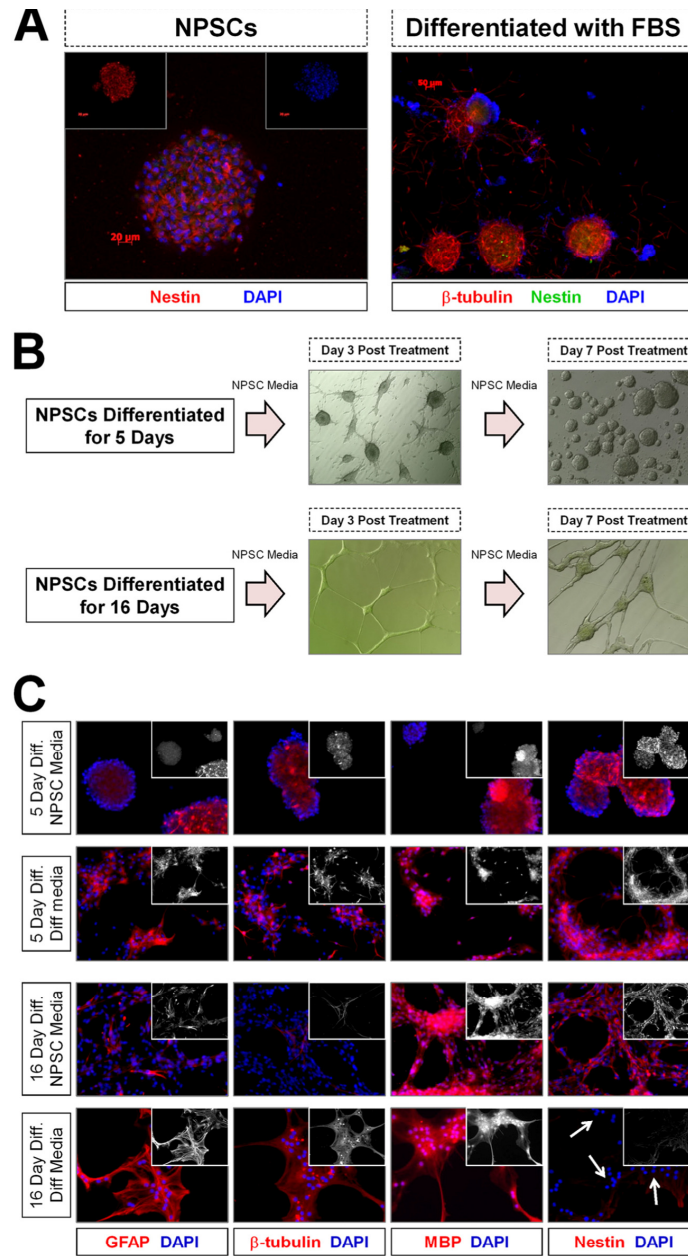


FIG. 5. Differentiation of NPSCs following treatment with fetal bovine serum. C57BL/6 NPSCs were evaluated for nestin and β -tubulin expression before and after FBS treatment. (A) NPSCs were grown in complete NPSC medium or, alternatively, were differentiated for 5 days in the presence of FBS. NPSCs or differentiated NPSCs were fixed with 4% paraformaldehyde and stained for nestin (red) or costained for both nestin (green) and β -tubulin (red). Cells were counterstained with DAPI (nuclear dye). (B) NPSCs differentiated for 5 or 16 days in the presence of FBS were placed into complete NPSC medium in the absence of FBS (NPSC medium) for an additional 3 or 7 days. Partial dedifferentiation was observed as soon as day 3 posttreatment for NPSCs differentiated for 5 days, with complete dedifferentiation at day 7 posttreatment. Also, partial dedifferentiation was observed by day 7 posttreatment for NPSCs differentiated for 16 days. (C) NPSCs were differentiated for 5 or 16 days and placed in NPSC medium or in the presence of FBS (Diff. Media) for 3 days, fixed with 2% paraformaldehyde, and immunostained for nestin, GFAP, neuronal class III β -tubulin (β -tubulin), or MBP. The 5-day- and 16-day-differentiated cells expressed high levels of nestin and reduced levels of GFAP and β -tubulin in the presence of complete NPSC medium, suggesting their dedifferentiation in these cultures. The 16-day-differentiated cells in differentiation medium expressed little or no nestin (white arrows), suggesting their differentiated status.

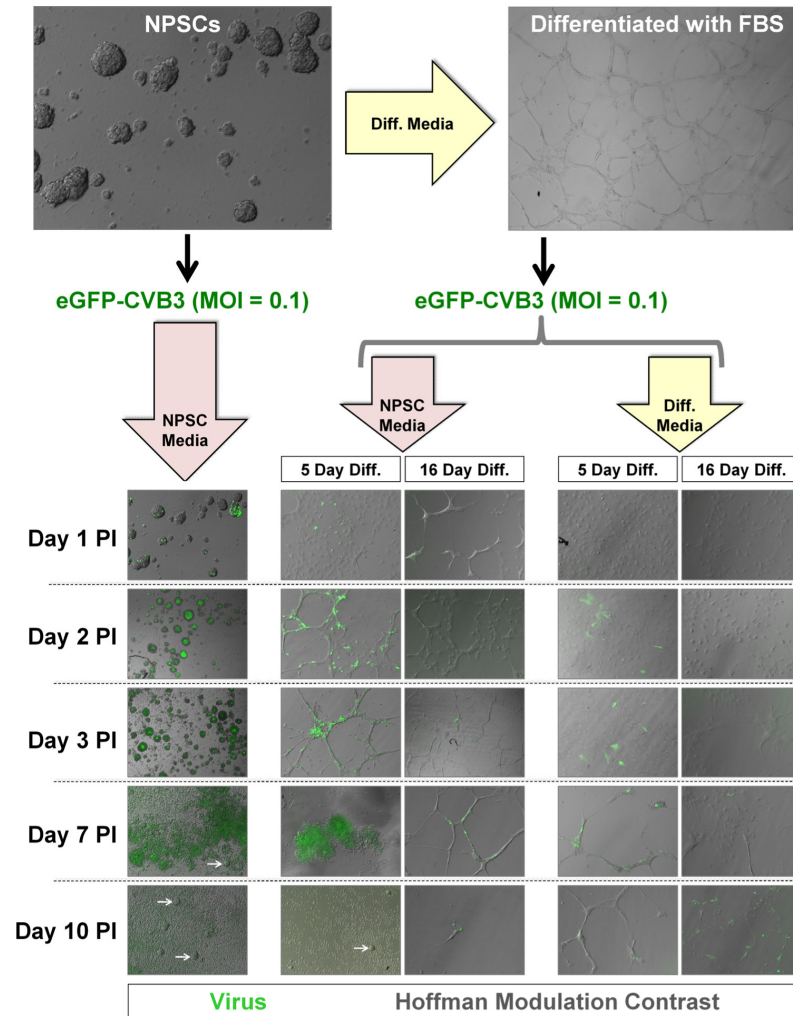


FIG. 6. Higher levels of viral protein expression and CPE were observed in NPSCs than in differentiated NPSCs. NPSCs or differentiated NPSCs (5 Day Diff. or 16 Day Diff.) were infected with eGFP-CVB3 (MOI of 0.1) and followed for virus protein expression for 10 days p.i. Following infection, NPSCs or differentiated NPSCs were cultured in complete NPSC medium lacking FBS (pink arrows). Alternatively, differentiated NPSCs infected with virus were cultured in medium containing FBS (yellow arrow). The greatest to least amount of virus protein expression and CPE were observed in the following order, from left to right: NPSCs in NPSC medium > 5-day-differentiated cells in NPSC medium > 16-day-differentiated cells in NPSC medium > 5-day-differentiated cells in differentiation medium > 16-day-differentiated cells in differentiation medium. Despite the relatively high level of CPE, surviving neurospheres continued to be observed in infected NPSCs in NPSC medium and in infected 5-day-differentiated cells in NPSC medium (white arrows).

extended time point (Fig. 7I and J, blue arrows), indicative of viral persistence in this long-term culture.

We measured viral titers in NPSCs differentiated with FBS and compared them to those of undifferentiated NPSCs up to 7 days p.i. Viral titers were evaluated in 5-day-differentiated cultures either continuously treated with FBS or replenished with NPSC medium (Fig. 7K). The highest viral titers (over 10^7 PFU/ml at day 2 p.i.) were observed in NPSCs cultured in

NPSCs medium over all time points. The 5-day-differentiated cultures replenished with NPSC medium supported lower levels of virus replication at all time points than infected NPSCs. The least amount of virus replication was observed in 5-day-differentiated cultures continuously treated with FBS. These results match the virus protein expression levels shown in Fig. 6 and suggest preferential CVB3 replication in NPSCs compared to that of their differentiated counterparts. A greater

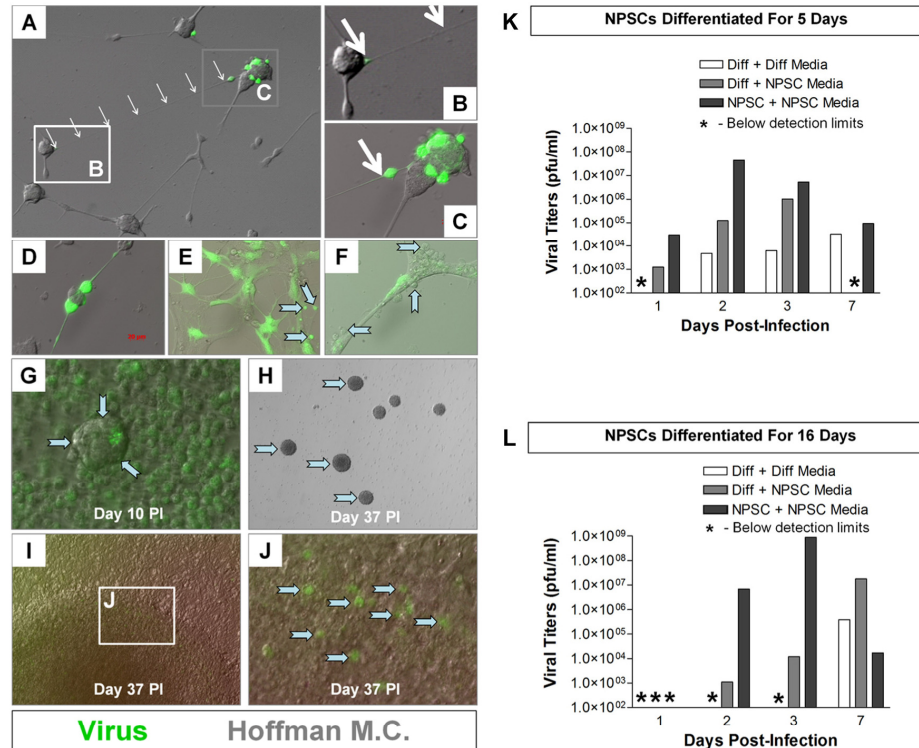
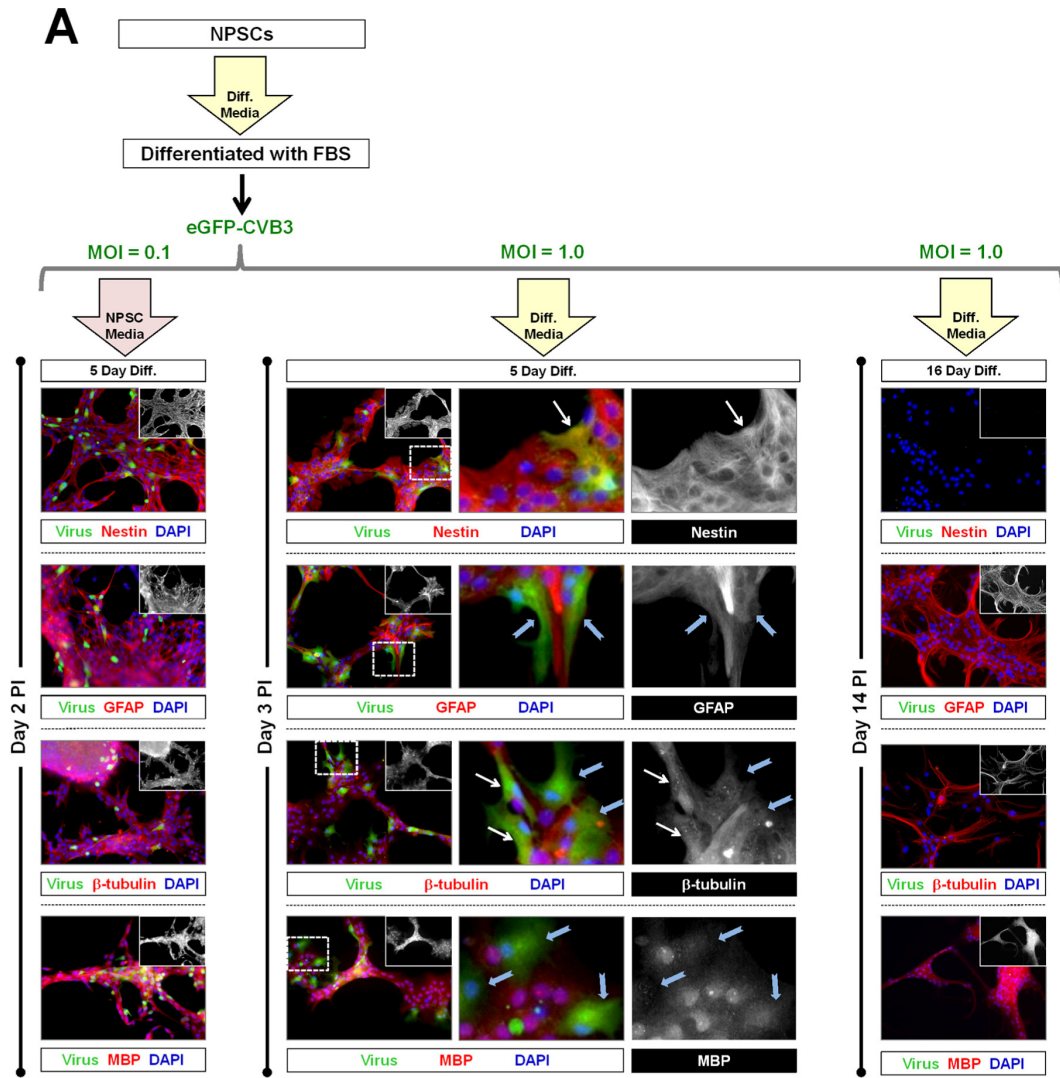


FIG. 7. Higher levels of viral titers observed in NPSCs than in differentiated NPSCs. NPSCs or differentiated NPSCs (5-day- or 16-day-differentiated [5 Day Diff. or 16 Day Diff.] cells) were infected with eGFP-CVB3 (MOI of 0.1) and observed by fluorescence microscopy over time. Also, viral titers were evaluated in these cultures up to 7 days p.i. Following infection, NPSCs or differentiated NPSCs were cultured in complete NPSC medium lacking FBS (NPSC medium). Alternatively, differentiated NPSCs infected with virus were cultured in medium containing FBS (Diff. Media). (A) Infected cells at day 3 p.i. with extended axonal processes were readily apparent in 5-day-differentiated cells in NPSC medium (white arrows). (B to D) Higher magnification of panel A showed the contact of infected cells with axonal processes to adjacent uninfected cells. (E and F) Cellular blebbing was seen in many differentiated NPSCs following infection, including 5-day-differentiated cells in NPSC medium at day 2 p.i. (blue arrows) and in 5-day-differentiated cells in differentiation medium at day 7 p.i. (blue arrows). Neurospheres surviving infection in NPSC medium were observed at day 10 p.i. (G) and day 37 p.i. (H). (I and J) Detectable levels of virus protein expression were observed in many surviving neurospheres at day 37 p.i. (blue arrows). (K) Viral titers were determined for NPSCs and compared to those of 5-day-differentiated NPSCs cultured in differentiation medium or NPSC medium. The cultures of 5-day-differentiated cells in differentiation medium produced the least amount of infectious virus over 7 days p.i. (L) Viral titers were determined for NPSCs and compared to those of 16-day-differentiated NPSCs cultured in differentiation medium or NPSC medium. Cultures of the 16-day-differentiated cells in differentiation medium failed to produce detectable levels of infectious virus for up to 3 days p.i.

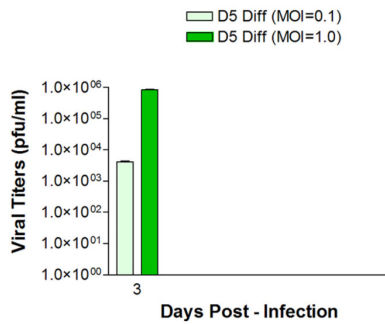
difference in viral replication was observed in 16-day-differentiated cultures continuously treated with FBS or replenished with NPSC medium (Fig. 7L). Viral titers were undetectable in 16-day-differentiated cultures continuously treated with FBS until day 7 p.i. Also, 16-day-differentiated cultures replenished with NPSC medium supported very low levels of infectious virus compared to levels in infected NPSCs. These results suggest that the longer NPSCs are differentiated in the presence of FBS (5 days versus 16 days), the less these cells support CVB3 replication.

We analyzed viral protein expression levels and viral titers in NPSCs during the course of well-defined differentiation to determine the susceptibility of the three neural cell lineages to CVB3 infection (Fig. 8). The 5-day- and 16-day-differentiated cultures were infected with eGFP-CVB3 at low (MOI of 0.1)

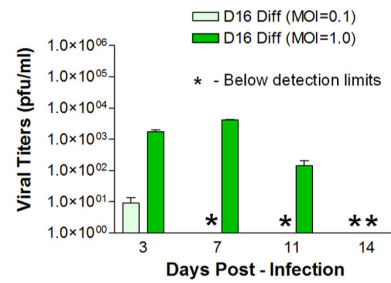
and high (MOI of 1.0) MOI. Differentiation medium was added back to infected cultures, and cells were harvested after a period of time (days 3 and 14 p.i.) based on the kinetics of viral protein expression, as determined for the experiment shown in Fig. 6. We evaluated infection by eGFP expression and the degree of NPSC differentiation utilizing nestin and three differentiation markers (GFAP, β -tubulin, and MBP) (Fig. 8A). For comparison, cells from 5-day-differentiated cultures were infected with eGFP-CVB3 at a low MOI (MOI of 0.1), cultured in the presence of NPSC medium, and stained for nestin or differentiation markers at day 2 p.i. As shown in Fig. 6, 5-day-differentiated cultures in NPSC medium showed relatively high levels of viral protein expression at day 2 p.i. Furthermore, these cultures expressed high levels of nestin as well as the three differentiation markers, suggesting that these



B NPSCs Differentiated For 5 Days + Diff Media



C NPSCs Differentiated For 16 Days + Diff Media



cells were not fully differentiated. The 5-day-differentiated cultures in differentiation medium showed less viral protein expression and more diffuse nestin staining. Higher-magnification images of hatched white boxes for 5-day-differentiated cultures in differentiation medium demonstrated colocalization of viral protein expression and either nestin-positive or β -tubulin-positive cells (Fig. 8A, white arrows). Also, we observed a lack of viral protein expression in 5-day-differentiated cultures in differentiation medium expressing high levels of GFAP or MBP (Fig. 8A, blue arrows). For the single time point examined before harvest (day 3 p.i.), low to moderate levels of viral titers were observed in cultures of 5-day-differentiated cells in differentiation medium (Fig. 8B), depending upon the initial viral inoculum. In contrast, 16-day-differentiated cultures in differentiation medium showed no viral protein expression at 14 days p.i., suggesting again that well-differentiated cells did not support CVB3 replication (as shown in Fig. 6). Furthermore, these cultures lacked nestin expression and expressed moderate to high levels of GFAP, β -tubulin, and MBP, which suggested their highly differentiated status. Also, low viral titers were observed until day 11 p.i. for cultures given a higher initial inoculum (MOI of 1.0) (Fig. 8C). These results suggest that the highly differentiated 16-day-differentiated cultures supported significantly less CVB3 replication than the 5-day-differentiated cultures.

Infection of NPSCs and alteration of the differentiation pathway. We inspected the ability of infected neurospheres to differentiate into the three downstream cell lineages following treatment with FBS. C57BL/6 NPSCs were mock infected or infected with eGFP-CVB3 (MOI of 0.1). In parallel, actin-GFP NPSCs were mock infected or infected with DsRed-CVB3 (MOI of 0.1). After 2 days p.i., the NPSC cultures were treated with FBS (differentiation medium) for an additional 3 days (Fig. 9). Infected NPSC cultures were observed for virus protein expression by fluorescence microscopy before (day 2 p.i.) and after (day 3 p.i.) FBS treatment. Intriguingly, infected NPSCs appeared less attached or flattened in the presence of FBS at day 3 p.i. than mock-infected NPSCs. By fluorescence microscopy, infected NPSCs were shown to express detectable levels of viral protein at day 2 and day 3 p.i. After 3 days of FBS treatment (day 5 p.i.), infected NPSC cultures were fixed and stained for three neural cell lineage markers (GFAP, β -tubulin, and Olig2). Olig2 expression has been utilized previously in other studies to identify cells in the oligodendrocyte lineage (5). The amount of fluorescent signal for each marker was

quantified by ImageJ analysis, and the relative fluorescence was calculated as a percentage of the total number of cells for each stain. For C57BL/6 NPSCs, DAPI was utilized to calculate relative fluorescence values. For actin-GFP NPSCs, GFP signal was utilized to calculate relative fluorescence values.

We compared the relative fluorescence value for each marker between mock-infected and infected NPSCs differentiated with FBS. For C57BL/6 NPSCs, no statistically significant changes were observed in the relative fluorescence levels for all three markers following infection. In contrast, a statistically significant increase in relative β -tubulin levels ($P = 0.02$, Student's t test) was observed in actin-GFP NPSCs following infection, compared to mock-infected control cultures. Also, the percentage of GFAP⁺ cells was reduced in actin-GFP NPSCs following infection although not by a statistically significant level ($P = 0.06$, Student's t test). No statistically significant change was observed in the relative fluorescence levels of Olig2 within actin-GFP NPSCs following infection. A direct comparison of actin-GFP and C57BL/6 NPSCs was problematic due to the methodology applied in obtaining the ratios of the representative markers. For example, the downstream cell lineages for actin-GFP NPSCs were determined based on cytoplasmic GFP expression, compared to nuclear staining (DAPI) for C57BL/6 NPSCs. Alterations in the relative population of downstream cell lineages following differentiation of infected NPSCs may be dependent upon isolation differences during stem cell harvesting, isolation, and cell culture, as well as on potential stochastic differences inherent during infection and after the FBS treatment. Also, infected NPSCs were reduced in number at 5 days p.i. compared to the number of mock-infected NPSCs, suggesting either CPE or a reduction in cellular proliferation during the differentiation procedure. Each downstream progenitor cell lineage may be differentially susceptible to CVB3-induced CPE. These results indicate that CVB3 may bias neural stem cell differentiation by increasing the percentage of immature β -tubulin-positive neuroblasts.

DISCUSSION

The ability of CVB3 to target neural stem cells in the neonatal CNS raises many questions regarding stem cell function and normal brain development within the surviving host. We previously established a murine model for neonatal coxsackievirus B3 (CVB3) infection, and proliferating nestin-positive progenitor cells were identified as primary targets for early

FIG. 8. Reduction in CVB3 replication and viral protein expression in highly differentiated NPSCs expressing neural differentiation markers and lacking nestin expression. C57BL/6 NPSCs were differentiated in the presence of FBS for 5 or 16 days and infected with eGFP-CVB3 (MOI of 0.1 or 1.0). After infection, differentiated NPSCs were cultured in NPSC medium or differentiation medium. Also, viral titers were evaluated in these cultures up to 14 days p.i. (A) After day 2, 3, or 14 p.i., cultures were stained for nestin and three downstream cell lineage markers (GFAP, β -tubulin, and MBP). Moderate to high levels of all three cell lineage markers were observed in all cultures. Single-channel black and white images for insets show the expression level for each cell lineage marker. Also, little to no nestin expression was observed in cultures of 16-day-differentiated cells in differentiation medium, indicating well-defined differentiation of these cells. The highest level of viral protein expression was observed in 5-day-differentiated cells in NPSC medium. Detectable levels of viral protein expression were seen in 5-day-differentiated cells in differentiation medium. Higher magnification of boxed areas showed colocalization of viral protein expression in cells with moderate levels of diffuse nestin and in some β -tubulin-positive cells (white arrows). In contrast, a lack of colocalization was observed for GFAP and MBP staining (blue arrows). Little to no viral protein expression was observed in 16-day-differentiated cells in differentiation medium. (B) Cultures of 5-day-differentiated cells in differentiation medium supported low to moderate levels of viral replication depending upon the MOI utilized at the single time point analyzed. (C) In contrast, cultures of 16-day-differentiated cells in differentiation medium supported lower levels of viral replication at either MOI utilized, and these levels dropped to below detection limits at day 14 p.i.

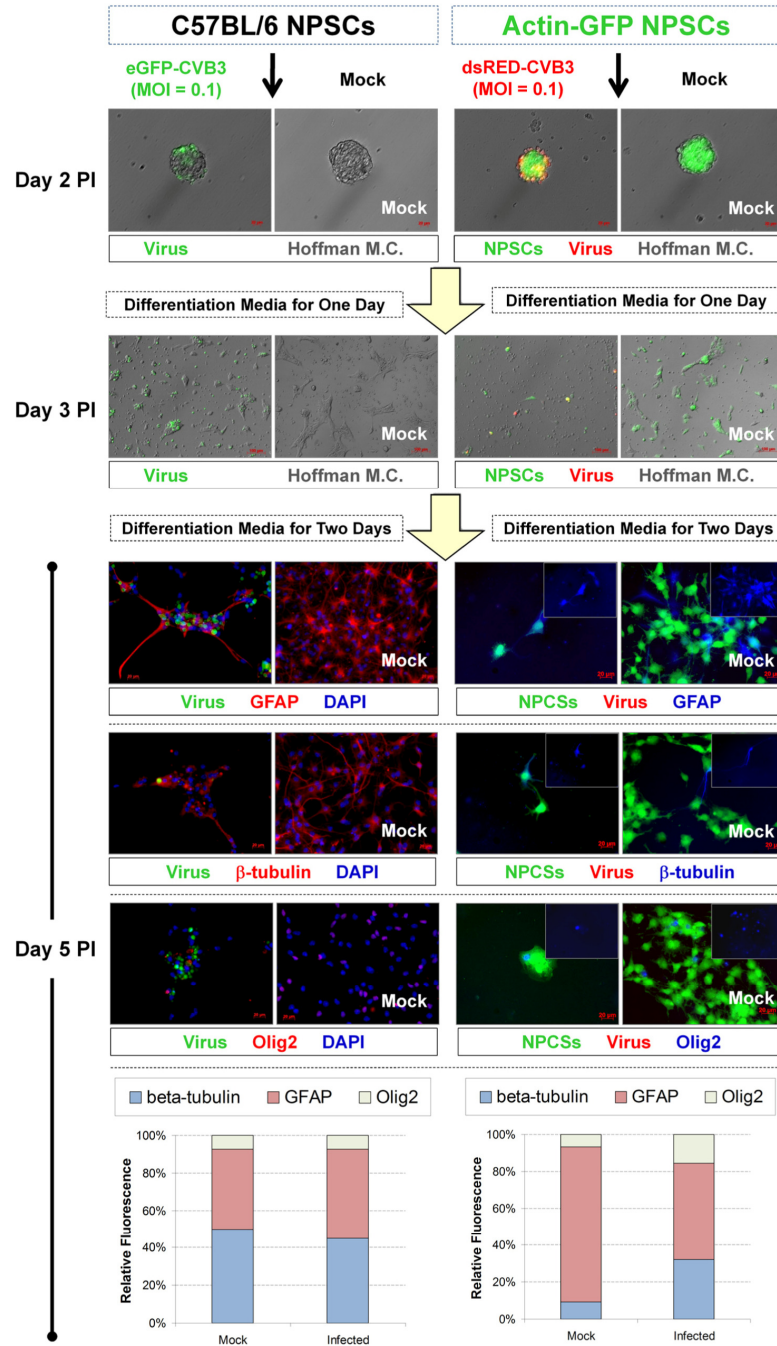


FIG. 9. CVB3 infection and alteration of the NPC differentiation pathway. C57BL/6 NPSCs were infected with eGFP-CVB3 (MOI of 0.1). In parallel, actin-GFP NPSCs were infected with DsRed-CVB3 (MOI of 0.1). After day 2 p.i., infected NPSCs were differentiated in the presence of FBS for 3 days and harvested for immunofluorescence staining. Infected NPSCs were stained for three downstream cell lineage markers (GFAP, β -tubulin, and Olig2). For C57BL/6 NPSCs, the relative fluorescence of each marker following infection was calculated and normalized to DAPI signal using the ImageJ program. For actin-GFP NPSCs, the relative fluorescence of each marker following infection was calculated and normalized to GFP signal using the ImageJ software (inset images are shown for a single blue channel).

infection (15, 16). In addition, CVB3 established a persistent infection in mice surviving a neonatal infection, characterized by the continued detection of viral RNA by reverse transcription-PCR (RT-PCR), along with long-lasting lesions and chronic signs of inflammation and microgliosis up to 9 months following infection (17).

To more easily discriminate the effects of CVB3 infection on neural stem cell function and differentiation, we thought it imperative to duplicate any findings observed *in vivo*, in parallel with neural stem cells grown in culture. Given that CVB3 is a cytolitic virus, we wished to determine if neural stem cells were susceptible to infection and exhibited cytopathic effects (CPE) following infection. Therefore, we inspected the susceptibility of neurospheres or NPSCs grown in culture to CVB3 infection. Also, we wished to determine whether CVB3 infection might alter the differentiation path of NPSCs. The benefits of using NPSCs grown in culture include the ability of using a relatively pure population of target cells, controlling the multiplicities of infection (MOI) at the onset of infection, and discriminating the initial time of infection during time course assays, factors difficult to control *in vivo*.

Despite the benefits of examining infected NPSCs grown in culture, we realized that neurosphere aggregates form relatively complex mixtures of both stem and progenitor cells expressing a variety of cell markers. In fact, infection of cultured primary NPSCs may be a particularly intriguing and dynamic model of CVB3 infection, given the complex mixture of cell types with potentially differential antiviral responses induced during infection. In this regard, little is known about the ability of stem cells to induce and respond to interferon following infection. We expect that the interferon response within our primary stem cell culture system may be responsible for the observed carrier state infection observed in NPSCs, which may ultimately parallel the establishment of viral persistence within the CNS. Also, our results suggest that susceptibility to infection may reflect the heterogeneity of progenitor cells in neurosphere aggregates; each progenitor cell type may have a slightly different susceptibility to coxsackievirus infection and CPE depending upon the progenitor type or stage of differentiation. Also, some adherent cells with a flattened, stretched morphology remained in culture and appeared to be resistant to infection, as judged by viral protein expression. Adding to the complexity, susceptibility to infection may be altered as progenitor cells differentiate into the downstream lineages. A recent publication suggests preferential coxsackievirus replication within immature neurons expressing relatively high levels of coxsackievirus-adenovirus receptor (CAR) compared to their fully differentiated counterparts (1).

Two independent neurosphere isolations from C57BL/6 mice and actin promoter-GFP transgenic mice generated NPSCs which were shown to be highly susceptible to CVB3 infection. Also, virus-mediated cell death in NPSCs following CVB3 infection was observed by trypan blue staining. The ability of CVB3 to infect neonatal NPSCs and induce CPE may shed light on potential CNS development defects following neonatal infection. In addition, possible long-term consequences may be detected in the surviving host, given the substantial number of functional neural stem cells in the adult CNS. However, the capacity of adult NPSCs to support CVB3 infection remains to be determined. Also, distinct populations of NPSCs from dif-

ferent regions of the murine CNS may be differentially susceptible to infection. Our previous published *in vivo* data suggest that NPSCs in the subventricular zone (SVZ) and hippocampus are both susceptible to infection (15, 16). However, the degree of susceptibility and the ability to establish a persistent infection may be reflected by the particular anatomical location of isolated NPSCs.

Despite clear CPE in infected NPSCs following CVB3 infection, surviving neurospheres were observed in cultures replenished with complete NPSC medium. These results suggest that NPSCs may mount functional antiviral responses, perhaps by inducing and/or responding to interferon following infection (38). In this respect, very little is known regarding the ability of stem cells to induce innate immune responses in response to pathogens. It remains unknown if prolonged antiviral responses or chronic interferon may alter or compromise normal neural stem cell function and the proper generation of downstream cell lineages. The possibility remains that a particular nestin-positive stem cell population may exist within the neurosphere aggregate which is both resistant to CVB3 infection and yet can reestablish the NPSC culture. Nestin-positive progenitor cells have been previously shown to be responsible for neurosphere regeneration in culture (32).

Our results also indicate the ability of CVB3 to persist in NPSCs grown in culture. This finding may be particularly relevant, given our recent work indicating the ability CVB3 to persist in the adult CNS following neonatal infection (17). We speculate that neural stem cells in the adult CNS may be a site of viral persistence and that CVB3 may undergo active viral replication during stem cell proliferation and division. Conversely, we expect that viral replication and viral protein expression may become substantially reduced within quiescent primary stem cells, as opposed to rapidly proliferating progenitor cells (14). As we have shown, acute CVB3 replication may harm NPSCs in culture, and this injurious effect on stem cell function may occur *in vivo* as well. In fact, viral RNA by itself may be damaging to normal brain function, as shown for myocytes in culture (39). Also, the expression of viral proteins during CVB3 replication may activate the host immune response, which may compromise neural stem cell function.

We evaluated the ability of CVB3 to target neuronal, oligodendrocyte, and astrocyte precursor cells through immunofluorescence colocalization studies using antibodies against neuronal class III β -tubulin (immature neurons), NG2/Olig2 (oligodendrocyte precursor markers), myelin basic protein ([MBP] mature oligodendrocyte marker), and GFAP (glial/astrocyte precursor marker) (13, 22, 33). Oligodendrocytes are critical cells in the CNS and provide axons with insulating myelin sheaths. Astrocytes, once considered merely support cells in the brain, are now thought to play a more active role by affecting the activity of neurons (22). CVB3 appeared to preferentially target nestin-positive and NG2⁺ cells for infection. It is not clear from our studies which cells might preferentially undergo CPE following infection. However, any reduction in nestin-positive and NG2⁺ progenitor cells following infection/CPE might alter the percentage of downstream oligodendrocyte precursor cells and potentially impact normal myelination in the developing CNS. Also, well-differentiated cultures expressing high levels of GFAP, β -tubulin, or MBP and lacking nestin expression failed to support

CVB3 infection, as determined by viral protein expression or by viral titers. Of note, differentiation of infected actin-GFP NPSCs resulted in an increase of neuronal class III β -tubulin-expressing cells compared to levels in mock-infected controls. However, no statistically significant changes within infected C57BL/6 NPSCs were observed following their differentiation.

In summary, we propose that CVB3 may target neural stem cells in culture, induce CPE preferentially in progenitor cells compared to their differentiated counterparts, and may persist in neurosphere cultures replenished with fresh complete NPSC medium. Taken together, our results suggest that virus protein expression was robust in undifferentiated neurospheres, yet differentiated cells adjacent to infected neurospheres appeared to be refractory to infection. Future studies will evaluate neural stem cell function and potential genomic alterations in the CVB3 genome within persistently infected NPSC cultures. Also, actin-GFP NPSCs will assist us with future experiments designed to track previously infected neural stem cells adoptively transferred within a new host. We will test the ability of NPSCs surviving infection to continue functioning normally, give rise to the three downstream neural cell lineages, and migrate correctly within an *in vivo* environment.

ACKNOWLEDGMENTS

This work was supported by National Institutes of Health awards R01 NS054108 (to R.F.), R01 AI042314, and HL093177 (to J.L.W.), a National Institutes of Mental Health Minority Research Infrastructure Support Program R24 Faculty Fellow Award MH065515 (to R.F.), an SDSU University Grants Program Award (to R.F.), and two Achievement Rewards for College Scientists Foundation Scholarships (to G.T. and J.M.T.-G.).

We declare that we have no conflicts of interest.

REFERENCES

- Ahn, J., et al. 2008. Primary neurons become less susceptible to coxsackievirus B5 following maturation: the correlation with the decreased level of CAR expression on cell surface. *J. Med. Virol.* **80**:434–440.
- Alexanian, A. R., and S. N. Kurpad. 2005. Quiescent neural cells regain multipotent stem cell characteristics influenced by adult neural stem cells in co-culture. *Exp. Neurol.* **191**:193–197.
- Alvarez-Buylla, A., B. Seri, and F. Doetsch. 2002. Identification of neural stem cells in the adult vertebrate brain. *Brain Res. Bull.* **57**:751–758.
- Baracska, K. L., G. J. Kidd, R. H. Miller, and B. D. Trapp. 2007. NG2-positive cells generate A2B5-positive oligodendrocyte precursor cells. *Glia* **55**:1001–1010.
- Chandran, S., et al. 2003. FGF-dependent generation of oligodendrocytes by a hedgehog-independent pathway. *Development* **130**:6599–6609.
- Chapman, N. M., and K. S. Kim. 2008. Persistent coxsackievirus infection: enterovirus persistence in chronic myocarditis and dilated cardiomyopathy. *Curr. Top. Microbiol. Immunol.* **323**:275–292.
- Cheeran, M. C., et al. 2005. Neural precursor cell susceptibility to human cytomegalovirus diverges along glial or neuronal differentiation pathways. *J. Neurosci. Res.* **82**:839–850.
- Crocker, S. J., R. F. Frausto, J. L. Whitton, and R. Milner. 2008. A novel method to establish microglia-free astrocyte cultures: comparison of matrix metalloproteinase expression profiles in pure cultures of astrocytes and microglia. *Glia* **56**:1187–1198.
- Das, S., and A. Basu. 2008. Japanese encephalitis virus infects neural progenitor cells and decreases their proliferation. *J. Neurochem.* **106**:1624–1636.
- Das, S., S. Chakraborty, and A. Basu. 2010. Critical role of lipid rafts in virus entry and activation of phosphoinositide 3' kinase/Akt signaling during early stages of Japanese encephalitis virus infection in neural stem/progenitor cells. *J. Neurochem.* **115**:537–549.
- Das, S., D. Ghosh, and A. Basu. 2009. Japanese encephalitis virus induces immuno-competency in neural stem/progenitor cells. *PLoS One* **4**:e8134.
- David, P., et al. 1993. MRI of acute disseminated encephalomyelitis after coxsackie B infection. *J. Neuroradiol.* **20**:258–265.
- Dawson, M. R., A. Polito, J. M. Levine, and R. Reynolds. 2003. NG2-expressing glial progenitor cells: an abundant and widespread population of cycling cells in the adult rat CNS. *Mol. Cell Neurosci.* **24**:476–488.
- Feuer, R., I. Mena, R. Pagarigan, M. K. Slifka, and J. L. Whitton. 2002. Cell cycle status affects coxsackievirus replication, persistence, and reactivation *in vitro*. *J. Virol.* **76**:4430–4440.
- Feuer, R., et al. 2003. Coxsackievirus B3 and the neonatal CNS: the roles of stem cells, developing neurons, and apoptosis in infection, viral dissemination, and disease. *Am. J. Pathol.* **163**:1379–1393.
- Feuer, R., et al. 2005. Coxsackievirus targets proliferating neuronal progenitor cells in the neonatal CNS. *J. Neurosci.* **25**:2434–2444.
- Feuer, R., et al. 2009. Viral persistence and chronic immunopathology in the adult central nervous system following coxsackievirus infection during the neonatal period. *J. Virol.* **83**:9356–9369.
- Frisk, G., M. A. Lindberg, and H. Diderholm. 1999. Persistence of coxsackievirus B4 infection in rhabdomyosarcoma cells for 30 months. *Brief reports. Arch. Virol.* **144**:2239–2245.
- Gage, F. H. 2000. Mammalian neural stem cells. *Science* **287**:1433–1438.
- Graber, D., C. Fossoud, E. Grouteau, C. Gayet-Mengelle, and J. P. Carriere. 1994. Acute transverse myelitis and coxsackie A9 virus infection. *Pediatr. Infect. Dis. J.* **13**:777.
- Hack, M. A., M. Sugimori, C. Lundberg, M. Nakafuku, and M. Gotz. 2004. Regionalization and fate specification in neurospheres: the role of Olig2 and Pax6. *Mol. Cell Neurosci.* **25**:664–678.
- Horner, P. J., and T. D. Palmer. 2003. New roles for astrocytes: the nightlife of an "astrocyte." *La vida local! Trends Neurosci.* **26**:597–603.
- Kim, K. S., N. M. Chapman, and S. Tracy. 2008. Replication of coxsackievirus B3 in primary cell cultures generates novel viral genome deletions. *J. Virol.* **82**:2033–2037.
- Kim, K. S., et al. 2005. 5'-Terminal deletions occur in coxsackievirus B3 during replication in murine hearts and cardiac myocyte cultures and correlate with encapsidation of negative-strand viral RNA. *J. Virol.* **79**:7024–7041.
- Klingel, K., et al. 1992. Ongoing enterovirus-induced myocarditis is associated with persistent heart muscle infection: quantitative analysis of virus replication, tissue damage, and inflammation. *Proc. Natl. Acad. Sci. U. S. A.* **89**:314–318.
- Luo, M. H., et al. 2010. Human cytomegalovirus infection causes premature and abnormal differentiation of human neural progenitor cells. *J. Virol.* **84**:3528–3541.
- Luo, M. H., P. H. Schwartz, and E. A. Fortunato. 2008. Neonatal neural progenitor cells and their neuronal and glial cell derivatives are fully permissive for human cytomegalovirus infection. *J. Virol.* **82**:9994–10007.
- Mokry, J., J. Karbanova, and S. Filip. 2005. Differentiation potential of murine neural stem cells *in vitro* and after transplantation. *Transplant. Proc.* **37**:268–272.
- Odeberg, J., et al. 2006. Human cytomegalovirus inhibits neuronal differentiation and induces apoptosis in human neural precursor cells. *J. Virol.* **80**:8929–8939.
- Odeberg, J., et al. 2007. Late human cytomegalovirus (HCMV) proteins inhibit differentiation of human neural precursor cells into astrocytes. *J. Neurosci. Res.* **85**:583–593.
- Okamoto, S., et al. 2007. HIV/gp120 decreases adult neural progenitor cell proliferation via checkpoint kinase-mediated cell-cycle withdrawal and G₁ arrest. *Cell Stem Cell* **1**:230–236.
- Park, J. H., et al. 2007. Genetic modification does not affect the stemness of neural stem cells in nestin promoter-GFP transgenic mice. *Neurosci. Lett.* **421**:185–190.
- Rogister, B., T. Ben-Hur, and M. Dubois-Dalcq. 1999. From neural stem cells to myelinating oligodendrocytes. *Mol. Cell Neurosci.* **14**:287–300.
- Rothenaigler, I., et al. 2007. Long-term HIV-1 infection of neural progenitor populations. *AIDS* **21**:2271–2281.
- Sawyer, M. H. 2002. Enterovirus infections: diagnosis and treatment. *Semin. Pediatr. Infect. Dis.* **13**:40–47.
- Sharma, N., et al. 2009. Functional role of the 5' terminal cloverleaf in coxsackievirus RNA replication. *Virology* **393**:238–249.
- Tabor-Godwin, J. M., et al. 2010. A novel population of myeloid cells responding to coxsackievirus infection assists in the dissemination of virus within the neonatal CNS. *J. Neurosci.* **30**:8676–8691.
- Wellen, J., J. Walter, P. Jangouk, H. P. Hartung, and M. Dihn. 2009. Neural precursor cells as a novel target for interferon-beta. *Neuropharmacology* **56**:386–398.
- Wessely, R., A. Henke, R. Zell, R. Kandolf, and K. U. Knowlton. 1998. Low-level expression of a mutant coxsackieviral cDNA induces a myocytopathic effect in culture: an approach to the study of enteroviral persistence in cardiac myocytes. *Circulation* **98**:450–457.

Acknowledgements

Chapter 1, in full, is a reprint of the material as it appears in Journal of Virology 2011. Tsueng, G; Tabor-Godwin, JM; Gopal, A; Ruller, CM; Deline, S; An, N; Frausto, RF; Milner, R; Crocker, SJ; Whitton, JL; Feuer, R.. The dissertation author was the primary investigator and author of this paper.

**CHAPTER II: Coxsackievirus B3 Hypervirulence Followed by Virus Attenuation
Upon Establishment of Persistent Infection in Neural Progenitor and Stem Cells**

Introduction

Coxsackievirus targets neural stem and progenitor cells (NPSCs) during infections of the central nervous system (CNS), increasing the susceptibility of younger hosts over older ones (Feuer et al., 2005). The ability of this enterovirus to persist and cause disease in the central nervous system may have profound developmental effects, making it a subject of significant research interest. Previous *in vivo* experiments in neonatal mouse models of infection with coxsackievirus B3 (CVB3) demonstrated that the viral genome could persist in the central nervous system for at least 90 days post-infection, even though infectious virus was not detectable by plaque assay (Feuer et al., 2009). The persistence of the viral genome in spite of the lack of infectious particles suggests that the virus might be persisting at a low-level, attenuated form.

The mechanisms of Coxsackievirus attenuation and persistence have been of interest due to its implications for chronic heart inflammation, and much of the work investigating alterations in the coxsackievirus genomes following infection and persistence has come from studies of cardiovirulent Coxsackievirus. Deletions in cardiovirulent strains of Coxsackievirus have previously been observed to attenuate the virus in primary cell culture infection experiments (Kim et al., 2008). Mutations in the Kozak's sequence of CVB3 has been found to render the virus noninfectious (Harkins et al., 2005), and mutations in the VP2 have been found to attenuate cardiovirulent CVB3 (Stadnick et al., 2004) (Knowlton et al., 1996). The persistence of

Coxsackievirus in the CNS is likely to be accompanied by attenuating mutations the genomes of the persisting virus.

In order to better understand the how the virus might be changing during persistent infection *in vivo*, we performed infection experiments on murine NPSCs *in vitro*. Murine NPSCs were previously found to be highly susceptible to CVB3 infection (Tsueng et al., 2011), and can serve as a useful model for viral persistence *in vitro*. Infecting with a recombinant CVB3 expressing enhanced GFP, allows us to examine the progression of infection under fluorescent microscopy. Utilizing this model of infection enables us to visualize the effects of CVB3 on the resident stem cell population of the central nervous system, and how persistence of CVB3 in a dynamic cell population can, in turn, affect the selection and persistence of the CVB3 quasispecies population.

Materials & Methods

Isolation and production of a recombinant coxsackievirus. The generation of a recombinant coxsackievirus expressing eGFP has been described previously⁵. Briefly, the CVB3 infectious clone (pH3) (obtained from Dr. Kirk Knowlton at University of California at San Diego) was engineered to contain a unique *SfiI* site which facilitates the insertion of any foreign sequence into the CVB3 genome. The generation of recombinant coxsackievirus expressing the enhanced green fluorescent protein (eGFP-CVB3) has been described previously (Feuer et al., 2002). Virus stocks were grown on HeLa RW cells. Virus titrations were carried out as described previously (Feuer et al., 2002a). Viral stocks were prepared on HeLa RW cells maintained in Dulbecco's modified Eagle's medium (DMEM; Invitrogen, Gaithersburg, MD) supplemented with 10% fetal bovine serum. Viral stocks were diluted in DMEM before inoculation.

Isolation, culture, and infection of neurospheres. Mouse experimentation conformed to the requirements of the San Diego State University Animal Research Committee and the National Institutes of Health. BALB/c and C57BL/6 mice were obtained from the Scripps Research Institute animal facilities or Harlan Sprague Dawley (Harlan Laboratories, San Diego CA). Breeding pairs were checked every day. C57 mouse neural progenitor and stem cells (NPSCs) were isolated as previously described, vigorously triturated and resuspended in culture medium to a concentration of 10^5 cells/mL in a T-

25 flask (BD falcon). The NPSC culture medium consisted of DMEM/F12 supplemented with 2% B27 (Invitrogen), 20ng/mL EGF (Invitrogen), 20ng/mL bFGF (Preprotech), 5µg/mL Heparin (Sigma), and 0.5% pen/strep. The complete culture was inoculated with eGFP-CVB3 at an MOI = 1.0, and examined over time using fluorescence microscopy. After day nine post-infection (PI), surviving NPSCs were pooled, centrifuged (4°C, 1200 rpm, 3min), washed once with 1x Phosphate Buffered Saline (PBS), centrifuged again, and resuspended in NPSC culture medium to allow the re-establishment of surviving NPSCs. The infection experiment was continued until 51 days PI.

Cell counts. At each time point, 300µL aliquots of the infected NPSC cultures were obtained from each triplicate sample. Thereafter, the flask was replenished with 900µL NPSC culture media. An additional 1.5 mL of culture was removed and replenished with media for time points spaced more than three days apart. Aliquots were triturated vigorously, and 250µL were transferred into a Eppendorf tube and frozen at -80°C for viral titrations. The remaining 50µL of each aliquot was trypsinized, and cell counts were obtained by mixing 10µL sample with 10µL trypan blue using a hemacytometer.

Detection and isolation of viral variants. Viral isolates from plaque assay plates were purified from plaques or eGFP-expressing regions, by demarcating the plaque of interest, and then utilizing a wide-bore pipette to obtain an agar

plug containing the plaque of interest. The agar plugs were then placed onto fresh HeLa RW cell cultures and viral isolates were expanded. For the Day 51 isolates, two rounds of expansion in HeLa RW cell cultures were necessary in order to generate sufficient levels of virus, thus the Day 51 isolates may have mutations introduced from the additional passaging in HeLa RW cells. For sequencing 50 μ L of the newly generated stocks of viral isolates were inoculated onto HeLa RW cells in T-150 flasks and subjected to freeze/thaw when cells reached ~80-90% cell death.

Virus multi-step growth curves. HeLa RW cell cultures were plated and infected at an MOI of 0.01 with each viral isolate in a 24-well format. At each time point, a plate of the infected cultures was carefully sealed with parafilm and then frozen at -80C. At the last time point, the frozen plates were thawed. The lysate from each well was triturated vigorously and subsequently transferred into sterile, pre-labeled eppendorf tubes and stored at -80C until plaque assays could be performed.

Examination of viral virulence by plaque assay. To minimize experimental variation, standard plaque assay was performed on all viral isolates on the same day. Plaque assay plates were scanned and analyzed using ImageJ to determine average plaque size per isolation time point. Plaque size data obtained by ImageJ was then analyzed by ANOVA and Student's t-test.

Differentiation and immunostaining. Differentiation and immunostaining of the cultures was performed as previously described (Tsueng et al., 2011), utilizing the same antibodies and antibody concentrations for GFAP, β -tubulin III, MBP, and Nestin. All cultures were plated at 10^5 cells/mL in differentiation media. The differentiation media consisted of DMEM supplemented with 1% FBS (Mediatech), 1x N1 supplement (Sigma), and 0.5% pen/strep.

Fluorescence microscopy and ImageJ analysis. Live cultures were imaged using a Zeiss Axio Observer D.1 fluorescent microscope. Three to five representative images of the cultures were taken for each sampling time point at multiple magnifications. For fixed cultures, six to nine representative images were taken for each marker, per condition, per experiment. To examine relative fluorescent protein expression, black/white threshold images were generated for each channel of each image separately. The quantifications of the marker were then divided by that of the corresponding DAPI channel to determine expression levels relative to cell number.

Western blots. To verify the results of the Immunostaining, Western blots were performed as previously described (Tabor-Godwin et al., 2012) using NuPAGE® Novex 4-12% Bis-Tris Gels (Invitrogen, NP0323Box) in an XCell SureLock® Mini-Cell CE (Invitrogen, EI0001). Separated proteins were transferred from the gel onto Invitrolon™ PVDF (Invitrogen, LC2005). Primary antibodies were added to the blots at the following concentrations and

incubated overnight in 0.5X BLOK-BSA solution (G-bioscience, 786-195): GFAP (1:6000), β -tubulin III (1:6000), Nestin (1:6000), and GapDH (1:6000). Membranes were rinsed with 1x TBSTx and then incubated for 1hr in HRP-conjugated anti-rabbit antibody at (1:6000). Membranes were, then treated with Novex® ECL Chemiluminescent Substrate Reagent Kit (Invitrogen, WP20005), and then exposed to Kodak® BioMax™ XAR Film (Sigma, F5888).

Sequencing and analysis. Three time points were selected to be the focus of genomic sequencing of the virus. Full length viral genomes were obtained for days 6, 27, and 48 PI. To obtain the sequence data, a reverse transcriptase polymerase chain reaction (RT-PCR) approach was taken. Eight overlapping primer pairs (Integrated DNA Technologies), each amplifying a 1.2 KB region, were designed using the Clone Manager Basic 9 software to anneal to the positive sense viral genome (Table 1) (Eppendorf Mastercycler - 94°C for 60 seconds - 30 cycles of 94°C for 15 seconds, 51.2°C for 15 seconds, and 72°C for minute – 72°C for 10 minutes – 4°C hold. Initially, RNA was isolated from the viral supernatant samples taken at the three time points (QIAamp Viral RNA Minikit from Qiagen: 52904). Primer specific cDNA was then generated (50 μ M primer concentration) and used as the template for PCR (20 μ M primer concentration) (SuperScript Reverse Transcriptase III from Invitrogen: 18080-044). Each of the 24 PCR products were then independently T/A cloned using the pETBlue-1 AccepTor Vector kit from Novagen: 70598-4DFRZ into a vector containing the M13 forward and M13 reverse primer binding sites flanking the

insert region. The inserts were subsequently sequenced using the M13 forward/reverse primers (Retrogen). Sequence data was analyzed using the DNASTAR suite. Bioinformatic analysis of the viral sequences enabled the construction of three full length genomes from the 3 time points which was compared to the original eGFP-CVB3 sequence.

Results

Coxsackievirus B3 persists in cultured neural progenitor and stem cells. We recently described CVB3 persistence in the central nervous system (CNS) whereby viral RNA was detected for at least 90 days post-infection (PI) following neonatal infection (Feuer et al., 2009). The site of viral persistence in the CNS has not been identified. However, both neural progenitor cells and immature neurons were shown to be targets for infection. Lasting consequences of an early CVB3 infection in our pediatric model of infection included CNS development defects and astrogliosis. Furthermore, we have recently demonstrated that neural progenitor and stem cells (NPSCs) grown in culture were highly susceptible to CVB3 infection (Tsueng et al., 2011).

CVB3 infection induced cytopathic effects (cpe) in NPSCs at early time points, yet these cells appeared to support a carrier-state infection at least up to 16 days PI if cultures were replenished with fresh complete media (Tsueng et al., 2011). We hypothesized that our model of NPSC infection might reveal similar mechanisms responsible for the establishment of CVB3 persistence in the CNS. To more clearly define potential target cells contributing to persistent

infection, NPSCs were infected with a recombinant CVB3 expressing eGFP (eGFP-CVB3; MOI = 0.1), and cultures were passaged for 51 days and inspected for viral protein expression by fluorescence microscopy. By Day 9 PI, remaining cells were washed, transferred, and replenished with complete media. Infected NPSCs were replenished by this methodology approximately every 3 days thereafter.

Viral protein levels were high at early time points following infection (**Figure 2.1**; green – eGFP; also by virus greyscale). Signs of cpe and cellular debris were evident as early as day 3 PI, as determined previously (Tsueng et al., 2011). Intriguingly, viral protein expression remained at detectable levels as late as day 42 and day 51 PI (**Figure 2.1**; high magnification, white arrows), suggesting continuous viral replication or carrier-state infection in NPSCs. The stability of our recombinant CVB3 in NPSCs was evident by the continuous detection of eGFP as determined fluorescence microscopy. In addition, HeLa cells infected with day 51 supernatants collected from persistently-infected NPSCs continued to express high levels of viral protein expression (**Figure 2.1**; black arrow). These results demonstrated the stability of our recombinant CVB3 over the course of 51 days of carrier-state infection in NPSCs.

Virus production over time in persistently-infected NPSCs. We quantified viral titers, cell viability, and interferon- β secretion over time in persistently-infected NPSCs. By trypan blue staining, a dramatic decline in cell viability (greater than 90%) was observed by day 3 PI **Figure 2.2A**; blue bars – dead cells, red

bars – live cells) which paralleled the visual observation of cpe by Hoffman Modulation Contrast (HMC) microscopy at this time point. However, infected NPSC cultures did not completely succumb to viral infection. Instead, NPSCs recovered and cell viability fluctuated inversely in near synchrony with viral titers over time although levels of cell death failed to reach the high levels observed at day 3 PI. Also, viral titers reached high levels early on, although these levels continuously decreased as cell viability increased over 51 days PI (**Figure 2.2A**; green line).

We hypothesized that Type I interferon production in NPSCs might contribute to NPSC survival during carrier-state infection, although few studies have determined the ability of stem cells to produce Type I interferons following microbial infection (Wellen et al., 2009) (McLaren et al., 2001) (Arscott et al., 2011) (Hirsch et al., 2009). Therefore, interferon- β production was quantified by ELISA in infected NPSCs over time. As shown in **Figure 2.2B**, detectable levels of interferon- β were observed in NPSC supernatants from day 9 to day 13 PI (**Figure 2.2B**; pink lines). Additional peaks of interferon- β production were observed at day 23 and day 47 PI. Intriguingly, these peaks of production occurred prior to a decrease in viral titers and partial recovery in cell viability.

These results suggest that interferon- β release in response to infection might be protective for NPSCs. However, the low levels of interferon- β were significantly delayed temporally, similar to the expression patterns of interferon- β seen in other cell types infected with CVB3 (Heim et al., 2000). The

delayed and low levels of interferon- β within these cultures may reflect recent results suggesting that CVB3 proteases may cleave critical proteins controlling efficient Type I interferon response in the host cell (Mukherjee et al., 2011).

Changes in CVB3 plaque size observed over time in supernatants sampled from infected NPSC cultures. Upon inspecting plaque sizes from viral supernatants sampled from infected NPSCs described in **Figure 2.2A**, we discerned an initial increase in plaque size at early time points (day 6 PI), followed by a continuous reduction in plaque size over time (data not shown). We also examined the presence of the eGFP insert within our recombinant virus over time by counting the number of eGFP⁺ plaques. Using this technique, we observed that the eGFP insert remained within the recombinant viral population until at least day 21 PI (data not shown). Therefore, the observed plaque size increase in day 6 PI NPSC supernatants was not a reflection of any loss of the eGFP insert in recombinant CVB3, which might be expected to increase CVB3 replication kinetics thereby leading to greater plaque sizes.

Thereafter, the percentage of plaques expressing eGFP dropped continuously. By day 35 PI, no eGFP⁺ plaques were identified in viral plaque assays taken from infected NPSC supernatants. This was unexpected, considering viral protein expression (as measured by eGFP signal) continued to be observed in NPSCs by fluorescence microscopy throughout 51 days of infection. With this in mind, we re-examined some of the later time-point NPSC

supernatant samples by plaque assay. However instead of searching for viral plaques, we scanned the plates for GFP expression. Using this methodology, we observed 'patches' of eGFP⁺ cells in samples obtained from Day 27 and Day 30 PI supernatants. These eGFP-expressing 'patches' did not appear to be forming plaques, further suggesting the presence of attenuated viral variants expressing the eGFP transgene. Also, the lack of eGFP in plaques from later time point NPSC supernatant samples (Day 35 and beyond) suggested the loss of the eGFP insert in viral populations retaining the ability to form plaques.

To better characterize the progressive attenuation of eGFP-CVB3, three viral isolates were plaque-purified from the supernatants of infected NPSCs from each of the following time points: day 6, day 14, day 27, day 48, and day 51 PI. All virus isolates, except day 48 PI isolates, were obtained from eGFP-expressing plaques or eGFP-expressing 'patches' on HeLa cell monolayers at 24 hours. Two viral isolates from day 48 PI supernatants were obtained from extremely small plaques which failed to express eGFP on HeLa cell monolayers at 48 hours. Virus isolates were then titrated by standard plaque assay, and the size of the plaques obtained on HeLa cell monolayers were compared for each isolate (**Figure 2.3**). Similar to our preliminary observations for day 6 supernatant samples, day 6 viral isolates were consistently larger in plaque size as compared to our original eGFP-CVB3 stock (**Figure 2.3A**), indicating a possible increased virulence in viral variants obtained from infected NPSC cultures at this early time point. In contrast, day 14 viral isolates showed

consistently reduced plaque sizes which became progressively smaller for day 27 and day 48 viral isolates. These results suggested the presence of attenuated viral variants obtained from infected NPSC cultures at later time points which remained consistent with regards to plaque phenotype. ImageJ quantification of the plaque sizes confirmed the visually-observed changes in plaque size in a stepwise progression over time (**Figure 2.3B**). Average plaque sizes (in pixels) for day 6 viral isolates were significantly larger as compared the original eGFP-CVB3 stock. However, day 14 viral isolates showed significantly smaller plaque sizes, as compared to day 6 viral isolates or the original viral stock. Also, plaque sizes continuously declined for day 27 and day 48 viral isolates, respectively.

Multi-step growth curve for viral isolates obtained from persistently-infected NPSCs. To determine whether the differences in plaque sizes observed in viral isolates obtained from persistently-infected NPSCs over time were due to differences in viral growth kinetics, we performed a multi-step growth curve. We hypothesized that a multi-step growth curve, as opposed to a one-step growth curve, may discriminate small changes in virulence or attenuation which may be dependent upon cell spread (as might be reflected by an increase or decrease in viral plaque sizes). As a comparison, we evaluated a multi-step growth curve for our original eGFP-CVB3 stock and an additional recombinant CVB3 expressing dsRED protein (dsRED-CVB3) (Tabor-Godwin et al., 2010).

As shown in **Figure 2.4** both eGFP-CVB3 (green squares) and dsRED-CVB3 (red diamonds) stocks showed similar viral growth kinetics over 56 hours PI. In contrast, the day 6 viral isolate (dark blue circles) displayed enhanced viral growth kinetics reaching a peak viral titer near 10^{12} pfu/ml at 48 hours. Few studies have described CVB3 samples from any culture methodology exhibiting such elevated viral titers. Furthermore, a stepwise decrease in viral growth kinetics was observed for day 14 (blue circles), day 27 (light blue circles), and day 48 isolates (lighter blue circles) over 56 hours PI. The day 51 isolate showed slightly increased viral growth kinetics, as compared to the day 48 isolate. Nonetheless, the day 51 isolate (lightest blue circles) also showed decreased viral growth kinetics, as compared to the original eGFP-CVB3 stock. Taken together, the data suggested that the phenotype reflected by viral plaque size for each isolate paralleled the results obtained from the multi-step growth curves.

Sequence analysis of viral isolates from persistently-infected NPSCs. We wished to identify genomic alterations associated with increased virulence or attenuation in our viral isolates. Eight sets of primers were designed to amplify overlapping viral fragments by RT-PCR (**Table 2.1**). These fragments were cloned and sequenced for each viral isolate (**Figure 2.5**). Fluorescence images illustrated the plaque size after 24 hours, the presence (day 6 and 27 viral isolate) or absence (day 48 viral isolate) of eGFP (green) within each viral plaque, and the eventual expansion of each viral isolate in HeLa cells (**Figure**

2.5A). Day 6 and 27 viral isolates continued to express eGFP during expansion in HeLa cells, while the day 48 viral isolate failed to express eGFP in HeLa cells - as reflected by the lack of eGFP within the 24 hour plaque for the day 48 viral isolate.

Compared to our original eGFP-CVB3 sequence, genomic sequence analysis identified 8 mutations for the day 6 viral isolate, 18 mutations for the day 27 viral isolate, and 10 mutations for the day 48 viral isolate (**Figure 2.5B**). These mutations occurred in both structural and nonstructural viral proteins and represented both silent (blue symbols) and missense mutations (red symbols). Also, some mutations became fixed in the viral isolates over time (blue and red dashed arrows). Possible "hot spots" of fixed mutations were observed in the 2C and 3A regions of the genome (including amino acid changes), suggesting the contribution of these mutations to the establishment of carrier-state infection in NPSCs. A single nucleotide mutation was observed in the non-coding region of the day 27 viral isolate. Also, partial deletion of the eGFP transgene was observed for all sequenced isolates. While the 5' end of the transgene was deleted, the 3' end remained within the viral genome. The eGFP deletion consisted of approximately 75% of the transgene, although the ORF of the virus was maintained. Although eGFP expression was observed for both day 6 and day 27 during viral expansion in HeLa cells, we suggest that the partial deletion of the eGFP transgene determined for these viral isolates represents genetic alterations occurring during significant expansion in HeLa cells. Also, PCR amplification may preferentially amplify smaller fragments

representing partial eGFP transgene deletions which may predominate in these expansion cultures over time.

A summation of all mutations in table form is shown in **Figure 2.5C**. Unique amino acid substitutions were observed for both the day 27 and day 48 viral isolates, although these substitutions did not overlap for both isolates. Nevertheless, unique amino acid changes found in day 27 and day 48 viral isolates may independently lead to attenuation. Also, no unique amino acid mutations were observed in the day 6 viral isolate which may identify changes affecting CVB3 virulence. However, silent mutations may hypothetically influence CVB3 replication and cytopathicity. Alternatively, amino acid mutations associated with virulence in the day 6 viral isolate may also remain within the attenuated viral isolates in the presence of additional dominant amino acid mutations contributing to attenuation. Hence, the identification mutations in viral isolates obtained from infected NPSCs over time may reveal modified viral proteins affecting virulence or attenuation.

Persistently-infected NPSCs continue to express of nestin and other markers of neural cell lineage differentiation. To verify that persistently infected NPSCs continue to comprise neural progenitor cells, nestin staining was done day 48 PI. As a control, high passage NPSCs were simultaneously stained. As seen in **Figure 2.6A**, Nestin was still expressed in the persistently infected NPSCs, with no apparent change in cellular localization. To determine whether or not persistent infection biased the differentiation of the NPSC population towards

a specific lineage, multiple rounds of differentiation experiments were carried out with the persistently infected and uninfected NPSCs and then stained with lineage markers such as GFAP, β -tubulin III, and MBP. Cell counts were then performed for the differentiated cell types, revealing no apparent differences between persistently infected cultures and uninfected cultures (**Figure 2.6B**). This suggests that the virus does not alter the differentiation pathway of the cells it infects, and that during persistent infection, there is no apparent bias in the lineages that are likely to survive infection. Western blots were carried out on some of these cultures in order to verify the results of the cell counts (**Figure 2.6C**). ImageJ analysis of the western blots revealed no significant differences between the protein levels observed for the persistently infected and the uninfected NPSCs (**Figure 2.6D**).

Persistently-infected NPSCs have an increased propensity to spontaneously differentiate under normal culturing conditions. Although we did not observe differences in differentiation potentials between uninfected and persistently-infected NPSCs, we did notice that persistently-infected NPSCs had the tendency to stick to the culture flask during normal culture conditions. This led us to suspect that persistently-infected NPSCs might be more likely to spontaneously differentiate than uninfected NPSCs even if they did not appear to be biased towards a particular lineage type after differentiating. To test this suspicion, cultures were plated in 6-well plates and observed daily for up to three days after plating in normal NPSCs media. Confirming our

previous observations, the persistently infected NPSCs spontaneously adhered to the bottom of the well (**Figure 2.7A**). ImageJ quantification of the flattened, adherent (spontaneously differentiating) cells in both cultures revealed a significantly higher number of spontaneously differentiating cells in the persistently-infected cultures than in the uninfected cultures (**Figure 2.7B**).

mCAR expression levels in NPSCs vary depending on differentiation status, but are not entirely suppressed in persistently-infected NPSCs. What might contribute to CVB3 attenuation in NPSCs? Previous studies describing CVB3 carrier state infection in cardiac cell lines describing the downregulation of mCAR, a critical receptor for viral entry. Therefore, we inspected the level of mCAR expression on both uninfected and persistently-infected NPSCs by western blot and quantified by ImageJ analysis (**Figure 2.8**). Uninfected NPSCs expressed detectable levels of mCAR, although these levels were greatly reduced in NPSCs differentiated for 5 days in the presence of fetal bovine serum (**Supplementary Figure 2.1**). As expected, differentiated NPSCs also downregulated the expression levels of nestin. Surprisingly, mCAR expression was still observed in persistently-infected NPSCs. However, mCAR expression levels varied substantially, and tended to trend together with the levels of nestin. If nestin was high in a sample, mCAR would likely be high as well; when nestin was low, mCAR was also low. The handling of the cultures prior to use in the experiment could affect the expression levels of nestin and CAR, as cultures grown for longer may experience higher levels of spontaneous

differentiation (**Supplementary Figure 2.1**). Taken together, persistent infection of NPSCs may downregulate mCAR which, in turn triggers spontaneous differentiation, or the persistent infection may be triggering spontaneous differentiation, which in turn offers some resistance to CVB3 entry.

Discussion

The highly virulent virus may have contributed to the massive cell death observed during initial infection. However, the loss of highly-susceptible target cells in the NPSC culture may have contributed to the ultimate selection of attenuated viral variants which remained in the recovered cultures. NPSC cultures, or neurospheres, are composed of a heterogenic mixture neural stem and progenitor cells, and more differentiated neuronal or glial precursor cells. Each progenitor and stem cell may differentially support CVB3 infection (Tsueng et al., 2011), thereby potential leading to dynamic cycles of virus replication, cpe, and eventual recovery of the culture.

Previous experiments from our lab have shown that neural progenitor and stem cells (NPSCs) are highly susceptible to infection by eGFP-CVB3 in vitro (Tsueng et al., 2011). Following the initial acute phase of infection, a carrier state of infection is induced within NSPCs. This carrier state is characterized by persistence of the virus at low levels. Previous studies have described a carrier-state infection of myocardial fibroblasts in culture (Heim et al., 1997) (Schmidtke et al., 2000). Our interest in infected NPSCs stems from the fact that this population of cells may potentially serve as a site for long

term viral persistence of the virus within the CNS. Furthermore, the persistence of the virus in these cells could potentially perturb their function, subsequently contributing to developmental disorders. Finally, we were interested in documenting if viral evolution was occurring following cellular infection and passage. Viral mutation in general, is a well documented phenomenon and has been associated with drug resistance and increases in virulence. RNA viruses are especially prone to mutation due to the low fidelity of the RNA dependent RNA polymerase, which lacks a proofreading mechanism. Therefore, we were interested in documenting any mutations associated with persistence and virulence that occurred during infection of NPSCs with eGFP-CVB3. Our central hypothesis surmised that the virus establishes a persistent state of infection via genomic mutations that generate an attenuated form of the virus.

Initially, we observed some isolates in the quasispecies to become hypervirulent. While it is arguable that the observed increase in virulence could be associated with the deletion of the eGFP transgene, the GFP expression exhibited by the Day 6, hypervirulent isolates, suggested that this was not the case. In contrast, the Day 48 isolates were picked from small, non-GFP expressing plaques, demonstrating that even without the GFP transgene, the virus could still more attenuated than the original stock containing the GFP transgene. Interestingly enough, these hypervirulent isolates did not persist in the culture in spite of their apparent increased fitness suggesting the presence of selective pressures against the hypervirulent

quasispecies, and in favor of attenuation. This attenuation occurred in spite of the loss of the transgene, as the Day 48 isolates were picked from small, non-GFP expressing plaques. Even without the GFP transgene, the virus could still more attenuated than the original stock containing the GFP transgene. Our results implicate the presence of a functional innate immune response. This immune response in stem cells may protect the cells from virally-induced cell death, as well as generate selective pressures in favor of attenuated virions. We are currently investigating the role of the innate immune response in CVB3 persistence in NPSCs and the CNS.

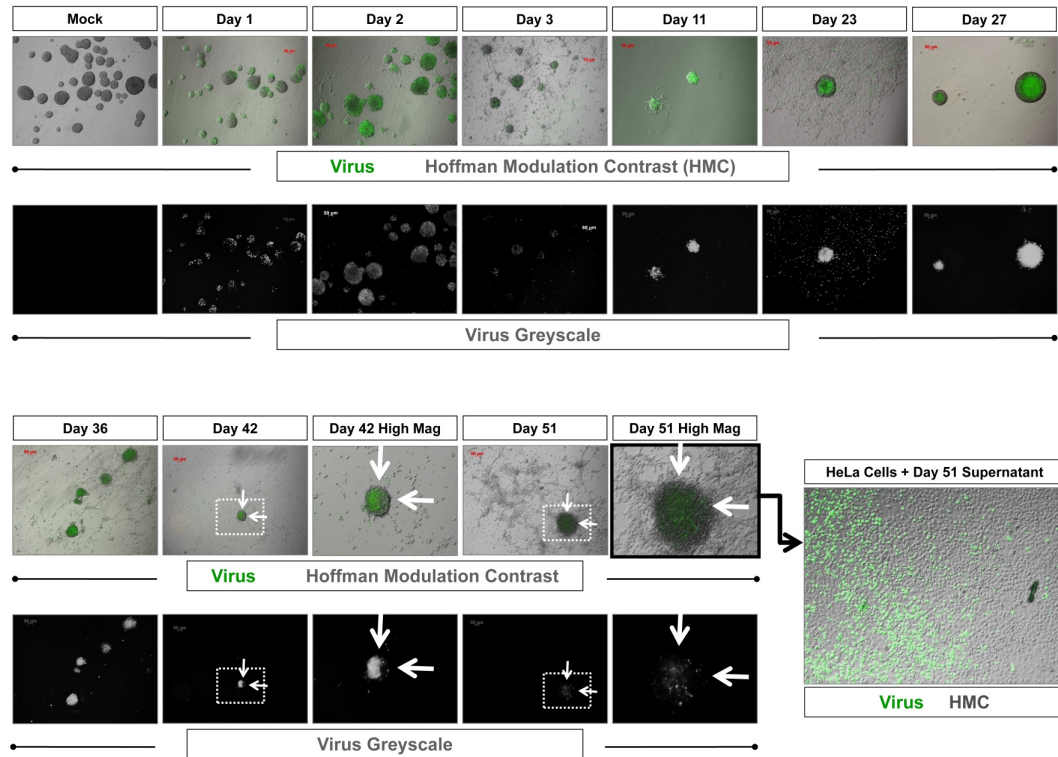


Figure 2.1. CVB3 persists as a carrier-state infection in cultured NPSCs.

Cultured neural progenitor and stem cells (NPSCs) were infected with eGFP-CVB3 (MOI = 1.0), and viral protein expression was determined by fluorescence microscopy over time. Detectable levels of viral protein expression (eGFP - green) were continuously observed in NPSCs, including at day 42 and day 51 PI (High Mag; white arrows). Viral protein expression levels are made clear by single channel greyscale images below each dual channel image. The highest levels of viral protein expression were observed in undifferentiated or free-floating neurospheres, as shown previously (Tsueng et al., 2011). Little to no viral protein expression was observed in more differentiated cells in culture adhering to the surface. HeLa cells infected with supernatants from day 51 infected NPSC cultures continued to express high levels of viral protein (eGFP) at 24 hours PI. All images were captured at 50x total magnification; except High Mag images - an additional four-fold digital magnification).

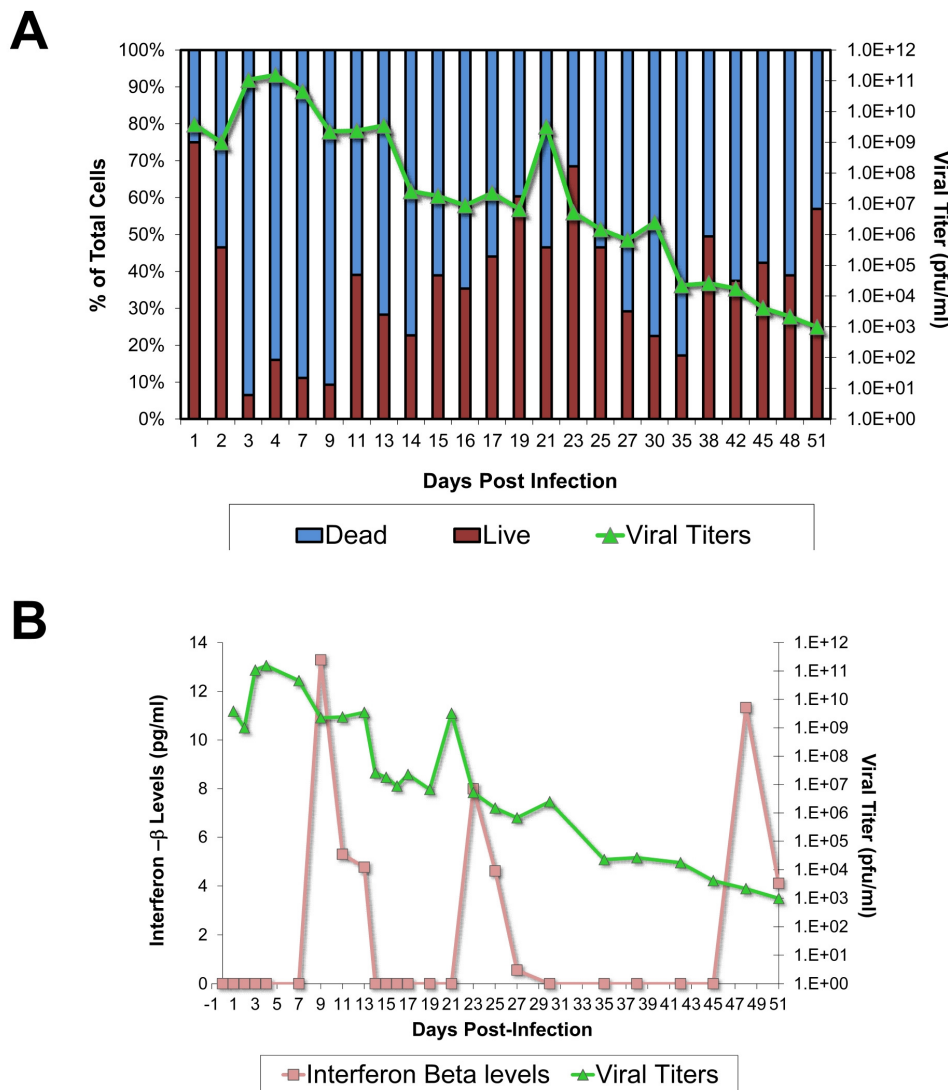


Figure 2.2. Quantification of viral titers, viable cells, and interferon- β production over time in persistently-infected NPSCs.

(A) NPSCs were infected with eGFP-CVB3 (MOI = 1.0), and cell viability was quantified by trypan blue staining. At day 9 post-infection (PI), infected cultures were washed twice in 1x PBS to remove extracellular virus and dead cells. Surviving NPSCs were allowed to expand in fresh complete media, and cell survival was quantified over a total period of 51 days PI. Bars indicate the percentage of live (red bar) and dead (blue bar) cells and the line graph (green) shows viral titer levels over time. Viral titers peaked following a precipitous drop in the number of viable cells at multiple time points during the experiment. However, total viral titers slowly decreased over 51 days. **(B)** Interferon- β production in supernatants from infected NPSCs (pink line) was quantified by ELISA over time.

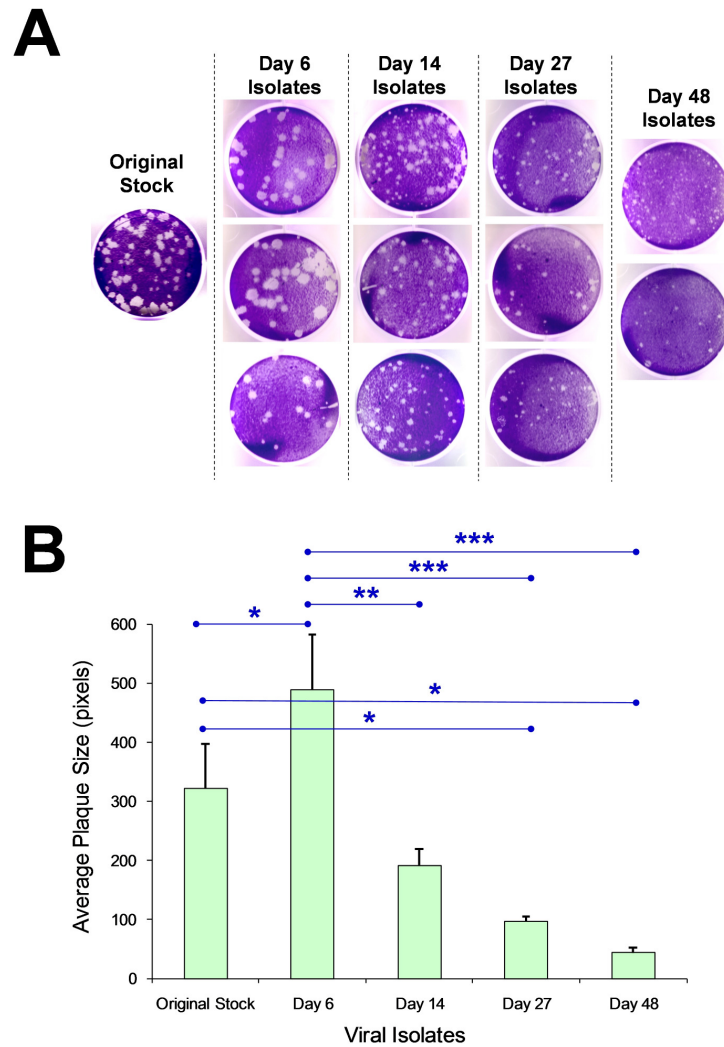


Figure 2.3. Viral isolates obtained at different time points during the establishment of persistent infection in NPSCs exhibited an initial increase, followed by a gradual reduction in plaque size.

Viral isolates were plaque-purified from infected NPSCs supernatants sampled at Day 6, 14, 27, and 48 PI. **(A)** Day 6 isolates generated larger plaques in comparison to our original eGFP-CVB3 stock. Day 14 isolates generated plaques slightly smaller in size compared to our original viral stock. Day 27 and Day 48 isolates showed a stepwise decrease in plaque size. **(B)** Plaque sizes from viral isolates were quantified by ImageJ analysis. Day 6 isolates showed statistically significant larger plaque sizes than those generated by our original viral stock. Day 14 isolates plaque sizes were not significantly different from our original viral stock, although significantly smaller than the Day 6 isolates. Day 27 and Day 48 isolates showed significantly smaller plaque sizes than those generated by our original viral stock. ANOVA and Student's t-test was utilized for statistical analysis.

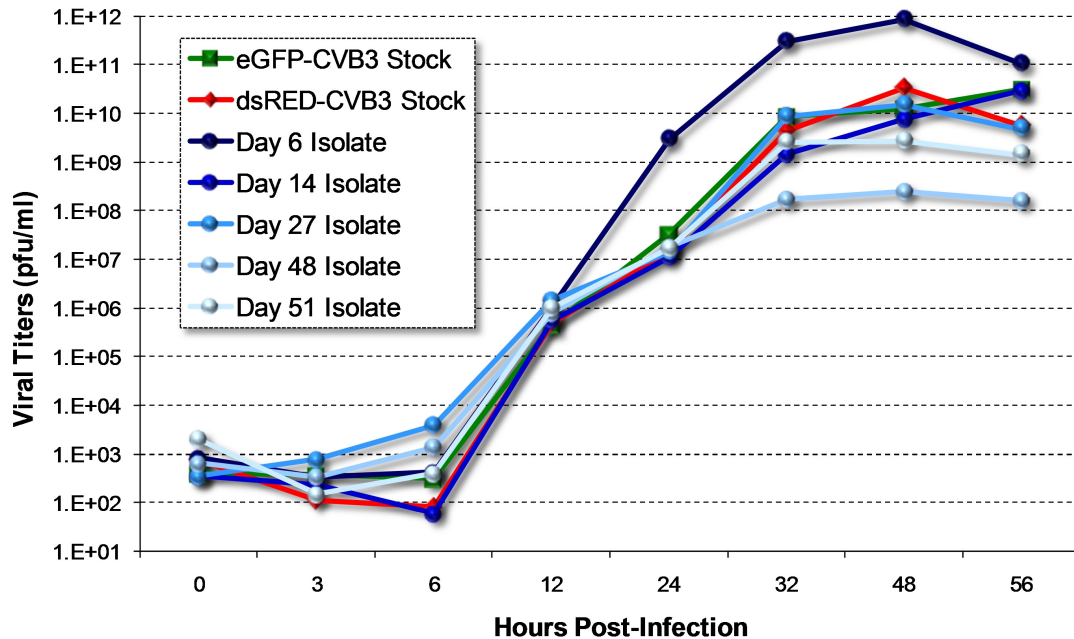


Figure 2.4. Viral isolates obtained temporally from persistently-infected NPSCs showed an initial increase, followed by a step-wise reduction in growth curve kinetics.

Hela cells were infected at an MOI of 0.01 with each of the viral isolates. At each time point, the cultures were frozen and stored for plaque assays. The plaque assays were performed for the different samples simultaneously. Triplicate samples were taken for each time point. Displayed are the average titers for each viral isolate at each time point. As seen in dark green, the Day 6 isolates reached higher titers than the original eGFP-CVB3 stock. In contrast, the Day 48 isolates reached lower titers (dark blue line). The Day 14 isolate and Day 27 isolate appeared to have similar growth rates as the eGFP-CVB3 stock, as did the dsRed-CVB3 viral stock. The Day 51 isolates appeared to reach higher titers than the Day 48 isolates, but this may have been due to the changes induced by the serial passaging necessary in order to generate the D51 viral isolate stock.

Table 2.1. Primer sequences utilized for viral genome amplification and sequence analysis for hypervirulent and attenuated viral isolates.

Primer Pair	Forward Sequence	Reverse Sequence
Primer Pair #1	5' TAAAACAGCCTGTGGGTTGATCCC 3'	5' CTCCGGCCCCCATTTTGTTG 3'
Primer Pair #2	5' GTTGGATTATACCACTTAGCTTGAGAGAGG 3'	5' CGTGTAGTGAATAATGGAATTGCCGCTAG 3'
Primer Pair #3	5' GTATCAACGCAAAGACTGGGGC 3'	5' CGCTTCATGGAGTTGACCTTCTCTCC 3'
Primer Pair #4	5' GATGAGGATACCTGGTGAGGTGAAGAAC 3'	5' CCCCGTTCCTGGAAAATTCAGACC 3'
Primer Pair #5	5' CCGTACCGTTTTTGAGCATTGGC 3'	5' GGGGGAGCTGTTTGAGTCTGTTTCAG 3'
Primer Pair #6	5' GGATAGCCATTAAGATTCAGAAATTCATTGAG 3'	5' CCTTGGGCTTCTGGTTGGGTATTC 3'
Primer Pair #7	5' CTACGTTTGTGTCAGTAGCTGGAATCATC 3'	5' CAGAGTCATTCAAACCTGGACGGGTC 3'
Primer Pair #8	5' GAAAGACGAACTCAGATCTGCAGAGAAG 3'	5' CCGCACCGAATGCGGAGAATTTAC 3'

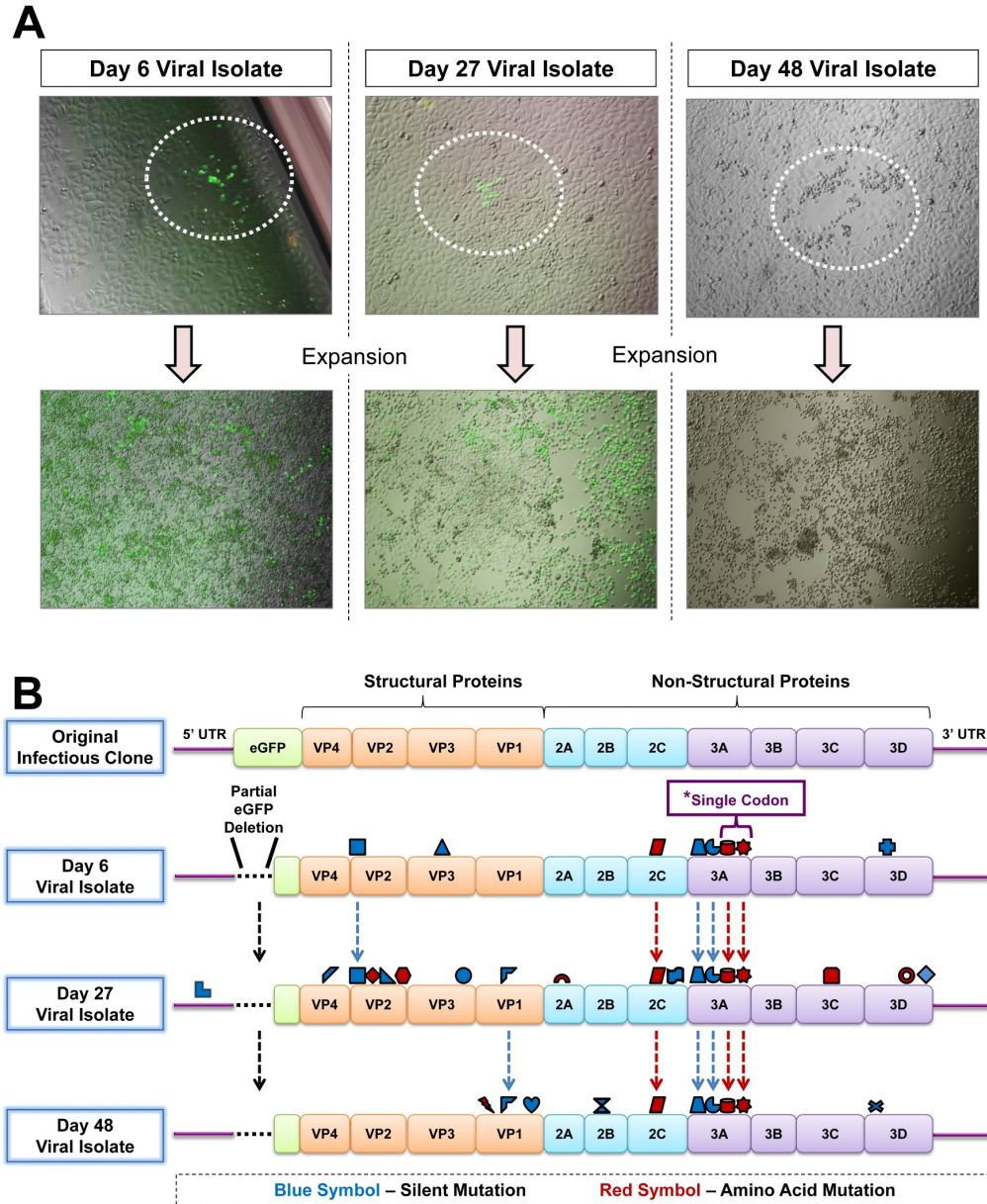


Figure 2.5. Unique mutations observed in viral isolates derived from persistently-infected NPSCs.

C




















Viral Isolate	Protein / Region	Nucleotide Substitution	Amino Acid Substitution
Day 6, 27	 VP2	A to G (1024)	-
Day 6	 VP3	C to T (2127)	-
Day 6, 27, 48	 2C	A to C (4705)	Lys to Asn
Day 6, 27, 48	 3A	T to C (5068)	-
Day 6, 27, 48	 3A	A to C (5071)	-
Day 6, 27, 48	 3A	C to G (5210)	Arg to Ala
Day 6, 27, 48	 3A	G to C (5211)	Arg to Ala
Day 6	 3D	A to G (6642)	-
Day 27	 5' UTR	T to C (610)	-
Day 27	 VP4	C to A (931)	-
Day 27	 VP2	C to T (1560)	Ser to Phe
Day 27	 VP2	G to A (1808)	-
Day 27	 VP2	A to G (1834)	Asn to Ser
Day 27	 VP3	T to C (2669)	-
Day 27, 48	 VP1	C to T (2951)	-
Day 27	 2A	G to A (3655)	Gly to Asp
Day 27	 2C	A to G (4710)	-
Day 27	 3C	G to A (4770)	Gly to Asp
Day 27	 3D	T to C (5073)	Met to Thr
Day 27	 3D	T to C (5076)	-
Day 48	 VP1	G to A (2810)	Glu to Lys
Day 48	 VP1	C to T (3148)	-
Day 48	 2B	C to T (3877)	-
Day 48	 3D	C to T (6142)	-

Figure 2.5 continued. Unique mutations observed in viral isolates derived from persistently-infected NPSCs.

(A) Following passage within NPSCs, eGFP-CVB3 genomic isolates were obtained at days 6, 27, and 48 PI. (B) Sequencing of the viral isolates identified post silent (blue) and missense mutations (red). Each symbol represents a unique nucleotide mutation present in the isolates. Both fixed and isolate specific mutations were identified. Symbols occurring in more than one isolate indicate fixed mutations. Partial deletion of the eGFP transgene occurred within all isolates. The conserved eGFP deletion consisted of approximately 75% of the transgene, with the deletion maintaining the ORF of the virus. While the 5' end of the transgene was deleted, the 3' end remained within the viral genome. Mutations occurred in both the structural and nonstructural proteins of the virus. The 2C and 3A regions of the genome represent 'hot spots' of fixed mutation due to the fact that a total of 5 mutations are conserved within these areas. Throughout the time course of the experiment, genomic mutation rate peaked at day 27, with the isolate containing a total of 18 mutations. In contrast, the day 6 isolate included 8 mutations, while the day 48 isolate had 10 mutations. (C) Column 1 illustrates the isolates containing the genomic mutation. Column 2 indicates the specific viral protein mutated. Column 3 shows the specific nucleotide substitution and the location of the mutation within the genome based upon the Woodruff strain of CVB3 (genomic ID: CXU57056). Column 4 demonstrates the specific amino acid substitution resulting from the genomic mutation.

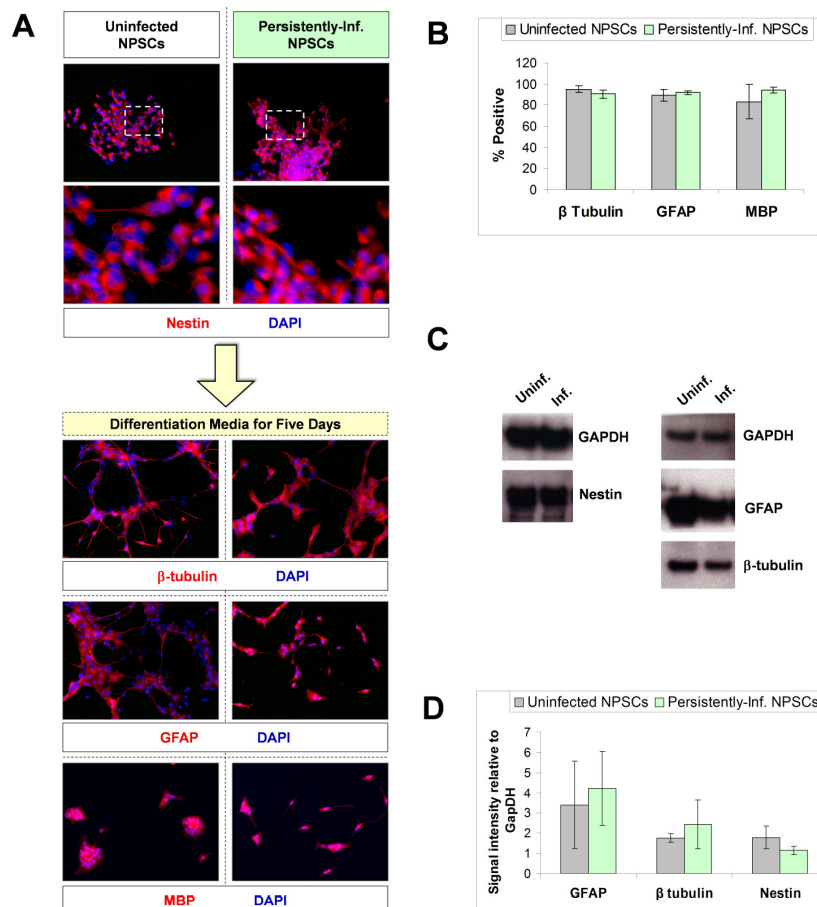


Figure 2.6. Persistently-infected NPSCs differentiate into the three downstream neural cell lineages similar to uninfected NPSCs.

(A) Top: Nestin staining (red) and Dapi (blue) in High passage (passage 60), uninfected NPSCs (left) and Persistently infected NPSCs (right) images taken at 200x total magnification. Digitally enhanced images placed below to show detail. Differentiated NPSCs stained for β -tubulin, GFAP, and MBP (all markers in red) from the middle to bottom. All images taken at 200x. **(B)** Cell counts performed on 50-80 Images (600-700 cells counted) per stain. Analysis by student T-test revealed no significant differences between the ratios obtained for the persistently infected and uninfected NPSCs. **(C)** Western blots were performed for 3 samples for each of the following markers: GFAP, β -tubulin, and Nestin to confirm the results of the immunostaining; GapDH (for normalization). Representative Images of the blots are shown. **(D)** Each of the 3 samples from C were analyzed with ImageJ and the quantifications normalized to the GapDH signal. Analysis of the quantifications using the Student T-test revealed no significant differences between marker expression in persistently infected and uninfected NPSCs.

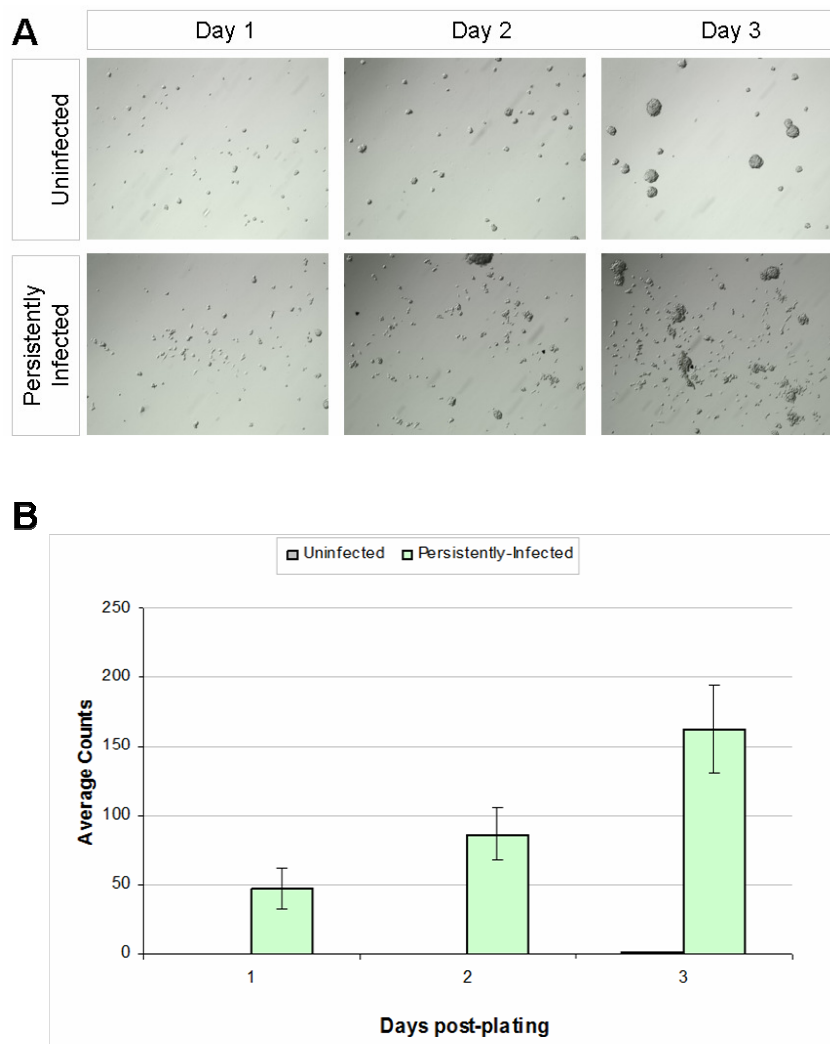


Figure 2.7. Persistently-infected NPSCs have an altered propensity to spontaneously differentiate.

Persistently infected NPSCs and uninfected NPSCs were plated in 6-well plates in fresh NPSCs media. For three days, the cultures were gently swirled to re-suspend non-adherent cells and imaged while focusing on the bottom of the well as seen in the representative images **(A)**. Six images per condition per day were taken and counted for flattened, adherent (partially differentiated) cells. In the uninfected NPSCs, few such cells were observed and counted as compared to the persistently infected cultures, in which an increasing number of such cells were seen over the three days **(B)**.

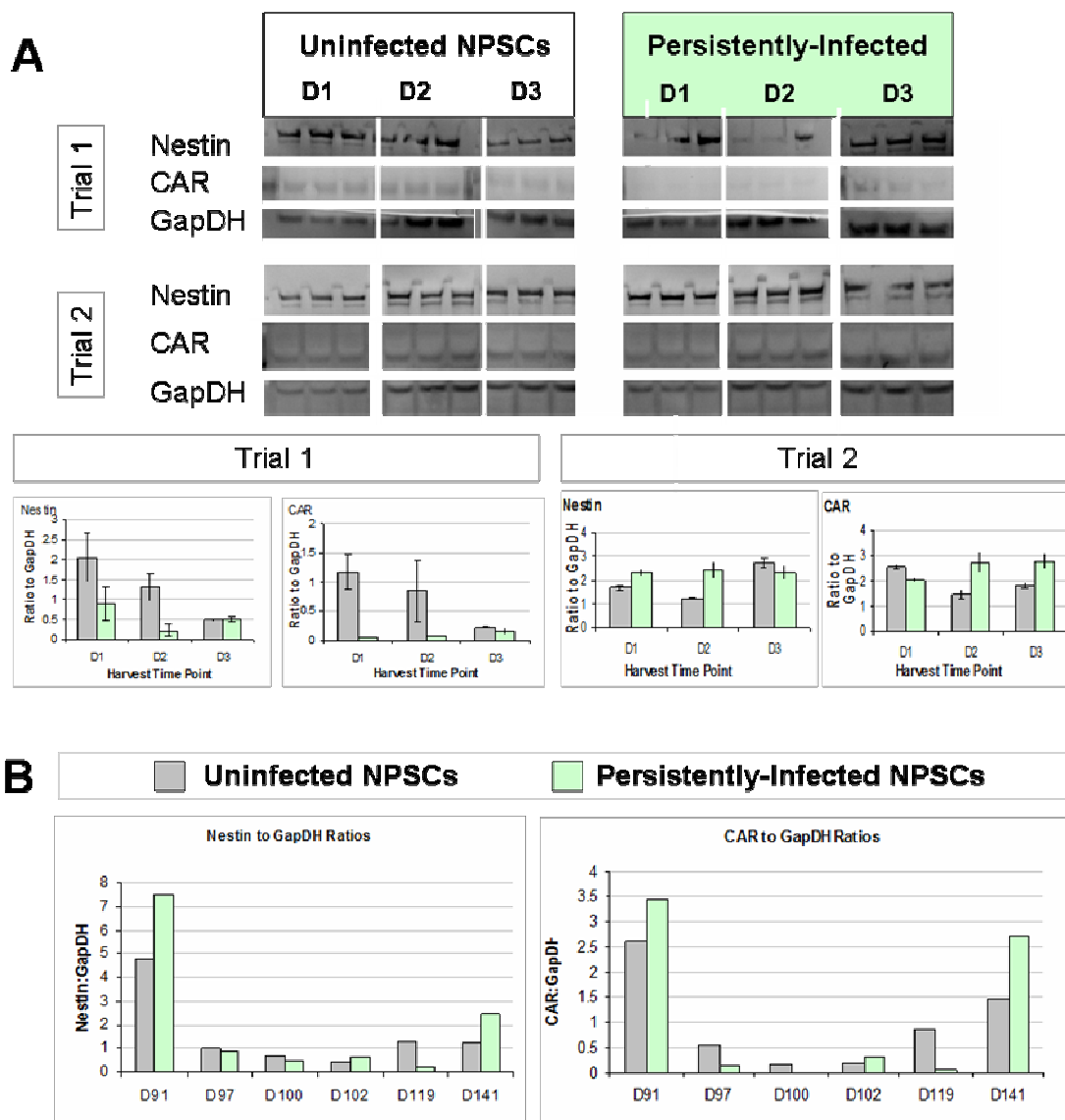
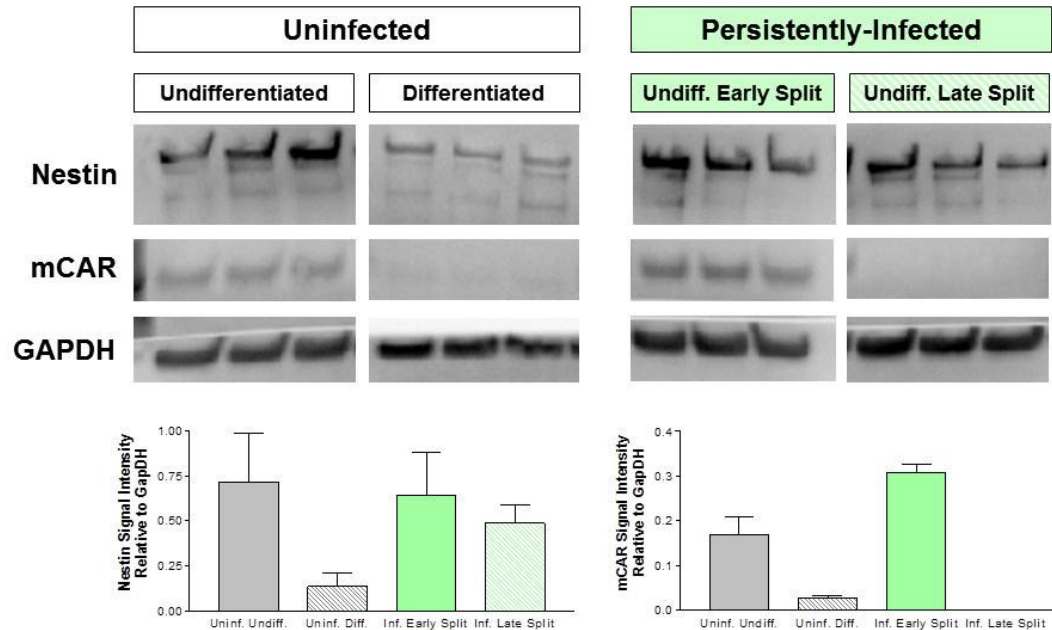


Figure 2.8. mCAR levels fluctuate in persistently-infected NPSCs, and are not necessarily suppressed.

Protein extracts were isolated from lysed uninfected or persistently infected NPSCs (survivors or surv) grown in NPSCs media. **(A)** Expression levels for nestin and mCAR was determined by Western blot. Protein loading was determined by endogenous GAPDH levels. The relative intensity of nestin or mCAR expression levels was determined relative to GAPDH and quantified using Image J software. **(B)** mCAR levels were observed to trend closely to nestin levels; however, mCAR was not entirely suppressed in persistently-infected NPSCs.



Supplementary Figure 2.1. mCAR levels fluctuate in persistently-infected NPSCs, and are not necessarily suppressed.

Protein extracts were isolated from lysed uninfected NPSCs grown in NPSC or differentiation media. Expression levels of mCAR and nestin were determined by Western blot. Protein loading was determined by endogenous GAPDH levels. The relative intensity of nestin or mCAR expression levels was determined relative to GAPDH and quantified using Image J software. mCAR was significantly reduced upon differentiation. Protein extracts were also isolated from lysed persistently-infected (survivor or surv) NPSCs from either a late or early split. The early split exhibited higher levels of mCAR as compared to the late split potentially due to the propensity of the persistently-infected cultures to spontaneously differentiate.

Acknowledgements

Chapter 2, in part is currently being prepared for submission for publication of the material. Tsueng, G; Rhoades, RE; Deline, S; Feuer, R. The dissertation author was the primary investigator and author of this material. This work was supported by National Institutes of Health (NIH) R01 Award NS054108 (to R.F.), an NIH Research Supplement to Promote Diversity in Health-Related Research Award 3R01NS054108-01A2S1 (to R.F.), and a National Institutes of Mental Health (NIMH) Minority Research Infrastructure Support Program (M-RISP) R24 Faculty Fellow Award MH065515 (to R.F.). Ginger Tsueng is recipient of an Achievement Rewards for College Scientists (ARCS) Foundation Scholarship, an Inamori Fellowship, and a Gen-Probe Fellowship. No conflicts of interest exist between the subject matter and the authors included in the manuscript.

**CHAPTER III: The role of Type I Interferons in Establishing a Carrier - State
Infection and Selecting for Attenuated Viral Variants Following Coxsackievirus
Infection in Neural Stem Cell Cultures**

Introduction

Newborn infants are particularly vulnerable to neurotropic infections of coxsackievirus which can potentially cause serious central nervous system (CNS) diseases such as meningitis and encephalitis. We previously described the susceptibility of murine neural progenitor and stem cells (NPSCs) grown in culture to a recombinant coxsackievirus B3 expressing the enhanced green fluorescence protein (eGFP-CVB3) (Tsueng et al., 2011). Utilizing this model, we determined that CVB3 mutates in the host enabling its persistence (chapter 2). The persistence of the virus in turn, can trigger an ongoing inflammatory response in the central nervous system, which may have important developmental implications for the host, and also raises questions as to how the persistent host response affects the virus.

RNA viruses like coxsackievirus have high rates of mutation and readily generate quasispecies dynamics. (Domingo et al., 2008) Host factors released in response to the initial and ongoing infection may generate selective pressures for the attenuation of the viral population during persistent infection. For example, a bottle-neck was observed to restrict the variability of the quasispecies during the spread of the virus from initial inoculation sites to the brain, in an artificial poliovirus quasispecies model (Pfeiffer and Kirkegaard, 2006). This bottle-neck was attributed to the innate immune response, rather than to an actual physical barrier. Similarly, the innate immune response of infected host tissues may generate selective pressure for the attenuation of CVB3 during persistent infection *in vivo*.

Type I interferons are key members of the antiviral innate immune response and play an important role in controlling the pathology associated with chronic coxsackievirus infection in the heart. In addition to its inhibitory effects on CVB3 replication in cultured cardiomyocytes (Kandolf et al., 1985), type I interferons can also affect the generation of CVB3 T-cell epitopes (Jakel et al., 2009). Mice deficient in type I interferons have a higher morbidity following myocardial infections by coxsackievirus than wild-type mice (Deonarain et al., 2004), illustrating the importance of type I interferons and interferon- β has been successfully used to treat chronic viral myocarditis (Kuhl et al., 2003). While coxsackievirus has been found to suppress interferon- β transcript levels during the first 48hrs post-infection (Richtsteiger et al., 2003), it was also previously found to be induced at 5 and 10 days post-infection in the CNS (Feuer et al., 2009). At 30 days post-infection, interferon- β levels were similar to those of control—demonstrating how dynamic the expression of type I interferons is in response to persistent viral activity.

Materials & Methods

Isolation and production of a recombinant coxsackievirus. The generation of a recombinant coxsackievirus expressing eGFP has been described previously. Briefly, the CVB3 infectious clone (pH3) (obtained from Dr. Kirk Knowlton at University of California at San Diego) was engineered to contain a unique *Sfi*I site which facilitates the insertion of any foreign sequence into the CVB3 genome. The generation of recombinant coxsackievirus expressing the enhanced green fluorescent protein (eGFP-CVB3) has been described previously (Feuer et al., 2002). Virus stocks were grown on HeLa RW cells. Virus titrations were carried out as described previously (Feuer et al., 2002a). Viral stocks were prepared on HeLa RW cells maintained in Dulbecco's modified Eagle's medium (DMEM; Invitrogen, Gaithersburg, MD) supplemented with 10% fetal bovine serum. Viral stocks were diluted in DMEM before inoculation. GFP-VSV was provided by Dr. Jacques Perrault at San Diego State University.

Isolation, culture, and infection of neurospheres. Mouse experimentation conformed to the requirements of the San Diego State University Animal Research Committee and the National Institutes of Health. BALB/c, C57BL/6, GFP-actin, IFN α/β R k/o mice were obtained from the Scripps Research Institute animal facilities or Harlan Sprague Dawley (Harlan Laboratories, San Diego CA). Breeding pairs were checked every day. C57 mouse neural progenitor and stem cells (NPSCs) were isolated and cultured as previously described (Tsueng et al., 2011). Fresh cortical NPSCs were isolated from 1 day

old IFN α/β R k/o and C57BL/6 mouse pups utilizing the Miltenyl MACS Neural stem cell isolation kit (Miltenyl Biotec, Inc; cat #130-090-312 [kit], #130-092-333 [beads], #130-092-628 [dissociation kit]). The NPSC culture medium consisted of DMEM/F12 supplemented with 2% B12 (Invitrogen), 20ng/mL EGF (Invitrogen), 20ng/mL bFGF (Preprotech), 5 μ g/mL Heparin (Sigma), and 0.5% pen/strep.

Superinfection infection of uninfected or persistently-infected C57BL/6 NPSCs.

NPSCs surviving eGFP-CVB3 infection (carrier cultures) were harvested at day 23 PI, washed once in 1xPBS, and re-suspended in fresh media at a concentration of 10⁵ cells/mL. Uninfected NPSCs of similar passage were subject to the same treatment in parallel. The cultures were then mock-infected or infected with dsRed-CVB3 at an MOI of 1.0. Trypan blue counting was performed to determine live / dead cell ratios. Fluorescent microscopic images were taken using a Zeiss Axio Observer D.1 fluorescent microscope. Images were analyzed by ImageJ to quantify the level of primary infection (green or red) or super-infection (yellow). Carrier cultures were also passaged until green fluorescence could no longer be observed and the CVB3 superinfection experiment repeated with eGFP CVB3. Carrier cultures no longer exhibiting GFP fluorescence and uninfected C57 NPSCs of similar passage were also infected with LCMV or GFP-VSV at low MOIs and examine for superinfection based on fluorescence with or without immunostaining (LCMV and VSV respectively).

Interferon β treatment. C57BL/6 NPSCs were plated at a concentration of 10^5 cells/ml in T-25 flasks. Recombinant mouse Interferon β (Millipore; cat # IF011) was used to treat the NPSCs at a concentration of 100U/ml or mock treated with media. Cultures were then infected with eGFP-CVB3 at an MOI of 1 and then examined for green fluorescence and sampled for viral titering. Alternatively, 10^6 cells/mL of GFP-actin NPSCs were treated with Interferon β for two hours, while 10^6 cells/mL of C57BL/6 NPSCs were treated with 10^6 pfu/ml of dsRed-CVB3. Next, 2.5×10^5 cells of dsRed-CVB3 NPSCs were mixed with 2.5×10^5 cells of GFP-actin NPSCs which were either treated with media (mock), treated with Interferon β for 2hrs (IFN), or treated with interferon β for 2hrs and then washed to remove the interferon β . Cultures were imaged for fluorescent protein expression, and sampled for viral titering and cell counts.

Detection of Endogenous Interferon β . Samples taken from infected and uninfected NPSCs cultures were analyzed for endogenous interferon β using the Mouse Interferon β ELISA kit by PBL Biomedical Laboratories sold via R&D systems (R&D systems; cat# 42400-1) following the manufacturers instructions. Readouts were performed using a Beckman-Coulter DTX-880 multimode plate reader and then compared with the standard curve to determine the actual concentration of endogenous interferon β present in each sample.

Plaque Assays and Plaque Size Determination. Plaque Assays were performed as previously described. Plaque assay plates were scanned and each well containing distinct plaques was analyzed for plaque size using ImageJ. Plaque size data was analyzed for differences using the ANOVA and the student t test.

Priming of the Innate Immune Response in NPSCs. C57BL/6 NPSCs were grown to high density and centrifuged at 1200 rpm for 3 min. The supernatant was discarded and the pellet was resuspended in 6ml of fresh NPSCs media. The resuspended cultures were then subjected to 3 cycles of freeze/thaw in a -80C ethanol bath. The cell lysate was centrifuged at 3000 rpm for 10 min to pellet the cell debris, and the supernatant removed to be used as 'cell lysate priming media'. 5×10^4 cells/mL of C57BL/6 NPSCs were plated in T-25 flasks containing fresh NPSCs media (no priming), 5mL of cell lysate priming media (priming with cell lysate), 5mL of media with Poly I:C at a concentration of $10 \mu\text{g/ml}$, or 5ml of media containing 10^5 pfu of dsRed-CVB3 that was subjected to uv-inactivation. After priming the cultures for 2 days, the primed cultures were plated at 10^5 cells/ml and infected with eGFP-CVB3 at an MOI of 1. Cultures were then examined daily for GFP expression (as well as dsRed protein expression in the UV-inactivated CVB3 primed condition), and sampled for viral titering.

Results

CVB3-infected NPSCs are less susceptible to new CVB3 infections. We have observed that persistence can be established in culture and that the viral population is evolving over the course of infection (chapter 2), but we did not understand how the host was responding to the infection. To examine the how persistent infection affects the susceptibility of NPSCs to new infection, Day 20 post-eGFP-CVB3-infection NPSCs were washed once and infected with dsRed-CVB3 at an MOI of 1 or mock-infected with DMEM. Cultures were imaged (**Figure 3.1A**), and sampled for cell counts (**Figure 3.1B**) and viral titering up to 10 days post-infection. Additionally, uninfected C57 NPSCs of similar passage were infected with dsRed or mock infected with DMEM in parallel.

Similar to previous infection studies, the newly infected C57 NPSCs experienced a 90% cell death by 8 days post-infection. In contrast, the eGFP-CVB3 Day 20 infection survivors did not appear to be affected by secondary infection with dsRed-CVB3. Consistent with their percent survivor profile, the cultures expressed eGFP rather than dsRed, indicating that the expression of the secondary infection virus was inhibited. Percent survival also dropped abruptly between day 5 and day 7 post-infection for the mock-infected cultures due to nutrient depletion in the medium caused by the uninhibited cell proliferation in that condition. Image J quantification fluorescent protein expression from three to five representative images of each condition and

each time point demonstrated the lack of dsRed production in eGFP-CVB3 infection survivors (**Figure 3.1C & D**).

DsRed is known to be relatively more toxic than eGFP due to the oligomerization of the dsRed protein that's needed for the fluorescence to be readily detected. To address the possibility that the lack of observable superinfection is due to the toxicity of the dsRed protein killing superinfected cultures, we passaged the persistently-infected cultures long enough for the GFP to be deleted from the viral genome. Concurrently, we continued to passage uninfected cultures to high passages in order to address the possibility that observed differences were due to the age of the cultures. These high passage, persistently-infected cultures, and high passage uninfected cultures were then subjected to infection by eGFP-CVB3, and the course of the infection examined by fluorescence using a multimode plate reader. In this manner, we observed that our high passage NPSCs infected for the first time by eGFP-CVB3 exhibited an increase in GFP fluorescence over the course of infection (**Supplementary Figure 3.1**). In contrast, persistently-infected NPSCs which were no longer expressing GFP and then subjected to a fresh infection by eGFP-CVB3 expressed similar levels of GFP as their mock-infected counterparts. Taken together, it is clear that persistently-infected cultures are protected from superinfection by CVB3.

To determine if the observed protection from superinfection is a general phenomena associated with CVB3 infections or a phenomena specific to persistent CVB3 infections, we performed concurrent infection of

NPSCs using both eGFP-CVB3 and dsRed-CVB3. As seen in **Figure 3.2A**, superinfection could be observed based on the co-localization of eGFP and dsRed expression. ImageJ analysis of the red and green fluorescent signal per field revealed little background as red fluorescence was observed in dsRed-CVB3, but not eGFP-CVB3 infected cultures (**Figure 3.2B**), while green signal, but not red was observed in eGFP-CVB3 but not dsRed-CVB3 infected cultures. Although a slight difference was observed in terms of expression levels at 2 days post-infection, both viruses exhibited similar expression levels thereafter. Upon simultaneous infection of the cultures with both viruses at an MOI of 0.5, superinfection occurred in 20 to 40% of the NPSCs (**Figure 3.2C**), as compared to the 10 to 15% of the NPSCs infected by both viruses at an MOI of 1 (**Figure 3.2D**).

Statistical analysis using Jmp verified that superinfection rates in NPSCs simultaneously by eGFP and dsRed CVB3 was significantly different from that of eGFP-CVB3-Persistently-infected cells later infected with dsRed-CVB3. This experiment was also performed in Hela RW cells as an additional comparison (data not shown). Interestingly enough, when Hela RW cells were infected with dsRed-CVB3 at an MOI of 1 and then subsequently infected 24hrs later with eGFP-CVB3 at an MOI 1, little/no superinfection with the secondary virus was observed. This confirms the finding that a previous infection is somehow protective against subsequent infection resulting in strong limitations on CVB3's ability to superinfect cells.

NPSCs are capable of producing Type I Interferons. Wellen et al. previously described the presence of Type I interferon receptors on NPSCs and the ability of NPSCs to respond to the presence of interferon (IFN β) (Wellen et al., 2009); however, whether or not NPSCs produced interferons endogenously was still unclear. Additionally, coxsackievirus has previously been reported to downregulate the transcription of interferons in other cell types (Richtsteiger et al., 2003). To determine whether or not NPSCs could produce type I interferons, NPSCs were infected by VSV, which is known to increase the production of type I interferons within a few hours. Using an Elisa kit for IFN β , we determined that NPSCs are capable of producing IFN β (**Figure 3.3A**). Consistent with Richtsteiger et al's observations on CVB3 downregulation of IFN β mRNA in MRC5 fibroblast cells, we also did not detect the production of IFN β within the first 48 hrs of infection in NPSCs by ELISA. To determine whether or not type I interferons are produced at all during the course of persistent CVB3 infection in NPSCs we performed the IFN β Elisa on the samples from the persistent-infection experiment. As seen in **Figure 3.3B**, IFN β is transiently produced during the course of persistent CVB3 infection.

The type I interferon response is protective against CVB3 in NPSCs.

Type I interferons have been found to play an important role in cardioprotection during CVB3 infection in an *in vivo* murine model of CVB3-induced myocarditis (Wang et al., 2007). To determine whether or not Type I interferons were protective against CVB3 in NPSCs, NPSCs were infected with

eGFP-CVB3 at an MOI of 1 and then incubated in media or media containing 100U/mL of Interferon β . As seen in **Figure 3.4**, infected cultures treated with IFN β retained neurosphere morphology and did not exhibit observable cytopathic effects as untreated cultures at the same time point (**Figure 3.4A**). Furthermore, expression of the virus as determined by GFP expression was inhibited in the treated cultures as compared to the untreated cultures (**Figure 3.4B**). Viral titers in the treated cultures were also lower than that of the untreated cultures (**Figure 3.4C**); however, these differences were transient and depended on continued presence of IFN β . When the media was changed with fresh media between day 4 and day 5 post-infection, the differences between the treated and untreated cultures diminished. This experiment demonstrated that IFN β was protective in NPSCs cultures, but did not disaggregate the effect of the Type I interferon response from possible direct effects of IFN β on the virus itself.

To further examine the protective effects of the Type I interferon response, NPSCs isolated from actin-GFP transgenic mice were subjected to one of three treatments and then mixed with NPSCs isolated from C57 black mice which were infected for 1 hour with dsRed-CVB3. The GFP NPSCs were treated with 100U/mL IFN β and then mixed with equal parts dsRed-CVB3-infected C57 NPSCs (**Figure 3.5A**); treated with 100U/mL IFN β , then washed of the IFN β , and mixed with equal parts dsRed-CVB3-infected C57 NPSCs (**Figure 3.5B**); or left untreated and mixed with equal parts dsRed-CVB3-infected C57 NPSCs (**Figure 3.5C**). The cultures were then examined for red fluorescence,

green fluorescence, or both; as well as, stained with Trypan blue for live/dead counts. As seen in **Figure 3.5C**, treatment with IFN β suppressed viral protein expression (lack of red fluorescence), as well as the cell death associated with acute infections. In the condition where the GFP NPSCs were treated with IFN β for two hours, and then washed of IFN β prior to mixing with dsRed-CVB3-infected NPSCs, transient protection of both the GFP and C57 NPSCs is observed at day two post-infection. This is evident from the decreased expression of red fluorescence in figure 6B on day 2 pi as compared to the red fluorescence in figure 6A at the same time point. Additionally, the percentage of cell death in the IFN β -treated condition is also lower at the same time point than in the untreated condition. Taken together, this demonstrates that the Type I interferon response is transiently protective in the absence of exogenous Interferon β .

Finally, to ensure that the type I interferon response could be induced in the absence of exogenous IFN β , and to demonstrate that this induction could be transiently protective, we pre-treated NPSCs isolated from C57 black mice with media (no treatment), NPSC cell lysate, 10 μ g/mL Poly I:C, or UV-inactivated dsRed-CVB3. These cultures were then infected with eGFP-CVB3 at an MOI of 1, and the course of infection examined by GFP expression and plaque assay for viral titers (**Figure 3.6A**). Priming the cultures corresponded to lower levels of GFP expression at 1 day post-infection, suggesting a delay (protective effect) in the infection of the primed cultures; however by 2 days post-infection, the GFP expression was actually higher than that of the

unprimed cultures (**Figure 3.6B**). This higher GFP expression may be due to the transient protection of the primed cells against the cytopathic effects of the virus, which improves their ability to survive the first day of infection, increasing the number of GFP-expressing cells at 2 days post-infection. By day 3 post-infection, only the cultures primed with cell lysate had significantly different GFP expression. In terms of viral titers, only cultures primed with Poly I:C (a known inducer of the Type I Interferon response) exhibited lower titers throughout the duration of the experiment (**Figure 3.6C**). This data suggests that the type I interferon response can be induced without exogenous IFN β , and this response may be transiently protective.

The decreased susceptibility to superinfection in Persistently-infected NPSCs is specific to CVB3. Since the Type I interferon response is a generalized, innate immune system response, we designed infection experiments to examine whether or not this protection from superinfection was specific for CVB3 or could be generalized to other viruses. C57 NPSCs or NPSCs Persistently-infected with CVB3 were infected with eGFP-CVB3, LCMV, or both at a total MOI of 0.1 (**Supplementary Figure 3.1A**). Immunocytochemistry was performed to determine if CVB3-infected cells (green) could be superinfected by LCMV (red). Cultures infected by LCMV had a tendency to stick down and differentiate (either due to the virus or the vehicle), and the Survivor cultures which do not appear to get superinfected by CVB3 (no green expression), exhibited the same differentiating morphology, suggesting

superinfection by LCMV. Immunostaining confirmed the superinfection of NPSCs upon co-infection (simultaneous infection) of the NPSCs by both viruses.

The ability of naïve NPSCs and CVB3-persistently-infected NPSCs to get superinfected by a virus other than CVB3 was tested with a second virus: VSV. C57 and Survivors were treated either with media (mock infection), dsRed-CVB3, or GFP-VSV at an MOI of 0.1. Again, no superinfection by CVB3 was observed in the eGFP-CVB3 persistently-infected cultures as determined by fluorescence microscopy (**Figure 3.7A**) and by a multi-mode plate reader (**Figure 3.7B**). Both naïve and CVB3-persistently-infected NPSCs were treated with 100U/mL exogenous interferon- β prior to infection with GFP-VSV at an MOI of 0.1. While GFP fluorescence in these cultures was below the detection limit of the plate reader due to the high background of the media in the green channel (data not shown), a delayed expression of GFP could be observed by fluorescence microscopy (**Figure 3.7A**), indicating that the type I interferon response could transiently inhibit the expression of VSV viral proteins.

Finally, eGFP-VSV infected and killed all the cultures irrespective of whether or not the NPSCs had previously been survived an eGFP-CVB3 infection. This suggests that the strong protection against superinfection exhibited by CVB3-persistently-infected cultures is specific to CVB3. However, the GFP-VSV reached its highest level of expression sooner in naïve NPSCs as compared to CVB3-persistently-infected NPSCs suggesting that there may be a low level of generalized antiviral activity occurring in CVB3-persistently-infected cultures (**Figure 3.7A and C**). Additionally, CVB3-persistently-infected

NPSCs reached higher levels of GFP expression later on than naïve NPSCs suggesting that these persistently-infected NPSCs were hardier than their naïve counterparts. The persistently-infected NPSCs appeared better able to withstand the cytopathic effects of VSV, allowing them to survive for longer and express higher levels of GFP-VSV (**Figure 3.7C**). This data suggests that the type I IFN response may confer some protection against the cell death mediated by superinfection by VSV, even if it is unable to protect against superinfection by VSV.

The lack of a functional Type I interferon response affects the ability of the virus to evolve and persist. We previously observed the evolution of the CVB3 in the course of persistent infection and suspected that the type I interferon response played an important role in the attenuation of the virus, which enabled its persistence. To examine the role of the type I interferon response in the evolution of the virus, we isolated NPSCs from Interferon α/β receptor knock out mice (IFN α/β r k/o) as well as from C57/BLK6 mice, and then performed infections in these newly isolated NPSCs. As seen in **Figure 3.8A**, CVB3-infected NPSCs isolated from C57 mice exhibited shrinking viral plaque sizes over time. In contrast, CVB3-infected NPSCs isolated from IFN α/β r k/o mice did not exhibit shrinking viral plaque sizes at the same time points. The average plaque size was quantified using ImageJ and found to be significantly different at the later time points (**Figure 3.8B**).

Viral titers of both types of NPSCs were found to peak at day 3 post infection, though the NPSCs derived from C57 mice were found to support a lower viral titer overall as compared to NPSCs derived from IFN α/β r k/o mice. To verify that IFN α/β r k/o NPSCs did not respond to interferon treatment, both C57 and IFN α/β r k/o derived NPSCs were treated with exogenous interferon β and then infected. While viral titers could not always be observed in the cultures derived from C57 mice (viral suppression occurring), the presence of the exogenous interferon did not drastically alter the viral titers in the NPSCs derived from IFN α/β r k/o mice. Taken together this data confirms that the NPSCs derived from IFN α/β r k/o mice have a defective type I interferon response, and that this interferon response is important for the evolution and consequently the persistence of the virus in NPSCs.

Discussion

We have previously demonstrated that the differentiation status of NPSCs affects their susceptibility to CVB3 infection (Tsueng et al., 2011), and observed that CVB3 evolves in its host in order to persist in neural progenitor and stem cells. These observations led us to investigate the selective pressures in the environment which triggered the evolution of the virus—in particular, the host cell innate immune response. Type I interferons have been established as an important survival factor in cardiotropic infections of CVB3 (Deonarain et al., 2004). We therefore expected the Type I interferon response to play an important role in neurotropic infections by CVB3 and the establishment of viral

persistence. The interferon response of NPSCs has recently been investigated in the context of demyelization diseases such as Multiple Sclerosis.

While it is known that exogenous Type I interferons can help ameliorate some of the symptoms of MS, the mechanism by which this effect occurs is still under investigation. The addition of exogenous Interferon- β has been found to reduce apoptosis (Hirsch et al., 2009), and may be somewhat anti-proliferative—arresting NPSCs in the G1 phase of the cell cycle in mice (Lum et al., 2009). Our findings that NPSCs stimulated to produce interferons with Poly I:C or cell lysate were able to withstand CVB3 infection longer, could be attributed to this anti-apoptotic effect, which could be beneficial to the virus as it allows for longer production of virus on a per cell basis.

The Type I interferons are important in modulating dendritic cell differentiation and viruses have been found to manipulate the type I interferon response in order to modulate dendritic cell differentiation and evade the immune system (Hahm B). Different subtypes of type I interferons can induce differentiation of dendritic cells with different characteristics specific to the subtype of the interferon inducer (Garcin et al., 2013), thus type I interferons play an extremely important role in differentiation during an immune response, but what about differentiation in the central nervous system? Modified interferon- β (betaseron) has been found to induce proliferation at high doses, as well as induce differentiation of human NPSCs in a dose-dependent fashion (Arscott et al., 2011).

We also previously observed an increased propensity to differentiate in these cultures, though we did not observe any changes in proliferation. Here we demonstrated that NPSCs are capable of producing and are responsive to interferon- β in the context of coxsackievirus infection. While we detected only low levels of interferon- β globally, the local concentrations might be sufficiently high to protect individual clusters of cells from the harmful effects of the virus.

The chronic exposure of the NPSCs to endogenous type I interferons may be increasing the propensity of the NPSCs to spontaneously differentiate as differentiation may confer increased survivability of these cells in the context of CVB3 infection. Not only do more differentiated neural cell types express lower levels of the Coxsackievirus and Adenovirus Receptor (CAR) thus limiting the ability of the virus to enter the cell (Ahn et al., 2008), but differentiation may increase the type I interferon response to stimulation (Farmer et al., 2013). The induction of the type I interferon response and the increased propensity of CVB3-persistently-infected NPSCs to differentiate contributes to the selective pressures that drive the evolution of the virus. Taken together, the type I interferon response plays an important role in protecting the host during neurotropic infections; but this protection comes at a potential cost as this protective response is the very one that forces the virus to evolve, enabling its persistence in the host. Furthermore, premature differentiation of the NPSCs is a potential consequence of the chronic exposure to type I interferons due to

the ongoing presence of the virus, and this can have serious implications in the development of the neurological diseases.

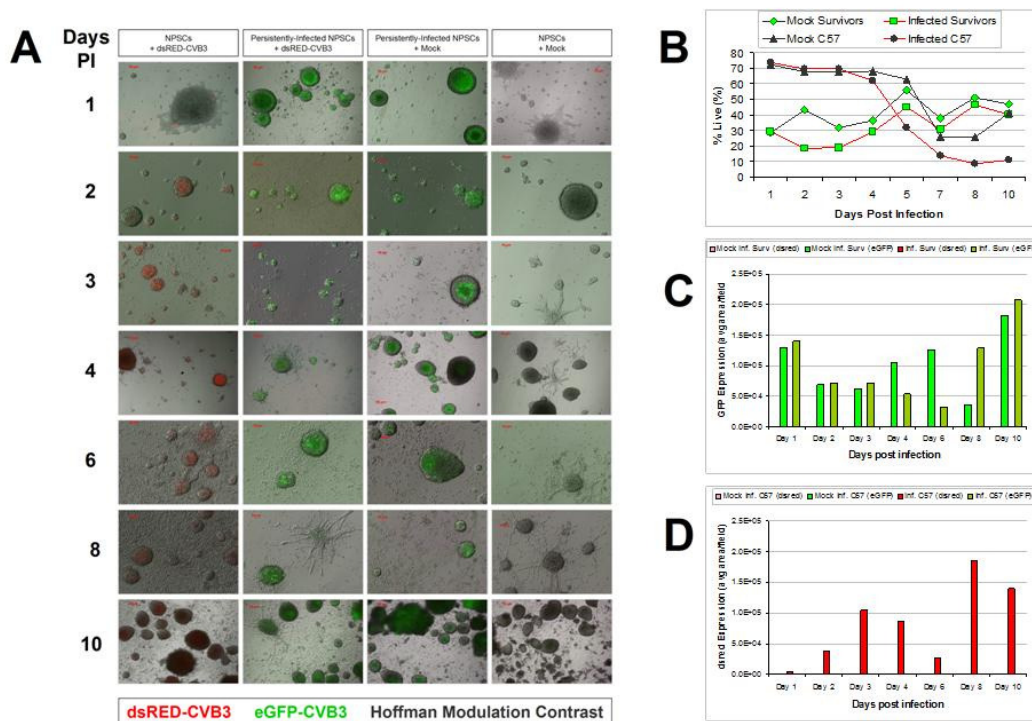


Figure 3.1. Persistently-infected cells are resistant to superinfection.

NPSCs, and NPSCs Persistently-infected with GFP-CVB3 (carrier-state/survivors) are Infected with media (mock) or dsRed-CVB3 and examined for superinfection. Representative images **(A)** reveal red fluorescence upon infection in NPSCs, but not upon infection in carrier-state NPSCs. **(B)** Infected and mock infected NPSCs and carrier-state NPSCs were examined for viability, and a reduced viability was observed in the NPSCs infected by dsRed. Viability of the NPSCs in the mock-infected condition dropped precipitously after 5 days in culture due to overgrowth and subsequent exhaustion of the media. ImageJ analysis of representative images shows that GFP is only observed in the carrier-state cultures **(C)**, and dsRed is not observed in carrier-state NPSCs in spite of dsRed-CVB3 inoculation into both uninfected and carrier-state NPSCs **(D)**.

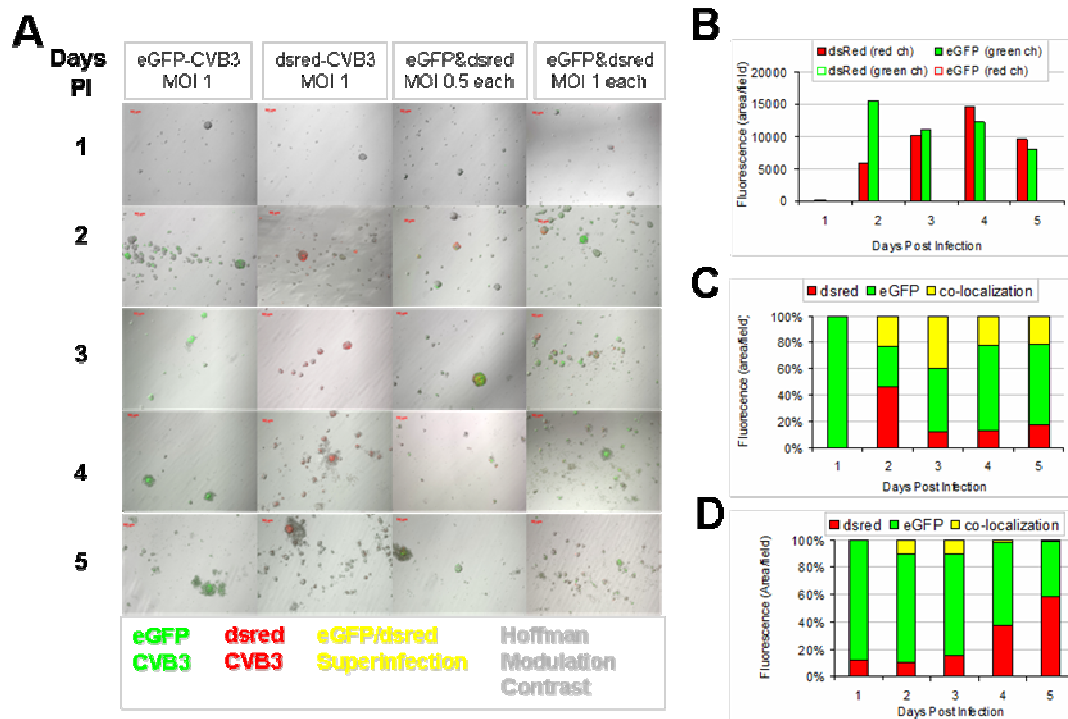


Figure 3.2. Superinfection occurs in naïve NPSCs upon concurrent inoculation.

Representative images **(A)** of NPSCs upon infection with eGFP-CVB3 at an MOI of 1, dsRed-CVVB3 at an MOI of 1, both viruses at an MOI of 0.5, or both viruses at an MOI of 1 reveal that alone, each virus reaches similar expression levels after two days post-infection, with little background signal **(B)**. Furthermore, slightly higher levels of superinfection can be observed upon simultaneous infection at an MOI of 0.5 **(C)**, than at an MOI of 1 **(D)**.

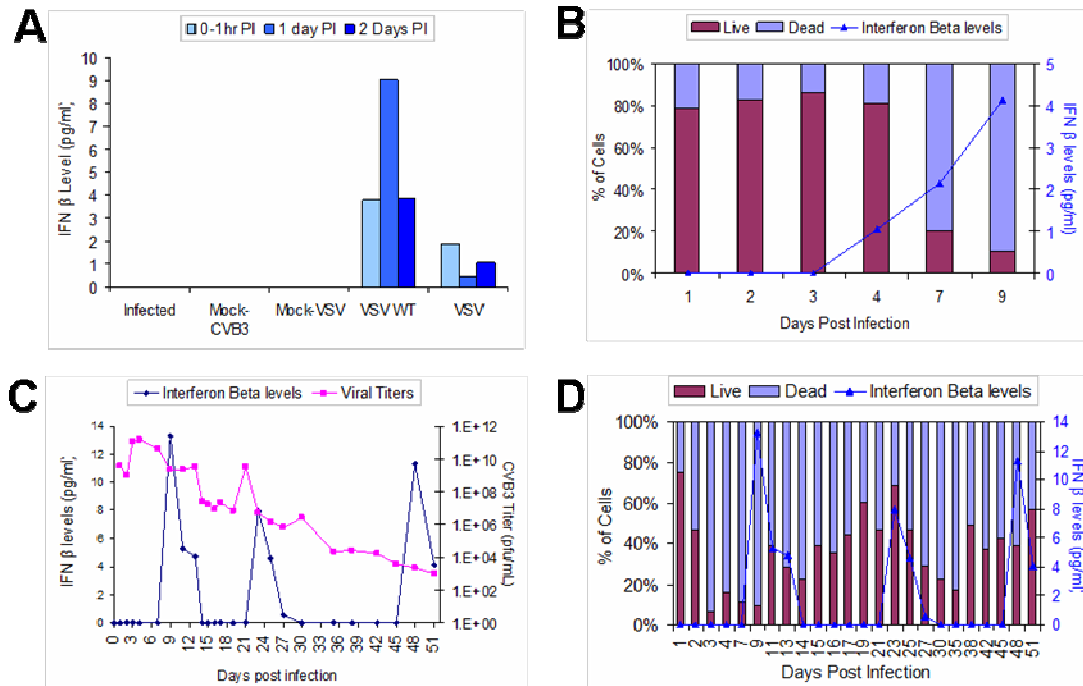


Figure 3.3. Interferon is produced during the course of infection.

Interferon β production is observed within 2 days post-infection in VSV-infected, but not CVB3-infected or Mock-infected cultures (**A**). Interferon β is produced in mock-infected cultures after prolonged culturing as cell viability decreases due to overgrowth and media exhaustion (**B**). During prolonged/persistent infection, interferon β is observed to spike periodically (**C**), generally following a spike in viral titer, and subsequently followed by a decrease in viral titers. The infected NPSCs exhibit robust cycles of proliferation and cell death, with viability increasing slightly after each spike in endogenous interferon β (**D**).

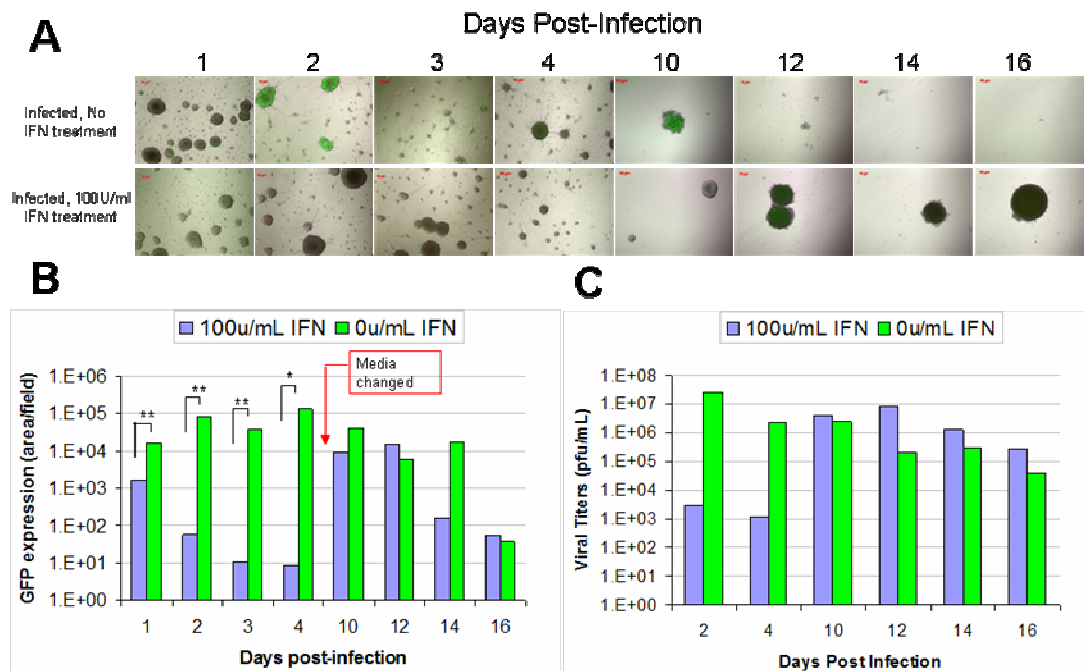


Figure 3.4. Interferon β treatment inhibits viral protein expression.

The addition of 100u/ml severely inhibits viral protein expression as seen by the lack of green fluorescence in the representative images of IFN-treated cultures vs untreated cultures (**A**). When quantified by ImageJ (**B**), the differences in green fluorescence in the untreated cultures was significantly lower than those of IFN treated cultures up until the media was changed (and the exogenous interferon washed out). Viral titers (**C**) mirror the GFP expression.

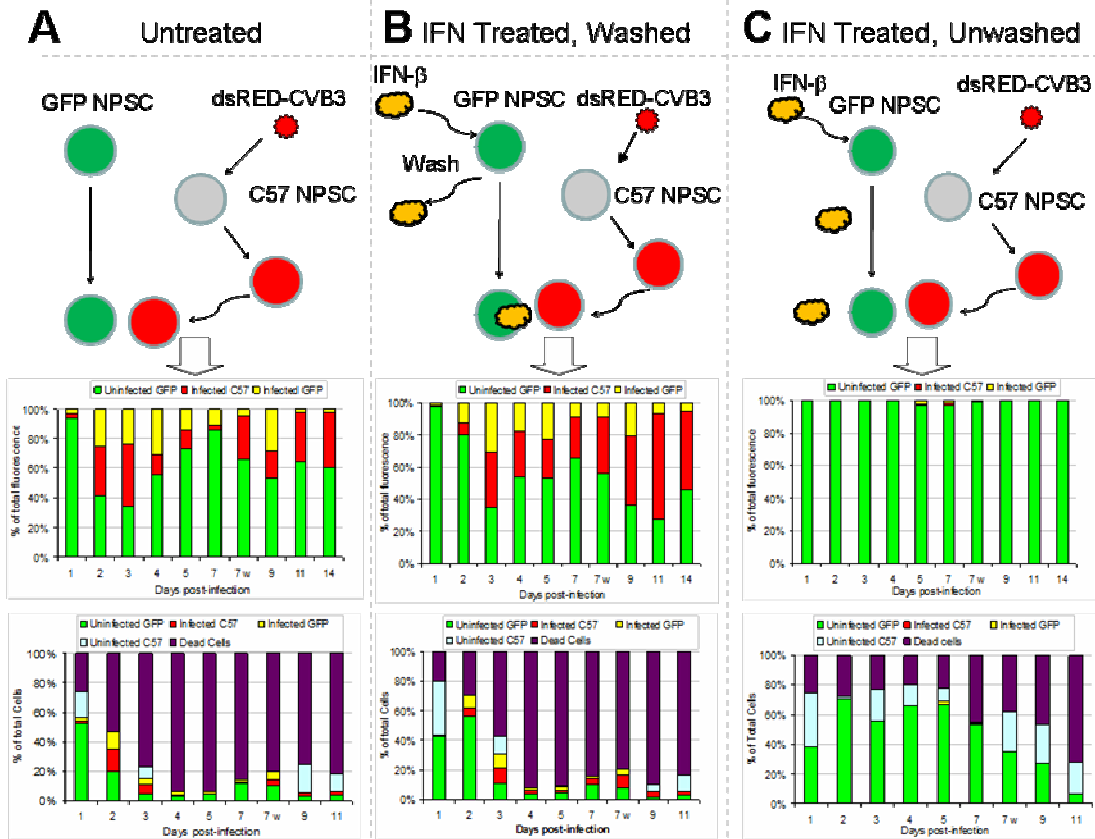


Figure 3.5. The induction of the type I interferon response is transiently protective in the absence of exogenous interferons.

NPSCs derived from GFP-actin transgenic mice were treated with media or exogenous interferon β for two hours while C57-derived NPSCs were incubated with dsRed-CVB3. The equal parts of the untreated GFP-actin NPSCs were then mixed with the dsRed-CVB3 infected NPSCs and co-cultured (**A**), revealing the course of a normal infection. The interferon-treated GFP-actin derived NPSCs was mixed with dsRed-CVB3 infected C57 NPSCs and co-cultured to reveal the effects of the prolonged presence of interferon (**C**), or the interferon-treated NPSCs were washed prior to co-culturing with dsRed-CVB3 infected C57 NPSCs to reveal the stimulation of protective factors which offer transient protection to the cultures in the absence of exogenous interferon β (**B**).

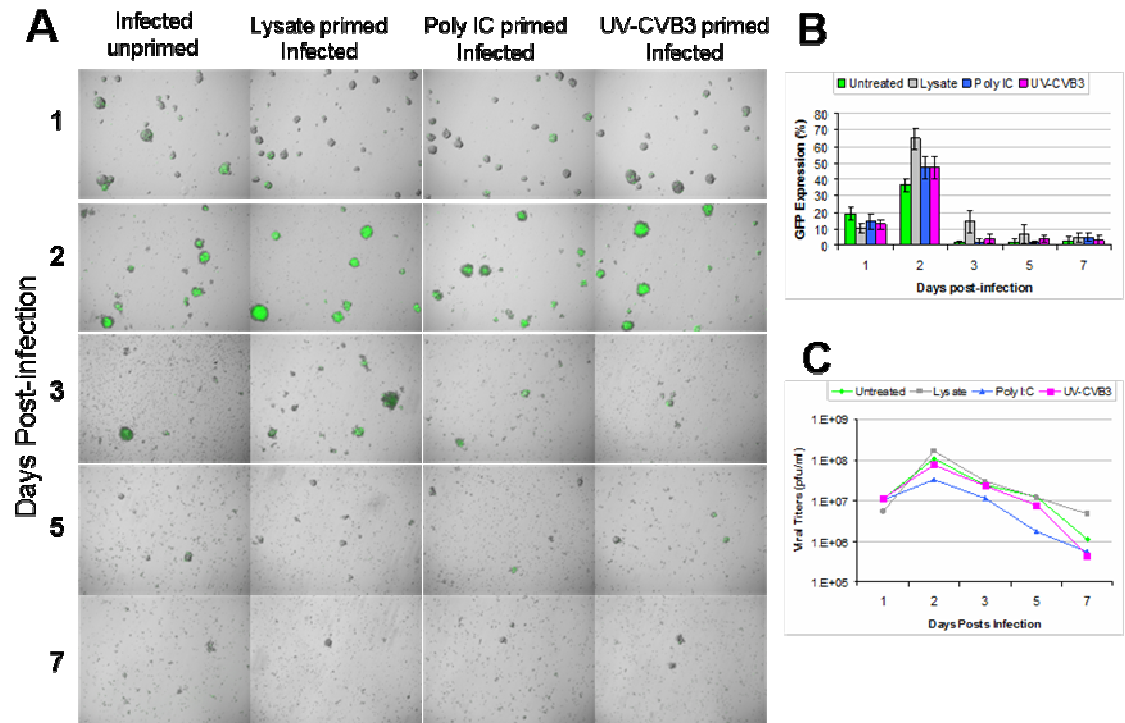


Figure 3.6. Priming the innate immune response may protect cells from virus-induced CPE.

NPCs were primed with nothing (mock/unprimed), lysate, Poly I:C, or UV-irradiated dsRed-CVB3 and then infected with eGFP-CVB3 and imaged over the course of 7 days (**A**). ImageJ analysis revealed significantly higher GFP expression levels in the untreated cultures at 1 day post-infection as compared to the primed cultures, suggesting that priming of the innate immune response may be protective (**B**). At 2 days post-infection and beyond, primed cultures exhibited higher GFP expression levels, suggesting that priming the cultures allows them to survive better, thus allowing for greater viral protein expression. Viral titers in the Poly I:C primed cultures (**C**) were consistently lower than any of the other conditions.

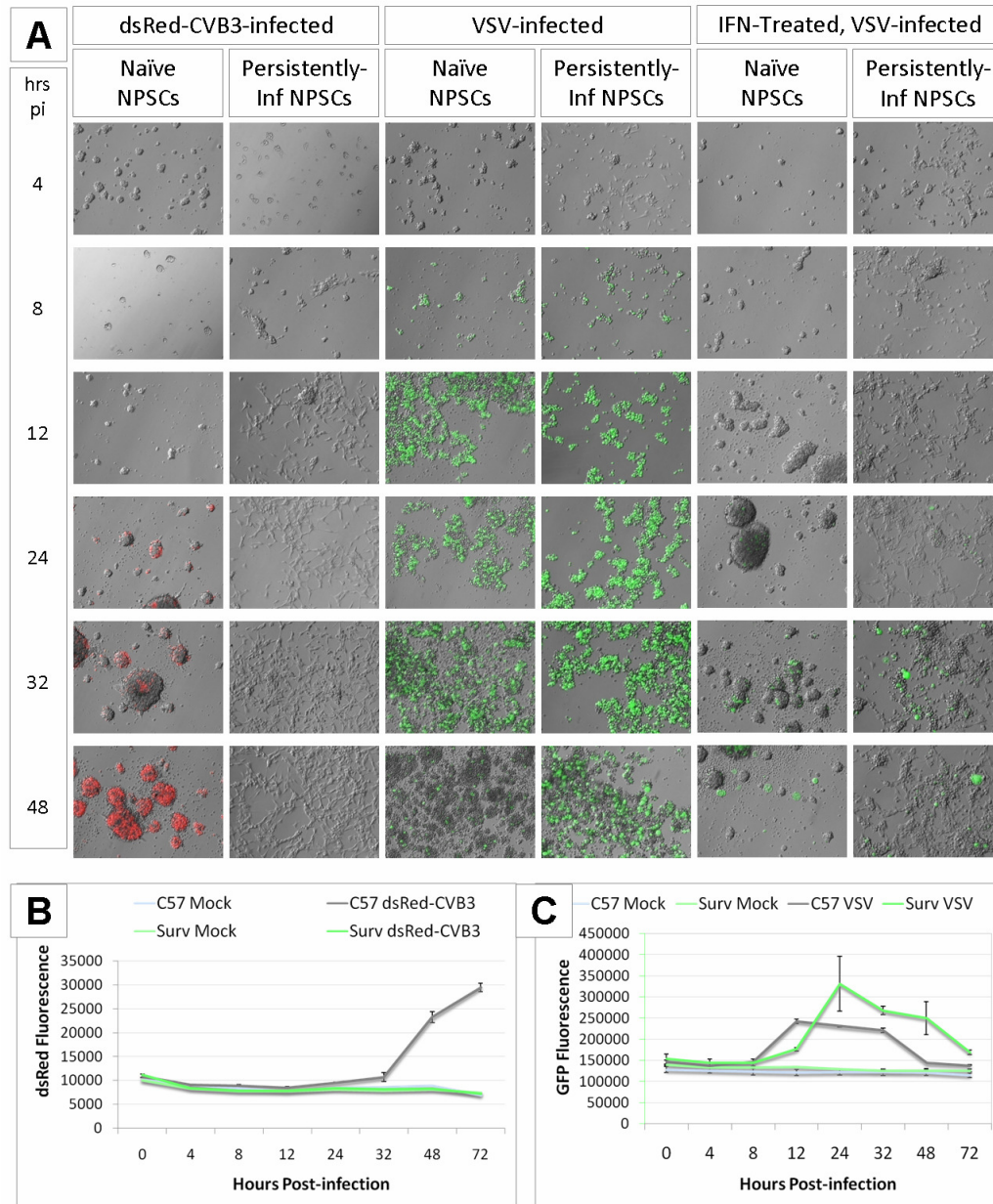


Figure 3.7. Persistently-infected NPSCs are still vulnerable to superinfection by VSV.

Again, persistently-infected NPSCs do not exhibit successful infection by dsred-CVB3 as compared to naïve/uninfected C57 NPSCs (**A and B**). Both naïve and survivor NPSCs exhibit green fluorescence upon infection with eGFP-VSV (**A**), although the green fluorescence peaked earlier in the naïve cultures and did not reach the levels exhibited by the persistently-infected cultures as determined by a multi-mode plate reader (**C**). This suggests that NPSCs previously infected by CVB3 may survive slightly better than naïve NPSCs when infected with VSV.

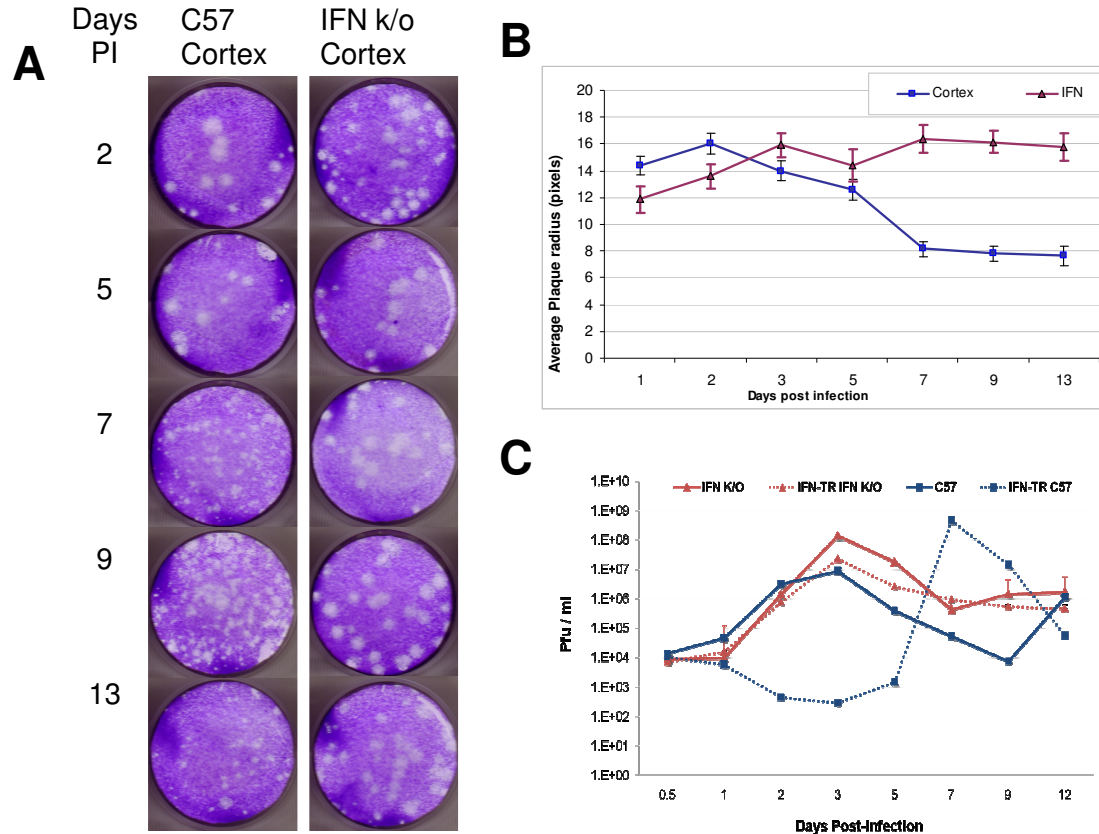
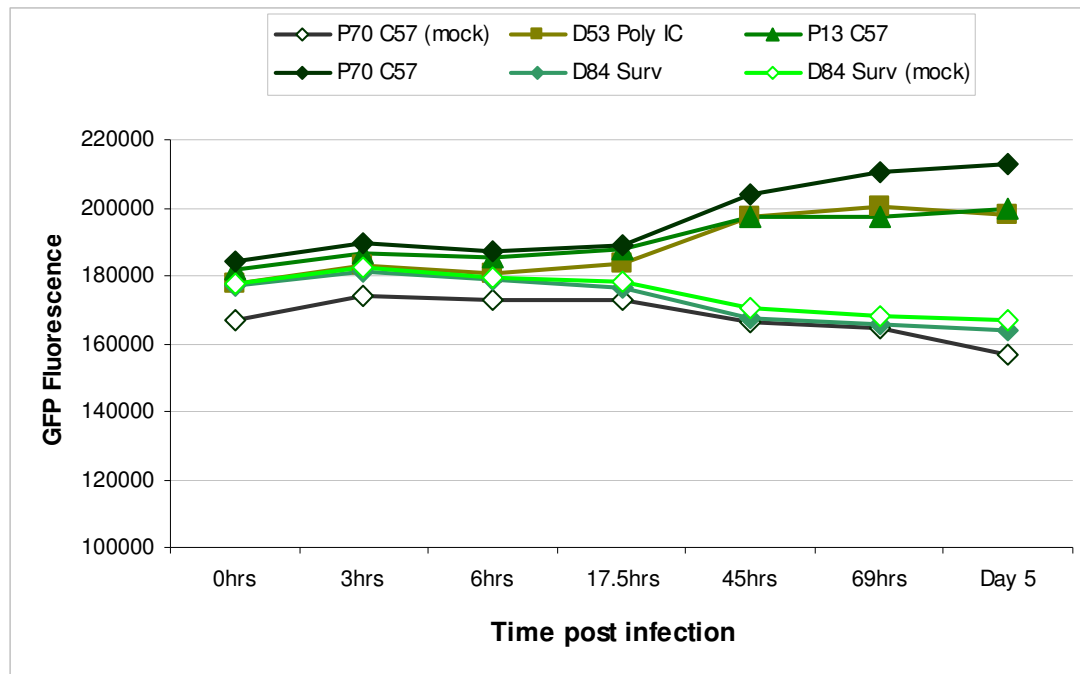


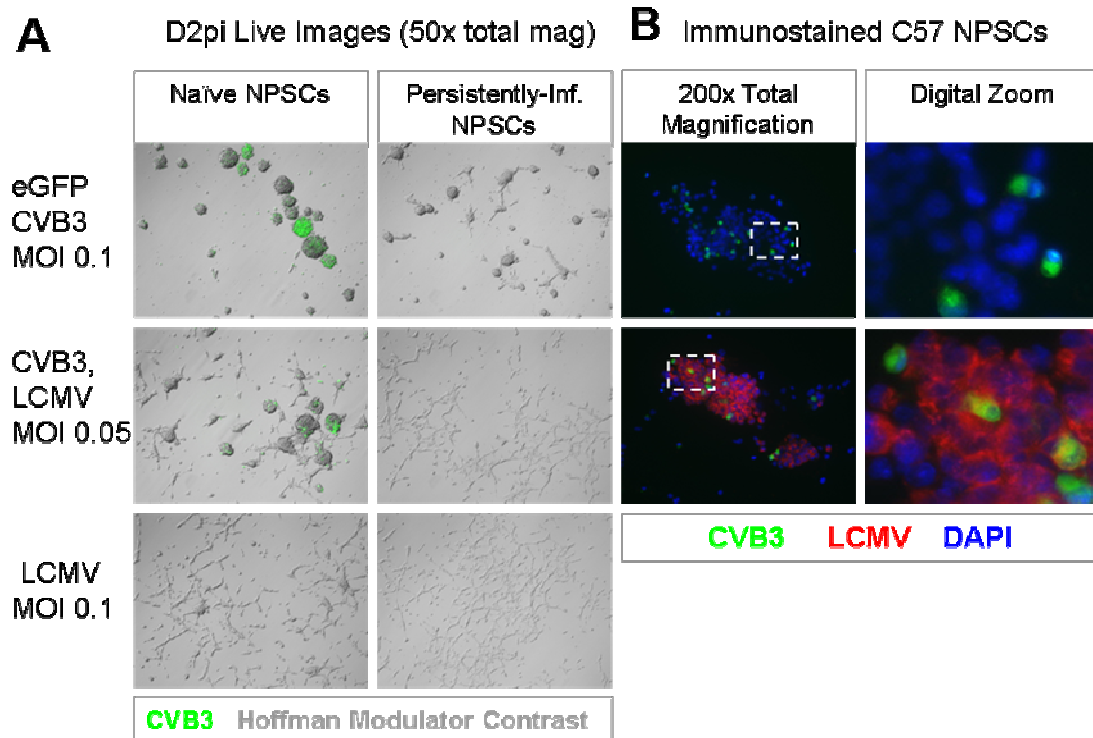
Figure 3.8. The type I interferons are important for CVB3 evolution.

Plaque assays for viral titers reveal that infectious virus from NPSCs derived from C57 mice change over time as compared to those infecting NPSCs derived from Interferon α/β r k/o transgenic mice (**A**). ImageJ analysis of the plaque size reveals that the decrease in plaque size in the cells with the type I interferon response intact is significant at the later time points (**B**), and that the viral titers are higher in the cultures with the type I interferon response knocked out (C).



Supplementary Figure 3.1. Persistently-infected NPSCs do not exhibit superinfection by CVB3.

Cultures previously infected by GFP-CVB3 (survivors/carrier-state cultures) were passaged until GFP could no longer be detected by microscopy. Survivor cultures and similar passage NPSCs were then infected with GFP-CVB3 and examined for green fluorescence using a plate reader, confirming the lack of green fluorescence in the mock-infected carrier-state cultures (GFP is really gone), and the lack of green fluorescence in the re-infected carrier-state cultures (ie- lack of superinfection) as compared to the freshly infected naïve NPSCs.



Supplementary Figure 3.2. Infected and persistently-infected NPSCs can still be superinfected by LCMV.

Again, carrier-state/survivor NPSCs do not exhibit successful infection by CVB3 as compared to naïve/uninfected C57 NPSCs. Both naïve and persistently-infected NPSCs exhibit differentiating morphology when infected by LCMV **(A)**. Immunostaining of the cultures reveals that LCMV can superinfect CVB3-infected cultures **(B)**.

Acknowledgements

Chapter 3, in part is currently being prepared for submission for publication of the material. Tsueng, G; Rahawi, S; Deline, S; Tabor-Godwin, JM; Ruedas, J; Perrault, J; Cornell, CT; Whitton, JL; Feuer, R. The dissertation author was the primary investigator and author of this material. This work was supported by National Institutes of Health (NIH) R01 Award NS054108 (to R.F.), an NIH Research Supplement to Promote Diversity in Health-Related Research Award 3R01NS054108-01A2S1 (to R.F.), and a National Institutes of Mental Health (NIMH) Minority Research Infrastructure Support Program (M-RISP) R24 Faculty Fellow Award MH065515 (to R.F.). Ginger Tsueng is recipient of an Achievement Rewards for College Scientists (ARCS) Foundation Scholarship, an Inamori Fellowship, and a Gen-Probe Fellowship. No conflicts of interest exist between the subject matter and the authors included in the manuscript.

CONCLUSION OF THE DISSERTATION

CVB3 can cause encephalitis and meningitis upon acute infection of the central nervous system. CVB3 targets proliferating neural stem and progenitor cells in the CNS (Feuer et al., 2005) has been found to persist for at least 90 days in a neonatal mouse model of infection (Feuer et al., 2009). CVB3 infection of the CNS has been correlated with several long-term neurological disorders such as learning disorders (Chamberlain et al., 1983), schizophrenia (Dalman et al., 2008) (Koponen et al., 2004) (Rantakallio et al., 1997), and demyelinating diseases (Berger et al., 2009) (Agin et al., 2010) (Verboon-Maciolek et al., 2006). Although the initial targets of infection have been identified, it is unclear which cells harbor the virus long-term, how the virus is able to persist in the CNS, and how the persistence of the virus affects the development of neurological disorders. In order to better understand the tropism and susceptibility of neural targets in the CNS, we developed an *in vitro* model of acute CNS infection using cultured mouse neural progenitor and stem cells (NPSCs) (chapter 1).

Using this model, we determined that more differentiated cell types were less susceptible to infection than less differentiated cell types in the CNS. We also observed blebbing the infected cells which we initially attributed to apoptosis. Further studies with a recombinant CVB3 containing a timer protein have elucidated these blebs to be infectious microvesicles which are being shed through the autophagic pathway (data not shown). In this manner, the

normally cytolytic CVB3 may be spread to uninfected cells without destruction of the host cell. We also observed that we could potentially extend this model from acute CNS infection to persistent CNS infection and that stem cells could potentially serve as a reservoir for the virus during viral persistence.

We next extended this model to understand previously observed CVB3 persistence *in vivo* through the development of carrier-state cultures *in vitro* (chapter 2). While no alterations in the gross differentiation and proliferation potentials were observed in these carrier-state cultures, a propensity to spontaneously differentiate was observed. Additional studies are needed to determine if carrier-state NPSCs are altered in terms of functional differentiation. Although we have demonstrated no bias in the propensity of the NPSCs to differentiate towards oligodendrocytes, neurons and astrocytes; there may be alterations in the differentiation potential towards a particular type of neuron or astrocyte. Are the NPSCs biased to differentiate into Type I vs Type II astrocytes? Are they more likely to differentiate towards glutamatergic vs dopaminergic neurons? Even if there is no bias, are neurons from differentiated carrier-state cultures even functional?

Mutations in the GABA (A) receptor has been associated with autism (Pizzarelli and Cherubini, 2011), but a deficiency in the development of functional gabanergic signaling may be the culprit (Kang and Barnes, 2013). Furthermore, differentiating NPSCs migrate from the site of neurogenesis, and alterations in differentiation propensity could affect the proper migration of these cells resulting in neurological disorders. IL-6 induced alterations of neural

migration in the cerebellum is thought to be at least partially responsible for the pathogenesis of autism (Wei et al., 2011). Levels of neural progenitors in the hippocampal region have been associated with memory impairment and addictive behavior (Recinto et al., 2012). If CVB3 preferentially targets the neurogenic region of the brain and CVB3-infected NPSCs have an increased propensity to differentiate, then the net effect could be similar to neural precursor depletion. CVB3-induced alterations in differentiation propensity and functional differentiation could have an important impact on the development of neurological diseases following persistent CNS infection.

In examining the virus receptor levels in differentiated and undifferentiated cultures, we learned that the previously observed decrease susceptibility of differentiated NPSCs could be attributed to the decreased CAR expression levels in differentiated NPSCs as compared to the undifferentiated counterpart. Thus, the increased propensity to spontaneously differentiate may help to reduce the susceptibility of the NPSCs to the virus. This observed increase in propensity of carrier-state NPSCs to differentiate may be attributed to the selective advantage of these cells over ones that do not. Further work is needed to clarify whether the host downregulation of the CAR receptor is responsible for the observed increase in spontaneous differentiation, or if the spontaneous differentiation triggers the downregulation of the CAR receptor.

While the downregulation of CAR contributes to the decreased susceptibility to infection, it is only one part of the story. Differentiation status

can have profound effects on autophagy (Tabor-Godwin et al., 2012), proliferation/cell cycle status (Salomoni and Calegari, 2010), and vice versa—all of which may contribute to the decreased susceptibility of carrier-state NPSCs to infection by CVB3. Current comparative studies of cortical and cerebellar NPSCs from neonatal and adult mice implicate proliferative status as an important factor in NPSC susceptibility to CVB3 infection. The decreased proliferative status of NPSCs in the adult CNS may contribute to the decreased susceptibility of the adult CNS to infection as compared to that of the neonate (Feuer et al., 2004), and the decreased susceptibility of the cerebellar regions as compared to the cortical regions (Gauntt et al., 1984). Cell cycle status is known to affect CVB3 replication (Feuer et al., 2002b) and has been proposed to be a potential regulatory mechanism for CVB3 persistence (Feuer et al., 2004) as CVB3 replicates best in the G1 and G1/S phase. The length of the G1 phase is suspected to directly influence the differentiation of neural precursors (Salomoni and Calegari, 2010). Taken together, differentiation can affect susceptibility to infection, and infection can affect propensity to differentiate. Additional studies are currently underway to understand how neonatal infections affect the NPSCs populations after the neonate has developed into an adult.

Using our carrier-state model, we also confirmed the previous *in vivo* observation that persistent virus was different from the virus from the initial infection. We isolated and sequenced virus from the carrier-state cultures to understand how the virus was changing over the course of infection. We not

only observed mutations in the VP2 capsid proteins which could affect the ability of the virus to bind to the CAR receptor and affect its ability to infect new cells, we also observed mutations in the 2C and 3A proteins which can affect CVB3's ability to replicate (van Ooij et al., 2006) (van der Schaar et al., 2012). The mutations in the 3A protein also have implications for the formation of replication complexes in the host cell (Wessels et al., 2005), which may be linked to the aforementioned formation and release of infectious extracellular microvessicles. Current studies are underway to elucidate the ability of these infectious extracellular microvessicles as a new mechanism of infection and a potential method for evading the antibody response in the host. Future work is needed to confirm that the mutations observed in our carrier-state cultures are similar to those in the persistently-infected mice.

Finally, to understand the selection pressures that encouraged the evolution of this cytolytic virus into a non-cytolytic one, we utilized our *in vitro* of persistent infection to investigate the ability of NPSCs to produce type I interferons and the effects of the type I interferon response on CVB3 infections in the CNS. Not only were NPSCs capable of producing type I interferons like interferon- β , but NPSCs were also protected by the type I interferon response in the context of CVB3 infection. Additional studies are needed to understand the effects of chronic exposure to type I interferons on NPSC behavior. This transient protection offered a mechanism by which highly susceptible NPSCs could evade CVB3-induced cytopathic effects, and allow for not only the survival of NPSCs, but also the evolution of CVB3. To confirm the importance

of the type I interferon response in the evolution of the virus, we infected NPSCs isolated from transgenic knock out mice lacking the interferon α/β receptors. Taken together, the type I interferon is important for the survival of the host during CVB3 infections, and also the evolution of the virus and its persistence in the host CNS.

REFERENCES

- Agin H, Apa H, Unalp A, Kayserili E (2010) Acute disseminated encephalomyelitis associated with enteroviral infection. *Neurosciences (Riyadh)* 15:46-48.
- Ahn J, Jee Y, Seo I, Yoon SY, Kim D, Kim YK, Lee H (2008) Primary neurons become less susceptible to coxsackievirus B5 following maturation: the correlation with the decreased level of CAR expression on cell surface. *J Med Virol* 80:434-440.
- Arcott WT, Soltys J, Knight J, Mao-Draayer Y (2011) Interferon beta-1b directly modulates human neural stem/progenitor cell fate. *Brain Res* 1413:1-8.
- Berger JR, Fee DB, Nelson P, Nuovo G (2009) Coxsackie B meningoencephalitis in a patient with acquired immunodeficiency syndrome and a multiple sclerosis-like illness. *J Neurovirol* 15:282-287.
- Bez A, Corsini E, Curti D, Biggiogera M, Colombo A, Nicosia RF, Pagano SF, Parati EA (2003) Neurosphere and neurosphere-forming cells: morphological and ultrastructural characterization. *Brain Res* 993:18-29.
- Chamberlain RN, Christie PN, Holt KS, Huntley RM, Pollard R, Roche MC (1983) A study of school children who had identified virus infections of the central nervous system during infancy. *Child Care Health Dev* 9:29-47.
- Chapman NM, Kim KS (2008) Persistent coxsackievirus infection: enterovirus persistence in chronic myocarditis and dilated cardiomyopathy. *Curr Top Microbiol Immunol* 323:275-292.
- Cheung PK, Yuan J, Zhang HM, Chau D, Yanagawa B, Suarez A, McManus B, Yang D (2005) Specific interactions of mouse organ proteins with the 5'untranslated region of coxsackievirus B3: potential determinants of viral tissue tropism. *J Med Virol* 77:414-424.
- Dalman C, Allebeck P, Gunnell D, Harrison G, Kristensson K, Lewis G, Lofving S, Rasmussen F, Wicks S, Karlsson H (2008) Infections in the CNS during childhood and the risk of subsequent psychotic illness: a cohort study of more than one million Swedish subjects. *Am J Psychiatry* 165:59-65.
- Deonarain R, Cerullo D, Fuse K, Liu PP, Fish EN (2004) Protective role for interferon-beta in coxsackievirus B3 infection. *Circulation* 110:3540-3543.
- Domingo E, Martin V, Perales C, Escarmis C (2008) Coxsackieviruses and quasispecies theory: evolution of enteroviruses. *Curr Top Microbiol Immunol* 323:3-32.

Farmer JR, Altschaeffl KM, O'Shea KS, Miller DJ (2013) Activation of the type I interferon pathway is enhanced in response to human neuronal differentiation. *PLoS One* 8:e58813.

Feuer R, Mena I, Pagarigan R, Slifka MK, Whitton JL (2002a) Cell cycle status affects coxsackievirus replication, persistence, and reactivation in vitro. *J Virol* 76:4430-4440.

Feuer R, Mena I, Pagarigan R, Slifka MK, Whitton JL (2002b) Cell cycle status affects coxsackievirus replication, persistence, and reactivation in vitro. *J Virol* 76:4430-4440.

Feuer R, Mena I, Pagarigan RR, Hassett DE, Whitton JL (2004) Coxsackievirus replication and the cell cycle: a potential regulatory mechanism for viral persistence/latency. *Med Microbiol Immunol* 193:83-90.

Feuer R, Pagarigan RR, Harkins S, Liu F, Hunziker IP, Whitton JL (2005) Coxsackievirus targets proliferating neuronal progenitor cells in the neonatal CNS. *J Neurosci* 25:2434-2444.

Feuer R, Ruller CM, An N, Tabor-Godwin JM, Rhoades RE, Maciejewski S, Pagarigan RR, Cornell CT, Crocker SJ, Kiosses WB, Pham-Mitchell N, Campbell IL, Whitton JL (2009) Viral persistence and chronic immunopathology in the adult central nervous system following Coxsackievirus infection during the neonatal period. *J Virol* 83:9356-9369.

Garcin G, Bordat Y, Chuchana P, Monneron D, Law HK, Piehler J, Uze G (2013) Differential activity of type I interferon subtypes for dendritic cell differentiation. *PLoS One* 8:e58465.

Gauntt CJ, Jones DC, Huntington HW, Arizpe HM, Gudvangen RJ, DeShambo RM (1984) Murine forebrain anomalies induced by coxsackievirus B3 variants. *J Med Virol* 14:341-355.

Harkins S, Cornell CT, Whitton JL (2005) Analysis of translational initiation in coxsackievirus B3 suggests an alternative explanation for the high frequency of R+4 in the eukaryotic consensus motif. *J Virol* 79:987-996.

Heim A, Grumbach I, Pring-Akerblom P, Stille-Siegener M, Muller G, Kandolf R, Figulla HR (1997) Inhibition of coxsackievirus B3 carrier state infection of cultured human myocardial fibroblasts by ribavirin and human natural interferon-alpha. *Antiviral Res* 34:101-111.

Heim A, Zeuke S, Weiss S, Ruschewski W, Grumbach IM (2000) Transient induction of cytokine production in human myocardial fibroblasts by coxsackievirus B3. *Circ Res* 86:753-759.

Hirsch M, Knight J, Tobita M, Soltys J, Panitch H, Mao-Draayer Y (2009) The effect of interferon-beta on mouse neural progenitor cell survival and differentiation. *Biochem Biophys Res Commun* 388:181-186.

Hyypia T, Kallajoki M, Maaronen M, Stanway G, Kandolf R, Auvinen P, Kalimo H (1993) Pathogenetic differences between coxsackie A and B virus infections in newborn mice. *Virus Res* 27:71-78.

Jakel S, Kuckelkorn U, Szalay G, Plotz M, Textoris-Taube K, Opitz E, Klingel K, Stevanovic S, Kandolf R, Kotsch K, Stangl K, Kloetzel PM, Voigt A (2009) Differential interferon responses enhance viral epitope generation by myocardial immunoproteasomes in murine enterovirus myocarditis. *Am J Pathol* 175:510-518.

Kandolf R, Canu A, Hofschneider PH (1985) Coxsackie B3 virus can replicate in cultured human foetal heart cells and is inhibited by interferon. *J Mol Cell Cardiol* 17:167-181.

Kang JQ, Barnes G (2013) A common susceptibility factor of both autism and epilepsy: functional deficiency of GABA A receptors. *J Autism Dev Disord* 43:68-79.

Kim KS, Chapman NM, Tracy S (2008) Replication of coxsackievirus B3 in primary cell cultures generates novel viral genome deletions. *J Virol* 82:2033-2037.

Knowlton KU, Jeon ES, Berkley N, Wessely R, Huber S (1996) A mutation in the puff region of VP2 attenuates the myocarditic phenotype of an infectious cDNA of the Woodruff variant of coxsackievirus B3. *J Virol* 70:7811-7818.

Koponen H, Rantakallio P, Veijola J, Jones P, Jokelainen J, Isohanni M (2004) Childhood central nervous system infections and risk for schizophrenia. *Eur Arch Psychiatry Clin Neurosci* 254:9-13.

Kuhl U, Pauschinger M, Schwimbeck PL, Seeberg B, Lober C, Noutsias M, Poller W, Schultheiss HP (2003) Interferon-beta treatment eliminates cardiotropic viruses and improves left ventricular function in patients with myocardial persistence of viral genomes and left ventricular dysfunction. *Circulation* 107:2793-2798.

Lum M, Croze E, Wagner C, McLenachan S, Mitrovic B, Turnley AM (2009) Inhibition of neurosphere proliferation by IFNgamma but not IFNbeta is coupled to neuronal differentiation. *J Neuroimmunol* 206:32-38.

McLaren FH, Svendsen CN, Van der Meide P, Joly E (2001) Analysis of neural stem cells by flow cytometry: cellular differentiation modifies patterns of MHC expression. *J Neuroimmunol* 112:35-46.

Mori H, Fujitani T, Kanemura Y, Kino-Oka M, Taya M (2007) Observational examination of aggregation and migration during early phase of neurosphere culture of mouse neural stem cells. *J Biosci Bioeng* 104:231-234.

Mukherjee A, Morosky SA, Delorme-Axford E, Dybdahl-Sissoko N, Oberste MS, Wang T, Coyne CB (2011) The coxsackievirus B 3C protease cleaves MAVS and TRIF to attenuate host type I interferon and apoptotic signaling. *PLoS Pathog* 7:e1001311.

Pfeiffer JK, Kirkegaard K (2006) Bottleneck-mediated quasispecies restriction during spread of an RNA virus from inoculation site to brain. *Proc Natl Acad Sci U S A* 103:5520-5525.

Pizzarelli R, Cherubini E (2011) Alterations of GABAergic signaling in autism spectrum disorders. *Neural Plast* 2011:297153. doi: 10.1155/2011/297153. Epub; 2011 Jun 23.:297153.

Rantakallio P, Jones P, Moring J, Von WL (1997) Association between central nervous system infections during childhood and adult onset schizophrenia and other psychoses: a 28-year follow-up. *Int J Epidemiol* 26:837-843.

Recinto P, Samant AR, Chavez G, Kim A, Yuan CJ, Soleiman M, Grant Y, Edwards S, Wee S, Koob GF, George O, Mandyam CD (2012) Levels of neural progenitors in the hippocampus predict memory impairment and relapse to drug seeking as a function of excessive methamphetamine self-administration. *Neuropsychopharmacology* 37:1275-1287.

Richtsteiger R, Henke-Gendo C, Schmidtke M, Harste G, Heim A (2003) Quantitative multiplex real-time PCR for the sensitive detection of interferon beta gene induction and viral suppression of interferon beta expression. *Cytokine* 24:190-200.

Salomoni P, Calegari F (2010) Cell cycle control of mammalian neural stem cells: putting a speed limit on G1. *Trends Cell Biol* 20:233-243.

Schmidtke M, Selinka HC, Heim A, Jahn B, Tonew M, Kandolf R, Stelzner A, Zell R (2000) Attachment of coxsackievirus B3 variants to various cell lines: mapping of phenotypic differences to capsid protein VP1. *Virology* 275:77-88.

Stadnick E, Dan M, Sadeghi A, Chantler JK (2004) Attenuating mutations in coxsackievirus B3 map to a conformational epitope that comprises the puff region of VP2 and the knob of VP3. *J Virol* 78:13987-14002.

Tabor-Godwin JM, Ruller CM, Bagalso N, An N, Pagarigan RR, Harkins S, Gilbert PE, Kiosses WB, Gude NA, Cornell CT, Doran KS, Sussman MA, Whitton JL, Feuer R (2010) A novel population of myeloid cells responding to coxsackievirus

infection assists in the dissemination of virus within the neonatal CNS. *J Neurosci* 30:8676-8691.

Tabor-Godwin JM, Tsueng G, Sayen MR, Gottlieb RA, Feuer R (2012) The role of autophagy during coxsackievirus infection of neural progenitor and stem cells. *Autophagy* 8:938-953.

Tsueng G, Tabor-Godwin JM, Gopal A, Ruller CM, Deline S, An N, Frausto RF, Milner R, Crocker SJ, Whitton JL, Feuer R (2011) Coxsackievirus preferentially replicates and induces cytopathic effects in undifferentiated neural progenitor cells. *J Virol* 85:5718-5732.

van der Schaar HM, van der Linden L, Lanke KH, Strating JR, Purstinger G, de VE, de Haan CA, Neyts J, van Kuppeveld FJ (2012) Coxsackievirus mutants that can bypass host factor PI4KIIIbeta and the need for high levels of PI4P lipids for replication. *Cell Res* 22:1576-1592.

van Ooij MJ, Vogt DA, Paul A, Castro C, Kuijpers J, van Kuppeveld FJ, Cameron CE, Wimmer E, Andino R, Melchers WJ (2006) Structural and functional characterization of the coxsackievirus B3 CRE(2C): role of CRE(2C) in negative- and positive-strand RNA synthesis. *J Gen Virol* 87:103-113.

Verboon-Maciolek MA, Groenendaal F, Cowan F, Govaert P, van Loon AM, de Vries LS (2006) White matter damage in neonatal enterovirus meningoencephalitis. *Neurology* 66:1267-1269.

Wang YX, da C, V, Vincelette J, White K, Velichko S, Xu Y, Gross C, Fitch RM, Halks-Miller M, Larsen BR, Yajima T, Knowlton KU, Vergona R, Sullivan ME, Croze E (2007) Antiviral and myocyte protective effects of murine interferon-beta and -{alpha}2 in coxsackievirus B3-induced myocarditis and epicarditis in Balb/c mice. *Am J Physiol Heart Circ Physiol* 293:H69-H76.

Wei H, Zou H, Sheikh AM, Malik M, Dobkin C, Brown WT, Li X (2011) IL-6 is increased in the cerebellum of autistic brain and alters neural cell adhesion, migration and synaptic formation. *J Neuroinflammation* 8:52. doi: 10.1186/1742-2094-8-52.:52-58.

Wellen J, Walter J, Jangouk P, Hartung HP, Dihne M (2009) Neural precursor cells as a novel target for interferon-beta. *Neuropharmacology* 56:386-398.

Wessels E, Duijsings D, Notebaart RA, Melchers WJ, van Kuppeveld FJ (2005) A proline-rich region in the coxsackievirus 3A protein is required for the protein to inhibit endoplasmic reticulum-to-golgi transport. *J Virol* 79:5163-5173.